Phosphinic acids: Synthesis, acidity measurements and their application in asymmetric catalysis

E F GRIFFITHS

PhD 2024

Phosphinic acids: Synthesis, acidity measurements and their application in asymmetric catalysis

Emily Faye Griffiths

A thesis submitted in partial fulfilment of the requirements of Manchester

Metropolitan University for the degree of Doctor of Philosophy

Department of Natural Sciences

Manchester Metropolitan University

Abstract

Brønsted acids, such as phosphoric acids derived from chiral 1,1'-bi-2-naphthol (BINOL), are important catalysts, particularly in the formation of new carbon-carbon bonds and chiral centres. The asymmetric catalytic capabilities of these Brønsted acids are closely related to their structure and acidity. The synthetic routes towards this class of organophosphorous catalysts consist of low-yielding excessive steps, often using reagents with negative environmental impacts.

A novel route towards new BINOL-derived phosphorous Brønsted acids is reported, circumventing three steps with low atom economies and the use of restricted reagents. Brønsted phosphinic catalyst (R)-59 was synthesised in yields up to 78% over seven steps. A novel chiral fluorinated ester (R)-57 was synthesised in a yield of 78% over six steps. A ¹⁹F{¹H} NMR titration experiment was and validated and tailored towards the determination of the pK_a value of (rac)-59, which was calculated to be in the range of 8.47-8.71. Three sulfonamide compounds were synthesised as references during the ¹⁹F{¹H} NMR titration and novel crystallographic data of their coordinated sodium complexes are reported. A library of Brønsted acid catalysts, inclusive of the novel ester (R)-57, were screened in an asymmetric Friedel-Crafts reaction to enable direct comparisons of the effect of fluorinating BINOL-based phosphinic atropisomers at the α -position to the phosphorous atom on their catalytic ability.

Acknowledgements

I would like to thank Dr. Ryan Mewis for all of his support and encouragement, not only throughout my PhD but during all of my time at MMU. Without his expertise, kindness and incredible patience, this would not have been possible. Thank you.

I would also like to thank the rest of my supervisory team, Dr. Beatriz Macia-Ruiz and Dr. Vittorio Caprio, for all of their advice and encouragement throughout this project. I really appreciate all of their support, especially all of the tips and tricks in the lab. I am also grateful to Dr. Andrew Caffyn, Dr. Jay Dixon and Dr. Stuart Langley for their contributions and the time they each made to support me over the years.

I am grateful to the many technical staff that have supported me during my time at MMU but a special mention must be made for Jean, John, Muks, Gary, Sayeed and Tommy for always being happy to help me, no matter what.

I would like to thank all of the friends I have made on the 7th floor over the years, as well as the citizens of 5.41. I will always be thankful for the love and laughter that Dave, Molly and Alex surrounded me with, especially during some pretty tough times I had outside of the lab.

Thank you to Anna for cheering me on every Monday without fail. It has been an honour to witness her journey unfold for the last 3 years. Her determination was inspirational.

A big thank you to Evan. I could not have reached this point without his support and generosity over the years. Thank you for telling me daily that I could do it. A very special thank you to my friends back home, especially Jack, Mel, Romany and Gina for always being there for me. No matter where they are in the world, I know I can count on them all to be on the other side of the phone, encouraging me to "keep on keeping on".

Tom and Will, I don't think I would have enjoyed my time here in Manchester as much as I have done over the last decade if it weren't for you both. Fun Lunch Wednesdays have been an absolute staple over the years. I will also always be grateful to your family for always making me feel so welcome and for everything they continue do for me. You really are like brothers to me, thank you.

A very special thank you to all of my family, for their incredible support in absolutely everything I do. Especially to my sister Jenny, who has a talent for making me laugh until it hurts. Thank you for believing in me. Thank you to my grandparents, Julie and Vic, for their unwavering support and incredible recipes, which helped me so much when I missed home.

Finally, a huge thank you to my parents, Andrew and Wendy, for all of their love and support, both moral and financial. I could not have completed this PhD without them. In the last few months of this research, they showed me what it truly means to be resilient. Thank you for always believing in me and encouraging me to go further.

Table of contents

Tal	ole of	contents	6
Lis	t of Fi	gures	.10
Lis	t of S	chemes	. 16
Lis	t of Ta	ables	. 18
Lis	t of Al	bbreviations	.20
1.	Intro	oduction: The importance and versatility of phosphinates	.22
1	1.1	Organophosphorous catalysts: Atropisomers derived from BINOL	.23
1	1.2	Applications of BINOL-derived phosphorous atropisomers in	
a	asymı	metric catalysis	.27
2.	The	synthesis of chiral Bronsted phosphinic acid catalysts	.36
2	2.1	Introduction: The general composition of phosphinic acids	.36
2	2.2	The synthesis of alkyl phosphinic acids from hypophosphorous acid	.36
2	2.3	The synthesis of allylic and aryl phosphinic acids from hypophosphorou	JS
a	acid		.39
2	2.4	Phosphinic acids in the design of tuneable catalysts	.42
2	2.5	BINOL derived phosphonates as asymmetric catalysts	.44
2	2.6	The synthesis of BINOL derived phosphinic acids	.46
2	2.7	Enhancing BINOL derived phosphinic acid catalytic capability through	
f	luorin	ation	.47
5	2.8	Results and discussion	51

2.8.1	Synthesis of (R) -2,2-distribute-1,1-dinaphtnyl, 2	51
2.8.2	Synthesis of (<i>R</i>)-2,2'-dimethyl-1,1'-binaphthyl, 3	57
2.8.3	Novel synthetic step towards (<i>R</i>)-ethyl-2,2'-bis(methylene)-1,1'-	
binaphth	nyl phosphinic acid	63
2.8.4	Synthesis of (R)-2,2-bis(bromomethyl)-1,1'-binaphthyl	88
2.8.5	Synthesis of (R)-2,2'-bis(methylene)-1,1'-binaphthyl phosphinic a	cid
55		89
2.8.6	Synthesis of (R)-ethyl-2,2'-bis(methylene)-1,1'-binaphthyl	
phosphi	nate	89
2.8.7	Synthesis of (R)-ethyl-2,2'-bis(difluoromethylene)-1,1'-binaphthyl	
phosphi	nate 7	92
2.8.8	Synthesis of 3,3'-substituted phosphinic acid atropisomers	101
2.9 Cor	nclusions	104
2.10 Fut	ure Work	104
3. The syn	thesis of sulfonamides for the pK₂ determination of the	
Brønsted aci	d 2,2'-bis(difluoromethylene)-1,1'-binaphthyl phosphinic	
acid		105
3.1 Res	sults and Discussion	116
3.1.1	Synthesis of reference compounds	116
3.1.2	Control ¹⁹ F{ ¹ H} NMR titration using two synthesised sulfonamides	s as
referenc	e compounds	127

3.1	1.3	pKa Determination: preliminary chemical shift tests for Brø	insted acid
59			131
3.1	1.4	Optimised ¹⁹ F NMR titration data	135
3.2	Co	nclusions	146
3.3	Fut	ture Work	147
4. Uti	ilising	Brønsted phosphinic acids in asymmetric catalysis	148
4.1	Intr	roduction: Applications of phosphinic acids in asymmetric ca	ıtalysis 148
4.′	1.1	Aims	153
4.′	1.2	Results and discussion	155
4.1	1.3	Conclusion	159
4.′	1.4	Future Work	160
5. Ex	perin	nental	161
5.1	Ch	emicals	161
5.2	Ins	trumentation	162
5.3	Titr	ration of <i>n</i> -butyl lithium solutions	162
5.4	Ор	timised ¹⁹ F{ ¹ H} NMR titration experiments for the determina	tion of the
pK _a (of the	Brønsted acid 2,2'-bis(difluoromethylene)-1,1'-binaphthyl p	hosphinic
acid			163
5.5	X-r	ay data collection and structural refinement	164
5.6	Svr	nthesis of reference sulfonamides	165

	5.6.1	General procedure for the amination of sulfonyl chlorides16
	5.6.2	Amination of 4-nitrobenzenesulfonyl chloride ⁷⁸ 16
	5.6.3	Amination of 3-nitrobenzenesulfonyl chloride ⁷⁸ 16
	5.6.4	Amination of 4-toluenesulfonyl chloride ⁷⁸ 16
	5.6.5	Amination of 4-chlorobenzene sulfonyl chloride ⁷⁸ 16
	5.6.6	Synthesis of 2,3,4,5,6-pentafluoro-N-(4-nitrobenzene-1-
	sulfo	nyl)benzene-1-sulfonamide (84) ⁸⁶ 16
	5.6.7	Synthesis of 2,3,4,5,6-pentafluoro-N-(3-nitrobenzene-1-
	sulfo	nyl)benzene-1-sulfonamide (85) ⁸⁶ 16
	5.6.8	Synthesis of 2,3,4,5,6-pentafluoro-N-(4-chloro-1-sulfonyl)benzene-1
	sulfo	namide ⁸⁶ (86)17
5	5.7	Synthesis of Brønsted phosphinic acids for asymmetric catalysis 17
5	5.8 F	Friedel-Crafts reactions18
	5.8.1	General procedure for the catalytic asymmetric Friedel-Crafts
	react	ion of (<i>E</i>)- <i>N</i> -Benzylidene-4-methylbenzenesulfonamide with indole 18
6.	Conc	lusion and Future work18
6	6.1 (Conclusions18
6	6.2 F	Future work18
7.	Refe	rences18

List of Figures

Figure 1 - The synthetic versatility of phosphinates, as summarised by	
Montchamp 2013. ³	23
Figure 2 - Atropisomer phosphine and phosphoric catalysts reported by	
Beller, Terada and co-workers. ^{11, 15}	24
Figure 3 - Phosphoric acids used as catalysts in many reactions,	
summarised by Rueping <i>et al</i> . ¹⁷	26
Figure 4 - Hetero Diels-Alder reaction of glyoxylates by Terada <i>et al</i> . ^{17,}	
18	28
Figure 5 - Nazarov cyclisation reaction used by Leito and co-workers in	
determining the pKa of BINOL-derived atropisomer catalysts. ²⁰	30
Figure 6 - Leito and co-worker's acidity scale of BINOL derived	
catalysts, with comparison to commonly used acids. These pKa values	
are of acidic compounds in acetonitrile. ²¹	32
Figure 7 - Fluorinated phosphinic acids synthesised by Mikami <i>et al</i> . for	
use in asymmetric catalysis. ²⁵	34
Figure 8 - The generic structure of phosphinic acids. ²⁸	36
Figure 9 - Summary of alkyl phosphinic acid preparations from	
phosphinic acid, summarised by Montchamp. ¹⁰	38
Figure 10 - Synthesis of cinnamyl-H-phosphinic acid 33 by the	
palladium-catalysed dehydrative allylation of hypophosphorous acid	
using allylic alcohols, reported by Montchamp and Bravo-Altamirano. ³⁶	40

Figure 11 - The synthesis towards aromatic phosphinic acids, reported	
by Stawinski and Kalek in 2009 and some examples from their work. ³⁹	41
Figure 12 - General structure of initial tuneable, aromatic phosphinic	
acids designed for asymmetric catalysis by Cornforth in 1978. ¹⁷	43
Figure 13 - First (R)-BINOL derived phosphonic acids reported by	
Inanaga, Terada, Akiyama and their co-workers. 12, 16, 45	45
Figure 14 - Synthesis of BINOL derived phosphinic acid (S)-2,2'-	
bis(methylene)-1,1'-binaphthyl phosphinic acid 46 reported by Moberg	
<i>et al.</i> in 2003. ⁴⁷	46
Figure 15 - BINOL derived phosphinic acid catalysts with the	
incorporation of perfluoroalkyl groups at the α positions of phosphorous	
atoms to enhance acidity which were synthesised by Mikami et al.25	47
Figure 16 - ¹ H NMR spectrum of (<i>R</i>)-2,2'-bistriflate-1,1'-binaphthyl, 52	52
Figure 17 - ¹ H environments of compound 52	53
Figure 18 - ¹ H- ¹ H COSY NMR spectrum of compound 52	55
Figure 19 - ¹ H NOESY NMR spectrum of compound 52	56
Figure 20 - ¹ H NMR spectrum of (<i>R</i>)-2,2'-dimethyl-1,1'-binaphthyl, 53	59
Figure 21 - Proton environment labelling for compound 53	60
Figure 22 - Crystal structure obtained of compound 53.	61
Figure 23 - Different perspective of compound 53 showing emphasis on	
angles of atropisomer.	61

Figure 24 – Reported structure of the <i>n</i> -Bull/IMEDA dimer isolated as	
a single crystal by Collum <i>et al</i> . in 2000. ⁵³	64
Figure 25 - Dilithiated (S)-binaphthyl intermediate complexes previously	
published by Engelhardt <i>et al</i> . ⁵⁴	64
Figure 26 - The proposed mechanism for the novel, direct conversion of	
compound 53 to 56	65
Figure 27 - ¹ H NMR spectrum of (R)-2,2'-bis(methylene)-1,1'-binaphthyl	
phosphinic acid via novel synthetic step.	84
Figure 28 - Proton environments of phosphinic ester 56	86
Figure 29 - ³¹ P{ ¹ H} NMR spectrum of crude (<i>R</i>)-ethyl-2,2'-	
bis(methylene)-1,1'-binaphthyl phosphinate 56 via novel synthetic step	87
Figure 30 - ³¹ P{ ¹ H} NMR spectrum of novel (<i>R</i>)-ethyl-2,2'-	
bis(difluoromethylene)-1,1'-binaphthyl phosphinate 57	94
Figure 31 - Fluorine environments for novel fluorinated ester 57.	96
Figure 32 – Labelled proton environments for novel fluorinated ester 57	96
Figure 33 - ¹⁹ F NMR spectrum of novel (<i>R</i>)-ethyl-2,2'-	
bis(difluoromethylene)-1,1'-binaphthyl phosphinate 57	97
Figure 34 - ¹ H NMR spectrum of novel (<i>R</i>)-ethyl-2,2'-	
bis(difluoromethylene)-1,1'-binaphthyl phosphinate 57	98
Figure 35 - ¹ H- ¹ H COSY NMR spectrum of novel fluorinated ester 57	100
Figure 36 - Mass spectrum obtained for novel chiral fluorinated ester	
57	101

Figure 37 - Synthesis of 3,3'-substituted BINOL derived phosphorous	
esters10)2
Figure 38 - Thiourea and taddol are examples of hydrogen-bonding	
Brønsted acid catalysts. Stronger phosphoric Brønsted acid catalyst	
examples derived from BINOL. ⁴² 10)7
Figure 39 - The structures and pKa values in DMSO of some of the	
phosphoric acids determined by O'Donoghue et. al.71	8(
Figure 40 – Exemplar Brønsted acids from Rueping and colleague's	
summarised scale of pK _a values determined in his previous work with	
Leito <i>et al</i> . in 2014. ^{17, 20} 11	0
Figure 41 - Structure of 2,2'-bis(difluoromethylene)-1,1'-binaphthyl	
phosphinic acid (59)11	4
Figure 42 - ¹ H NMR spectrum of 4-nitrobenzenesulfonamide. Spectrum	
collected in DMSO-d ₆ at 400 MHz11	7
Figure 43 - ¹ H NMR spectrum of 3-nitrobenzenesulfonamide in DMSO-	
d ₆ . Spectrum acquired at 400 MHz11	8
Figure 44 - ¹ H NMR spectrum of 4-chlorobenzenesulfonamide in	
DMSO-d ₆ , acquired at 400 MHz12	20
Figure 45 - Stacked ¹⁹ F NMR spectra of reference sulfonamides	
synthesised, compounds 84 , 85 and 86 in acetonitrile12	22
Figure 46 - Ball and stick representation of the X-ray crystallographic	
structure of 85 that showcases the coordination to sodium ions by	

ligand molecules in lattice. Atom labelling: carbon (black), oxygen (red),	
nitrogen (blue), fluorine (pink), sulfur (yellow), sodium (silver)	124
Figure 47 - Ball and stick representation of the X-ray crystallographic	
unit cell contents of 86 with H atoms omitted for clarity. Atom labelling:	
carbon (black), oxygen (red), nitrogen (blue), fluorine (pink), sulfur	
(yellow), sodium (silver), chlorine (green)	126
Figure 48 - Ball and stick representation of the X-ray crystallographic	
unit cell contents of 86 viewed along the b-c plane. H atoms have been	
omitted for clarity. For atoms that are disordered over two positions,	
only one position is shown. Atom labelling: carbon (black), oxygen (red),	
nitrogen (blue), fluorine (pink), sulfur (yellow), sodium (silver), chlorine	
(green)	127
Figure 49 – Exemplar ¹⁹ F{ ¹ H} NMR spectra from a preliminary chemical	
shift test of Brønsted acid 59 using sulfonamide 84 as a reference.	
Spectrum 49a represents the fully protonated compounds 59 and 84 ,	
spectrum 49b represents the partially protonated and deprotonated	
forms of 59 and 84 and spectrum 49c represents the fully deprotonated	
forms of compounds 59 and 84	132
Figure 50 - Stacked ¹⁹ F{ ¹ H} NMR spectra results from the optimised	
titration of 59 using reference compound 84	139
Figure 51 - Early application of BINOL-derived phosphoric acid	
atropisomers in the direct Mannich reaction by Terada and Uraguchi. ⁴⁵	149

Figure 52 - Nine-membered zwitterion transition state proposed by	
Yamanaka et al., showing the dual interaction of new chiral phosphoric	
Brønsted acids	150
Figure 53 - Nazarov cyclisation reaction catalysed by Brønsted	
phosphorous acids, published by Rueping <i>et al</i> . 2007. ⁸⁴	151
Figure 54 - Friedel-Crafts reaction of indole 95 with imine 96 , catalysed	
by the BINOL-derived phosphoric acid 94a to obtain the biologically	
active adduct 97 in high enantiomeric excess. ⁸⁵	152
Figure 55 - Procedure for catalytic Friedel-Crafts reaction of (<i>E</i>)- <i>N</i> -	
benzylidene-4-methylbenzensulfonamide with indole	153
Figure 56 - Catalysts employed in the Friedel-Crafts reaction of (<i>E</i>)- <i>N</i> -	
benzylidene-4-methylbenzensulfonamide with indole	156

List of Schemes

Scheme 1 - The Fridel-Crafts reaction of Indole with an N-Tosylamide,	
using the catalysts 29-31 , by Mikami <i>et. al</i> . ²⁵	34
Scheme 2 - The synthetic route for the synthesis of phosphinic acids	
59 . The red arrow indicates the proposed methodology to circumvent	
three reaction steps. A novel substitution reaction at the 3,3' position of	
phosphinic ester 57 is also shown	49
Scheme 3 - The synthetic route towards (R)-2,2'-bistriflate-1,1'-	
binaphthyl, 52	51
Scheme 4 - The synthetic route towards (R)-2,2'-dimethyl-1,1'-	
binaphthyl, 53	57
Scheme 5 - Proposed novel synthetic step of (R)-ethyl-2,2'-	
bis(methylene)-1,1'-binaphthyl	63
Scheme 6 - An example from the extensive scope of rapid fluorinations	
of organophosphorous acids by Melvin and co-workers. ⁵⁷	90
Scheme 7 - Synthesis of methyl ester 68 by Mikami <i>et al.</i> ²⁵ in a two-	
step esterification of the chiral phosphinic acid 55	91
Scheme 8 - The one-pot reaction to convert racemic phosphinic acid 55	
to phosphinic ester 56 , via. the phosphonochloridate intermediate 69	
reported by the Caffyn group. ⁴⁹	91
Scheme 9 - Synthesis of the novel chiral (<i>R</i>)- enantiomer of fluorinated	
phosphinic acid 57	92

Scheme 10 - Terada <i>et al</i> . employed BINOL derived Bronsted acids as	
catalysts in an enantioselective direct Mannich reaction and an aza-ene	
type reaction. ¹⁵	.106
Schome 11. Synthetic route towards reference compounds 94.96 for	
Scheme 11 - Synthetic route towards reference compounds 84-86 for	
the pK _a determination by ¹⁹ F{ ¹ H}NMR spectroscopic titration	.116

List of Tables

Table 1 - Initial trials of novel esterification reaction for compounds 53 to	
56	66
Table 2 - Further reaction trials of the novel esterification reaction from	
racemic compound 53 to 56	69
Table 3 - Novel cyclization esterification reaction trials in which reaction	
concentrations were altered	72
Table 4 – Reaction conditions for using Et ₂ O as a reaction solvent for	
the novel cyclisation esterification step.	75
Table 5 – Reaction scale, and order of addition, for the novel cyclisation	
step towards compound 56	77
Table 6 – Summary of the final novel cyclisation reaction trials	80
Table 7 – ¹⁹ F{ ¹ H} NMR spectrum chemical shifts (ppm) for sulfonamides	
84 and 85 in neutral, fully protonated and deprotonated forms	129
Table 8 - Chemical shift values used for the fully protonated and fully	
deprotonated forms of 59 relative to the reference standards 84-86 in	
the ¹⁹ F{ ¹ H} NMR titration experiments performed	136
Table 9 - pK _a values determined by ¹⁹ F{ ¹ H} NMR titrations	142
Table 10 - Catalyst screening results for the reaction of (<i>E</i>)- <i>N</i> -	
benzylidene-4-methylbenzensulfonamide with indole to produce	
tosylamide 100	157
Table 11: Crystal data for the structural refinement of 85	169

Table 12: Crystal data for the structural refinement of 86	.171
Table 13: Crystal data for the structural refinement of (R)-2,2'-dimethyl-	
1,1'-binaphthyl (53)	.175

List of Abbreviations

AIBN 2,2'-Azobis(2-methylpropionitrile)

BINOL 1,1'-Bi-2-naphthol

CCI₄ Carbon tetrachloride

CD₃CN Deuterated acetonitrile

CDCI₃ Deuterated chloroform

CH₂Cl₂ Dichloromethane

CH₃CN Acetonitrile

CHCI₃ Chloroform

Conc. Concentration

DIPEA *N,N*-Diisopropylethylamine

DMSO-*d*₆ Deuterated dimethyl sulfoxide

Dppp (Diphenylphosphino)propane

Et₂O Diethylether

EtOAc Ethylacetate

GC-MS Gas Chromatography - Mass Spectrometry

HCI Hydrochloric acid

HFB Hexafluorobenzene

HPLC High-Performance Liquid Chromatography

MeOH Methanol

MgSO₄ Magnesium sulfate

NaHCO₃ Sodium hydrogen carbonate

NaOH Sodium hydroxide

NBS *N*-bromosuccinimide

*n***-BuLi** *n*-Butyllithium

NH₄CI Ammonium chloride

NH₄H₂PO₂ Ammonium hypophosphite

P₂O₅ Phosphorous pentoxide

PTSA *p*-toluenesulfonic acid

RE Rare Earth

THF Tetrahydrofuran

TLC Thin Layer Chromatography

TMEDA Tetramethlethylenediamine

Triflic acid Trifluoromethanesulfonic acid

Triflic anhydride Trifluoromethanesulfonic anhydride

UV Ultra Violet

Introduction: The importance and versatility of phosphinates

Organophosphorus chemistry has been studied for more than a century and is now one of the largest sub-groups of chemistry. Despite this, the importance of this area was often over-looked and organophosphorus compounds seldom used, even up until as late as the 1980's. Yet it is now a vital area, not only within academic research today but in many other industries, including: the agricultural industry as pesticides; pharmaceutical industry as medicines; materials industry as building units and many more. Not only are both chiral and achiral phosphinate ligands used in homogeneous catalysis and organometallic chemistry, numerous phosphorus(V) compounds can also be used to form pseudopeptides, utilised as enzyme inhibitors. Over time, the field has provided many named reactions, such as the Arbuzov and Wittig reactions.

Organophosphorus compounds, namely substituted phosphinates and other derivatives from H-phosphinates, have now been used extensively in organic synthesis.⁷ This is not only due to their wide scope of applications but also the fact that H-phosphinates exist in an intermediate phosphorous oxidation state. This characteristic enables these compounds to be converted into essentially any organophosphorous functionality. These were summarised by Montchamp in 2013 (Figure 1).³

Figure 1 - The synthetic versatility of phosphinates, as summarised by Montchamp 2013.³

Numerous reactions of these organophosphorous functionalities have been developed by Montchamp and co-workers, such as nucleophilic and radical reactions; palladium-catalysed cross-couplings; hydrophosphinylations; metal-catalysed and reductive allylations; benzylations; catalytic P-O bond formations; palladium-catalysed P-C bond formations and more.^{1, 3, 8-10} The versatility of phosphinates highlights the importance of these compounds across a number of different industries.

1.1 Organophosphorous catalysts: Atropisomers derived from BINOL

A significant portion of organophosphorous synthesis today is the design of novel, chiral phosphinates for use in asymmetric catalysis.¹¹ The successful synthesis of both monodentate and bidentate phosphorous-containing catalysts, derived from 1,1'-binaphthalene-2,2'-diol (BINOL), sparked substantial interest within the area. This was not only due to the very high enantioselectivities achieved utilising these catalysts (95-99% ee),^{11, 12} but also due to the atropisomerism these

catalysts possessed. A type of stereoisomerism, atropisomerism arises from axially restricted bond rotation in three-dimensional molecules.^{13, 14} Some of the initial phosphorous atropisomers within this class of catalyst are shown in Figure 2.

Figure 2 - Atropisomer phosphine and phosphoric catalysts reported by Beller, Terada and co-workers.^{11, 15}

Since the synthesis of this new class of organophosphorous ligands, derived from BINOL, many chiral, phosphorus-based ligands today are designed to have a similar atropisomeric backbone. The atropisomerism associated with such structures enables high enantioselectivities for many reactions when employed as Brønsted acid catalysts. ¹⁶ Some phosphoric acid catalysts in this now broad atropisomer class, that are extensively employed in many reactions, were summarised into categories by Rueping *et al.*, Figure 3. ¹⁷ Although **5a** was a simple catalyst that found early applications in

asymmetric catalysis, many of these catalysts now have substitutions at the 3,3'- positions.¹⁷ The substituents at these positions are often used to enhance steric bulk in order to increase enantioselectivity and **5e-6a** are common examples of this. The substituents with *para*- substituted benzene rings, **6b-6j**, have a dual purpose. As well as providing the catalysts with steric bulk, the groups also tune the electronics of the catalysts.¹⁷ Benzene rings with *ortho*-position substitutions have been synthesised, **7a-7d**, however, these are less common. Compounds **8a-10d** are all examples of a large category of catalysts with trisubstituted benzene rings at the 3,3-positions. Although catalysts **10a-10d** have the capability to have the electronics or solubility altered *via* the chiral catalyst backbone; 3,3'-bis(2,4,6-triisopropylphenyl)-1,1'-binaphthyl-2,2'-diyl hydrogen phosphate (TRIP, compound **8b**) is employed the most in asymmetric catalysis.¹⁷

Figure 3 - Phosphoric acids used as catalysts in many reactions, summarised by Rueping *et al*.¹⁷

9d, $R^1 = {}^{i}Pr$, $R^2 = 9$ -anthracenyl

10d, R = i Pr, X = C₈H₁₇

Though the simplest and most employed phosphoric acid catalysts are shown in Figure 3, this is not an exhaustive list and other types have been utilised in catalysis. Other less common examples include phosphoric acid catalysts with multiple chiral axis and miscellaneous chiral catalysts designed for specific purposes that are more highly specialised. It is important to note that there are few examples of similar atropisomers with phosphinic acid moieties.¹⁷

1.2 Applications of BINOL-derived phosphorous atropisomers in asymmetric catalysis

Phosphorous acid atropisomers, derived from BINOL, are employed as catalysts in numerous synthetic reactions. A large proportion of the substrates that can be activated by axially chiral Brønsted acids are imine components, however, there are a number of reports of successful carbonyl group activation as well.¹⁷ A notable example of such carbonyl group activation was the hetero Diels-Alder reaction published in 2009 by Terada *et al.* (Figure 4).¹⁸ The Diels-Alder reaction is a famous and widely used reaction in synthesis today, and is frequently empolyed for the formation of six-membered rings with multiple centres of chirality.^{17, 19} The reaction of glyoxylate **12** with diene derivatives **11** to produce chiral dihydropyran derivatives **13** was shown using the BINOL-based phosphoric acid **6a** as a chiral Brønsted acid, Figure 4.

transition state:

Ar
$$CO_2Et$$

$$Ar$$

$$R^2$$

$$R^3$$

Figure 4 - Hetero Diels-Alder reaction of glyoxylates by Terada et al. 17, 18

The catalysts usually employed for these reactions are Lewis acids, since Brønsted acids are often not acidic enough to activate substrates, leading to poor reactivities.¹⁷ Despite this, it was proposed that the glyoxylate aldehydes participate in a dual-activation with Brønsted acid catalyst **6a** and the transition state published (depicted in Figure 4) supports this.¹⁸ It was proposed that the aldehyde proton of glyoxylate is acidic enough to interact with the Lewis basic site of the BINOL-phosphoric catalyst **6a**, alongside the interaction between the Brønsted acidic proton of **6a** with the oxygen atom of the aldehyde **12**.¹⁷ The enantiomeric excesses reported were extremely

high, with many examples providing 99% ee.¹⁸ The success of such BINOL-based phosphorus containing ligands as asymmetric catalysts is dependent on the architecture of the catalyst, as well as the strength of the Brønsted acid.¹⁶ Although the enantioselectivity is determined by the design of the catalytic ligand structure, the reactivity is determined by the acidity.¹⁷ Leito and co-workers investigated the correlation between Brønsted acidity and reactivity, using a Nazarov cyclization as a model reaction (Figure 5), as no side products were formed to complicate the investigation.²⁰

Nazarov cyclisation

O CH₃ Brønsted acid 16-28
$$(2 \text{ mol}\%)$$
 Ph 15

Brønsted acid catalysts:

16, $R^1 = Ph$; **17**, $R^1 = 4-FC_6H_4$; **18**, $R^1 = 2,4,6-({}^{i}Pr)_3C_6H_2$; **19**, $R^1 = 9$ phenanthrene; **20**-[H₈], R^1 = 9-phenanthrene; **21**, R^1 = Ph, R^2 = CF₃; **22**- $[H_8]$, $R^1 = Ph$, $R^2 = CF_3$; **23**- $[H_8]$, $R^1 = Ph$, $R^2 = C_4F_9$; **24**- $[H_8]$, $R^1 = Ph$, R^2 $= C_8F_{17}$; **25**, $R^1 = 4$ -MeOC₆H₄, $R^2 = CF_3$; **26**-[H₈], $R^1 = 4$ -MeOC₆H₄, $R^2 = 4$ CF_3 ; **27**-[H₈], $R^1 = 4$ -FC₆H₄, $R^2 = CF_3$; **28** = $R^1 = 3.5$ -(CF_3)₂C₂H₃.

Mechanism:

Figure 5 - Nazarov cyclisation reaction used by Leito and co-workers in determining the pKa of BINOL-derived atropisomer catalysts.²⁰

Leito and co-workers determined the pK_a values of the catalysts shown using a previously established UV-vis spectrophotometric titration of a solution consisting of two acids in acetonitrile (MeCN); using trifluoromethanesulfonic acid to fully protonate the acids and *t*-BuP₁(pyrr) phosphazene as the base for deprotonation.²⁰⁻²² The pK_a values were then calculated from the changes in absorbance, resulting in the production of an acidity scale, which is depicted in Figure 6.

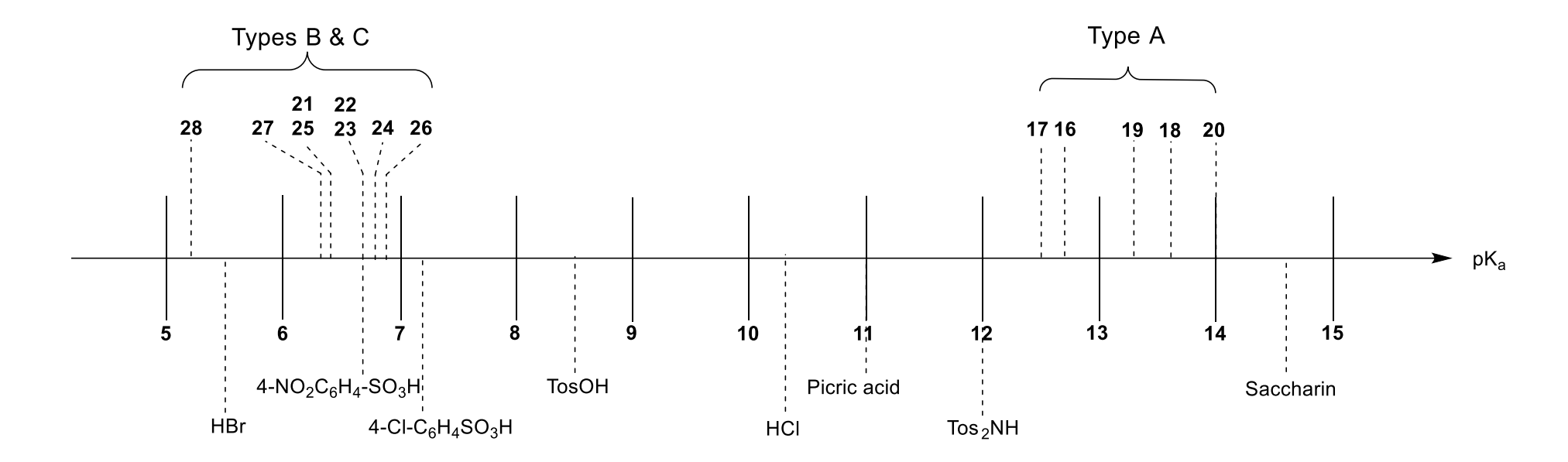


Figure 6 - Leito and co-worker's acidity scale of BINOL derived catalysts, with comparison to commonly used acids. These pKa values are of acidic compounds in acetonitrile.²¹

The pK_a values determined, as seen in Figure 6, have been plotted against the pK_a values of common acids in acetonitrile.^{17, 20, 21} From this scale, it is evident that the phosphoric acid Brønsted catalysts, Figure 5, type A, are significantly weaker than the type B and C catalysts shown. The type A phosphoric acids have pK_a values in the range of 12-14, comparable to *p*-toluenesulphonic acid (PTSA), whereas the acids with sulfonamide groups at the phosphorous moiety, type B, and the sulfonamide atropisomers, type C, are significantly stronger with pK_a values in acetonitrile comparable to hydrogen bromide (HBr). Notably, increasing the acidity of phosphorous Brønsted acids, while maintaining the phosphorous acid moiety has seldom been reported, despite the publication of the clear correlation between Brønsted acidity and reaction rate.²⁰

It has been reported that the presence of fluorine atoms near the phosphorus acid site can significantly increase the strength of the acid. 16, 23 Trifluoromethylphosphonic acid is one of the strongest known phosphorous-based acids²⁴ and perfluoroalkyl substituted phosphorus acids are also known to be strong acids. 24 The ability of the electronegative fluorine atoms to withdraw electrons from the neighbouring carbon atoms, which in turn withdraw electrons from the phosphorous atom at the acid site, through an inductive effect, causes the increased acidity. As the conjugate base of the acid is stabilised, the acid becomes stronger than the non-fluorinated counterpart and becomes an overall more successful ligand when utilised in asymmetric catalysis. This knowledge, alongside the lack of examples of BINOL derived phosphinic acids catalysts, led to the design of the potentially highly acidic Brønsted acid catalysts 29-31 by Mikami *et al.*, Figure 7.²⁵

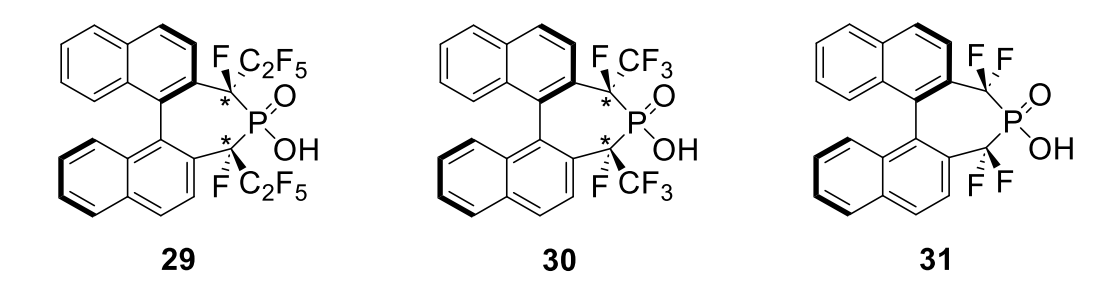


Figure 7 - Fluorinated phosphinic acids synthesised by Mikami *et al.* for use in asymmetric catalysis.²⁵

Mikami *et al.* synthesised phosphinic acids **29-31** for use in asymmetric catalysis, adding fluorine containing substituents at the methylene carbons in the heterocycles to enhance the catalyst acidity. They employed **29-31** as Brønsted acids in the Friedel-Crafts reaction of *N*-tosylimine with indole, Scheme 1, and compared their enantioselectivities and catalytic activities to similar non-fluorinated, phosphoric acids (**5a** and (*S*)-**6a**, Figure 3).

Scheme 1 - The Fridel-Crafts reaction of Indole with an N-Tosylamide, using the catalysts **29-31**, by Mikami *et. al.*²⁵

Unfortunately, the yields and ee values obtained were only slightly improved. For comparison, **31** gave the Friedel-Craft reaction product in yields up to 56%, an improvement from 42% for the non-fluorinated phosphonic acid **5a**. However, the ratios of *R*:*S* enantiomers reported were 54.5:45.5 for **31** and 44.5:55.5 for **5a**. These ee values are arguably close to racemic product mixtures and leaves room for improvement. The highest ee values reported were obtained when **29** was

used as the catalyst, with 82:18, though the product yield for this result was 60%. Higher product yields using **29** as a catalyst resulted in lower *ee* values.²⁵

Mikami *et al.* highlighted the significance of catalyst acidity within the design of these new fluorinated phosphinic acids, though they did not report the determination of their pK_a values. The synthesis of these catalysts also consisted of multiple steps with low atom economies and negative environmental impacts; using restricted reagents. This work aims to improve the synthetic route towards these new fluorinated phosphinic acid catalysts, as well as determining their pK_a values, prior to applying them as asymmetric catalysts.

2. The synthesis of chiral Bronsted phosphinic acid catalysts

2.1 Introduction: The general composition of phosphinic acids

Phosphinic acid compounds, derived from phosphinic acid (H₂P(O)OH), can exist as dialkyl and diaryl motifs, with the general formula R¹R²P(O)OH; where R¹ and R² are alkyl or aryl groups, as well as hydrogen (Figure 8).^{1, 4, 6} They are vastly diverse compounds with great versatility due to their beneficial characteristics, such as: their tetrahedral geometries; their capability of coordination to many metals; the ability to form electrostatic interactions; hydrogen bonding and more.²⁶ As such, phosphinic acids have found a wide range of applications across multiple fields. For example: within the materials industry, as coordination polymers; in the medicinal industry as anti-inflammatory agents and phosphinic pseudopeptides; in the agricultural industry as fertilisers and pesticides. They are also heavily utilised in organic and inorganic synthesis, as well as their uses as ligands in asymmetric catalysis. ^{1, 4, 6, 11, 17, 25-27}

 R^1 and $R^2 = H$, aryl or alkyl substituents

Figure 8 - The generic structure of phosphinic acids.²⁸

2.2 The synthesis of alkyl phosphinic acids from hypophosphorous acid

Since the synthesis of methylphosphinic acid, the first phosphinic acid, which was reported by Hofmann,^{29, 30} there have been extensive publications on the

synthesis of many different phosphinic acids. ^{3, 4, 8, 9, 28, 31, 32} Initially, Hofmann synthesised methylphosphinic acid from methylphosphine and nitric acid. More recently, phosphinic acid (otherwise known as hypophosphorous acid) is more frequently utilised for the synthesis of phosphinic acid derivatives, **32**. ^{31, 32} Montchamp previously summarised and reported improvements on the preparation methods of alkyl H-phosphinic acid derivatives. The examples utilising hypophosphorous acid are summarised in Figure 9. ¹⁰

1) Boyd & Regan, 2) Nifant'ev, 3) Gallagher, 4) Ciba-Geigy, 5) Montchamp

Figure 9 - Summary of alkyl phosphinic acid preparations from phosphinic acid, summarised by Montchamp.¹⁰

Figure 9 showcases some of the earlier methods of phosphinic acid compound synthesis from hypophosphorous acid. Each of the methods highlighted utilised reagents that limited their scope. For example, the use of (TMSO)₂PH by Boyd

and co-workers.³³ in preparation 1, produced symmetrically disubstituted phosphinates, unless a large excess of the reagent was used. This phosphinic acid preparation also led to significant amounts of decomposition, adding difficulty to their isolation. 10 The scope was limited by this as only the most reactive alkyl halides could be utilised to produce reasonable yields. 10 The scope of the radical reaction by Nifant'ev., 34 preparation 2, limited the number of substrates that could be employed due to the strongly acidic conditions required.³⁴ The use of the Ciba-Geigy reagent, preparation 4, was also a scope-limited preparation as it relied on the protection-deprotection method, which has drawbacks since the acidic cleavage of the acetal group is not always functional group compatible. 10 To improve the accessibility of phosphinic acid compounds (and other derivatives), Montchamp highlighted the importance of more practical and scalable reactions and as such, developed methodologies that could be replicated in any laboratory with standard equipment and utilising widely available and inexpensive reagents and catalysts. 10 These included multiple palladium-catalysed cross-couplings; radical hydrophosphinylations; nucleophilic reactions and esterifications. 9, 10 The development of the palladium cross-coupling reaction was extended to the direct coupling of alkyl phosphinic acids to aryl, heteroaryl, alkenyl, benzylic and allylic halides, as well as triflates, emphasizing the scope of the group's developments towards phosphinic acid derivatives. 10, 35

2.3 The synthesis of allylic and aryl phosphinic acids from hypophosphorous acid

Montchamp and Bravo-Altamirano went on to also publish a large scope of the synthesis of allylic phosphinic acids *via*. a palladium-catalysed dehydrative allylation of hypophosphorous acid with allylic alcohols.^{36, 37} More than twenty

examples utilising this reaction have been reported.²² An example using this synthetic pathway, for the synthesis of cinnamyl-H-phosphinic acid, **33**, is highlighted in Figure 10.

Ph OH
$$\frac{\text{Cat. Pd(OAc)}_2/\text{xantphos}}{\text{DMF, 85°C}}$$
 Ph OH H + H₂O

Figure 10 - Synthesis of cinnamyl-H-phosphinic acid **33** by the palladium-catalysed dehydrative allylation of hypophosphorous acid using allylic alcohols, reported by Montchamp and Bravo-Altamirano.³⁶

This synthetic publication on phosphinic acids was particularly poignant as a highly atom-economical and more environmentally benign approach in comparison to previous phosphinic acid synthesis from allylic alcohols.³⁷ Increasing the atom economy of reactions reduces the amount of waste produced, ensures resources are conserved and therefore minimises their environmental impact. Prior to the group's work, allylic H-phosphinic acids were prepared from the reaction of an allylic halide with (TMSO)₂PH, producing wasteful silylation products.^{37, 38}

Monoaryl and diarylphosphinic acids and their derivatives have attracted considerable research attention due to their vast applications, previously mentioned. Stawinski and Kalek built on the palladium-catalysis reactions by Montchamp and co-workers, 9, 35 towards a large scope of aromatic phosphinic acids. 39 The group developed an efficient method for the cross-coupling of H-

phosphinate diesters with aryl halides to produce monoaryl- and both symmetrical and unsymmetrical di-arylphosphinic acids, Figure 11.³⁹

Figure 11 - The synthesis towards aromatic phosphinic acids, reported by Stawinski and Kalek in 2009 and some examples from their work.³⁹

The microwave assisted palladium(0)-catalysed reaction of aryl halides and anilinium phosphinate (34), using Xantphos as a supporting ligand, is shown in Figure 11. The reported synthesis was microwave assisted and thus enabled reaction times as low as ten minutes.³⁹ Although the *in situ* synthesis of the diarylphosphinic acids was reported, the group isolated the monoaryl compounds prior to the second cross-coupling step towards the diaryl compounds. This was due to the fact that the synthesis of the unsymmetrical diarylphosphinic acids formed the symmetric compound simultaneously, significantly impacting the atom economy for the desired product.³⁹ Some examples (37-41) from the relatively

large scope (17 monoaryl and 7 diaryl derivatives) are highlighted in Figure 11. These examples showcase the capability of the palladium cross-coupling to produce monoaryl and diaryl phosphinic acids using aryl halides with a range of substituents, including highly electronegative groups **38** and more complex aromatic structures, **40** and **41**. This work enabled the practically simple preparation of highly tunable aryl phosphinic acids when compared to the previously reported palladium cross-couplings of such derivatives, with reactions times up to 64 hours.⁴⁰ This is particularly useful in the design of specialised molecular catalysts.

2.4 Phosphinic acids in the design of tuneable catalysts

Though phosphinic acids are now extensively utilised in catalysis, some of the first tuneable aromatic phosphinic acids were investigated by Cornforth in 1978.^{17, 41}

Cornforth designed phosphinic acid catalysts for use in the stereoselective hydration reactions of alkenes. The general structure of these phosphinic acids **42** is shown in Figure 12.

a = Backbone substituent potential

b = Tuneable aromatic groups

c = Narrow well-defined channel for substrates

Figure 12 - General structure of initial tuneable, aromatic phosphinic acids designed for asymmetric catalysis by Cornforth in 1978.¹⁷

Cornforth's phosphinic acids **42** had a rigid backbone (**a** in Figure 12), due to the five-membered dibenzo heterocycle. The backbone benzene rings were able to be finely tuned by adding sterically hindering groups at X, with the possibility of creating a chiral axis since the rings are restricted. The benzene rings at the stereocontrolling site b were also capable of tuning for certain reactions by substitution. These rings at **b** also created the narrow channel for substrate binding at the phosphinic acid site, **c**. These chiral phosphinic acid catalysts set the precedence of catalyst design utilising rigid aromatic backbones that are readily tuneable, more than 40 years ago. More recently, BINOL derived phosphinic acids have been extensively utilised for use in the asymmetric catalysis of numerous synthetic reactions. Rueping *et al.* reported that there were over 100 reports of BINOL derived phosphinic acids being designed for use in asymmetric catalysis in 2013 alone and they are as heavily investigated today. In recent years, organocatalysis work by List and co-workers, encompassing the use

of BINOL derived phosphinic acid catalysts, has been awarded the Nobel Prize, thus highlighting their significance.^{43, 44} This is again due to the rigid structure as a catalyst backbone, susceptibility to substitution for tuneability and stereocontrol, the capability of forming narrow channels for substrate interactions, as well as their chirality.

2.5 BINOL derived phosphonates as asymmetric catalysts

Inanaga, Terada, Akiyama and their co-workers were the first to introduce chiral 1,1'-bi-2-naphthol (BINOL) derived phosphonates for use as asymmetric catalysts. ^{12, 16, 45} Initially, phosphoric acid derivations were popular, due to their straightforward synthesis (phosphorylation with POCl₃)⁴⁶ from the commercially available atropisomer, (*R*)-BINOL. The structures of the first of these are shown in Figure 13.

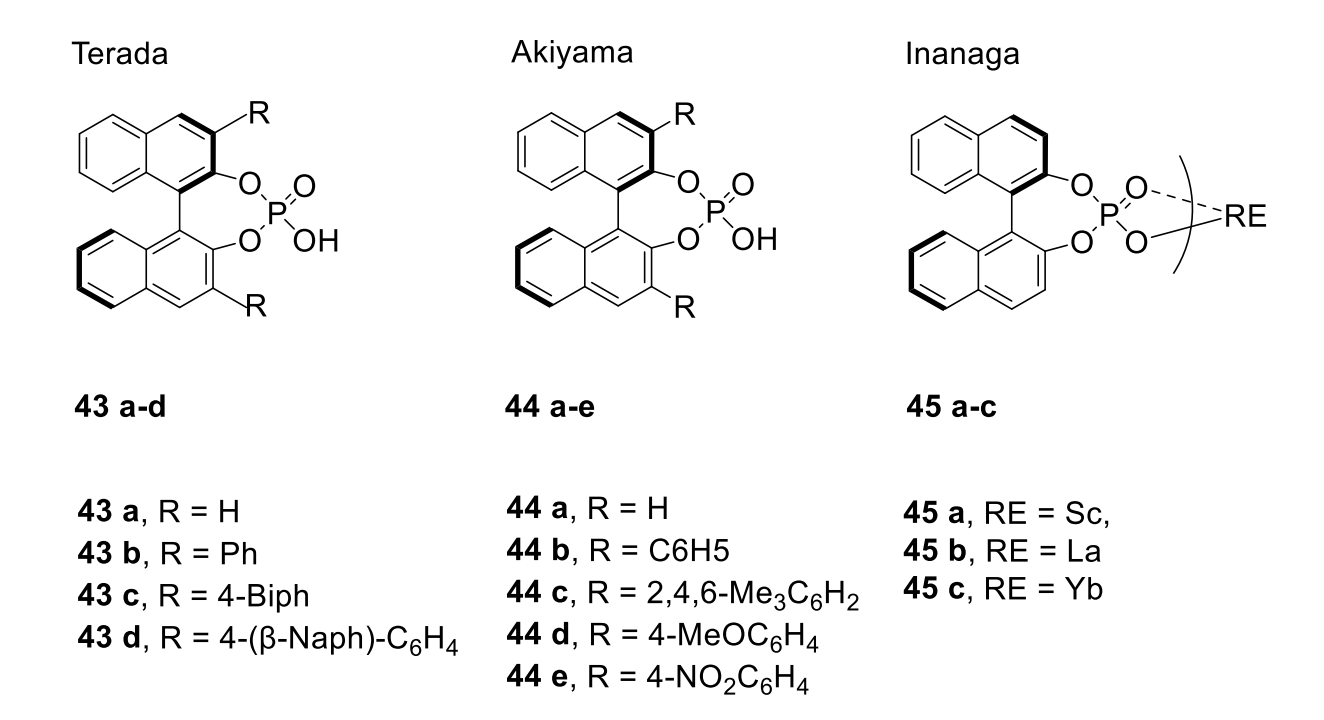


Figure 13 - First (*R*)-BINOL derived phosphonic acids reported by Inanaga, Terada, Akiyama and their co-workers.^{12, 16, 45}

Following Inanaga *et al.*'s work, employing the inorganic BINOL derived phosphonate-rare-earth (RE) metal complexes as asymmetric catalysts for a 1,4-addition reaction of an amine into an enone, ¹² Terada, Akiyama and their coworkers published the different uses of the organic phoshoric acids shown in Figure 13. Both publications showcased the (*R*)-BINOL phosphoric acids as Brønsted acids used in asymmetric direct Mannich reactions. ^{16, 45} These publications were the first metal-free examples of BINOL-based phosphoric acids and had significant success as asymmetric catalysts; products with high enantiomeric excesses (>99%) were obtained. ⁴⁵

2.6 The synthesis of BINOL derived phosphinic acids

Despite the extensive publications of the synthesis of many BINOL derived phosphoric acids for applications in asymmetric catalysis, few phosphinic acids derived from BINOL have been reported. Moberg and co-workers have, however, previously synthesised (*S*)-2,2'-bis(methylene)-1,1'-binaphthyl phosphinic acid **16**, Figure 14.⁴⁷

Figure 14 - Synthesis of BINOL derived phosphinic acid (*S*)-2,2'-bis(methylene)-1,1'-binaphthyl phosphinic acid **46** reported by Moberg *et al.* in 2003.⁴⁷

Moberg *et al.* synthesised the chiral phosphinic acid **47** from (S)-2,2'-bis(bromomethyl)-1,1'-binaphthyl **46**, using ammonium hypophosphite (NH₄H₂PO₂), diisopropylethylamine (DIPEA) and chlorotrimethylsilane (TMSCI) in CH₂Cl₂. The group synthesised numerous BINOL derived phosphinic ligands for asymmetric catalysis, using **47** yet interestingly, did not use **47** as a catalyst itself.

2.7 Enhancing BINOL derived phosphinic acid catalytic capability through fluorination

Mikami et al. reported the synthesis of multiple new BINOL derived phosphinic acids from (*R*)-2,2'-bis(methylene)-1,1'-binaphthyl phosphinic acid **47** for use in asymmetric catalysis.²⁵ The success of phosphinic acids as asymmetric catalysts is linked to their acidity. Berkowitz and Bose previously reported that increasing the acidity of phosphoric acids could be achieved by fluorination at the α position of the phosphorous atom.⁴⁸ This is caused by the electronegative fluorine atoms making very good electron withdrawing substituents, essentially weakening the O-H bond of the phosphoric acid and enhancing acidity. Following the report by Berkowitz and Bose on phosphoric acids, Mikami *et al.* designed BINOL derived phosphinic acids and incorporated perfluoroalkyl groups to them, at the α positions to phosphorous, to enhance their acidity for applications in asymmetric catalysis, Figure 15.

Figure 15 - BINOL derived phosphinic acid catalysts with the incorporation of perfluoroalkyl groups at the α positions of phosphorous atoms to enhance acidity which were synthesised by Mikami *et al.*²⁵

Despite the successful fluorination reactions towards phosphinic acids **48-50**, the application of these in the Friedel-Crafts reaction of an N-tosylimine and indole did not produce products with impressive yields or with high enantiomeric excesses,

obtaining the product with ee values of 9% in 56% yield using **48** as the catalyst. ²⁵ The best ee value reported was 64%, utilising catalyst **50**, though product yields were 63% over 2 days, showing relatively poor catalytic ability. The group did not trial tuning the newly fluorinated phosphinic acids with substituents at the 3,3'-positions of the backbone. The group also emphasised the importance of pKa in the design of catalysts for applications in asymmetric catalysis, but did not report the pKa of their fluorinated acids novel acids. Thus, there is scope to explore the fluorination of phosphinic acids, especially at the α position of the phosphorous acidic centre.

This work aims to improve the reported synthetic route of BINOL derived phosphinic acids, fluorinated at the α-position. It is proposed that such phosphinic acids will be more acidic and thus serve as better catalysts. The new synthetic route, Scheme 2, will be used to target a small library of novel phosphinic acids for applications in asymmetric catalysis. The route consists of two novel steps. One circumvents three steps with low atom economies in the original synthetic route, previously published by Mikami *et al.*^{25, 49} Another is a novel substitution reaction at the 3,3'-positions of the fluorinated esters to target a small library of catalysts with large substituents. Another novel aspect to this synthesis are the fluorination reactions of a phosphinic ester, which has not yet been fluorinated in the literature.

Both previously published synthetic routes towards racemic compound **59** consist of three steps with a low atom economy^{25, 49} and utilise solvents with a negative environmental impact, such as tetrachloroethylene, which is a required solvent for the synthesis of compound **54**, Scheme 2. Thus, to improve the overall atom economy of the synthesis of **59**, the synthetic route depicted in Scheme 2 is proposed.

Scheme 2 - The synthetic route for the synthesis of phosphinic acids **59**. The red arrow indicates the proposed methodology to circumvent three reaction steps. A novel substitution reaction at the 3,3' position of phosphinic ester **57** is also shown.

Scheme 2 shows the proposed synthetic route towards the chiral phosphinic catalysts **59** for use in asymmetric catalysis. The proposed synthetic route eradicates the three previously published^{25, 49} environmentally harmful steps with poor atom economy, indicated by the red curly arrow. The previous synthetic route towards the fluorinated phosphinic acid catalyst **59** also employed the radical initiator AIBN (2,2'-azobisisobutyronitrile), an explosive with a flashpoint of 50°C. The proposed synthetic route avoids the use of this compound, despite the step being relatively fast. The novel step proposed by the curly arrow in Scheme 2 utilises *n*-BuLi, chelated and activated by TMEDA (tetramethlethylenediamine) as a deprotonating complex, prior to the *in situ* formation of the 7-membered

phosphorous ring to obtain ethyl-2,2'-bis(methylene)-1,1'-binaphthyl phosphinate **56** directly from 2,2'-dimethyl-1,1'-binaphthyl **53**. Adding bulky substituents, and thus steric hinderance, to the phosphinic acids at the 3,3'-positions has the potential to create more enantio-selective/successful asymmetric catalysts. The proposed novel LICKOR step from compounds **57** to **58** applies Schlosser's base²³ as a deprotonating reagent at the 3,3'-positions of (*R*)-ethyl 2,2'-bis(difluoromethylene)-1,1'-binaphthyl phosphinate compound **57**, prior to the addition of large substituents; in order to add steric hindrance to the catalysts. The substituents targeted have similarities to the structure of TRIP **8b.**⁵⁰

2.8 Results and discussion

2.8.1 Synthesis of (R)-2,2'-bistriflate-1,1'-binaphthyl, 2

The synthesis of the chiral Brønsted acid catalyst, phosphinic acid **59** via the proposed novel synthetic route was instigated by the synthesis of compound **52** from 1,1'-bi-2-naphthol (BINOL), **51**, following literature procedures, ⁵¹ Scheme 3. The product was obtained as white crystals (100%). Analysis of the $^{19}F\{^1H\}$ NMR spectrum showed one sharp singlet at δ –74.45, providing initial evidence of successful synthesis, as this correlated to the literature chemical shift value for **52**. ²⁵ The 1H NMR spectrum also provided further evidence that compound **52** had been successfully synthesised and isolated as the data closely matched the literature value of δ –74.6. ²⁵ The aromatic region of the 1H NMR spectrum of **52** is shown in Figure 16.

Scheme 3 - The synthetic route towards (R)-2,2'-bistriflate-1,1'-binaphthyl, 52.

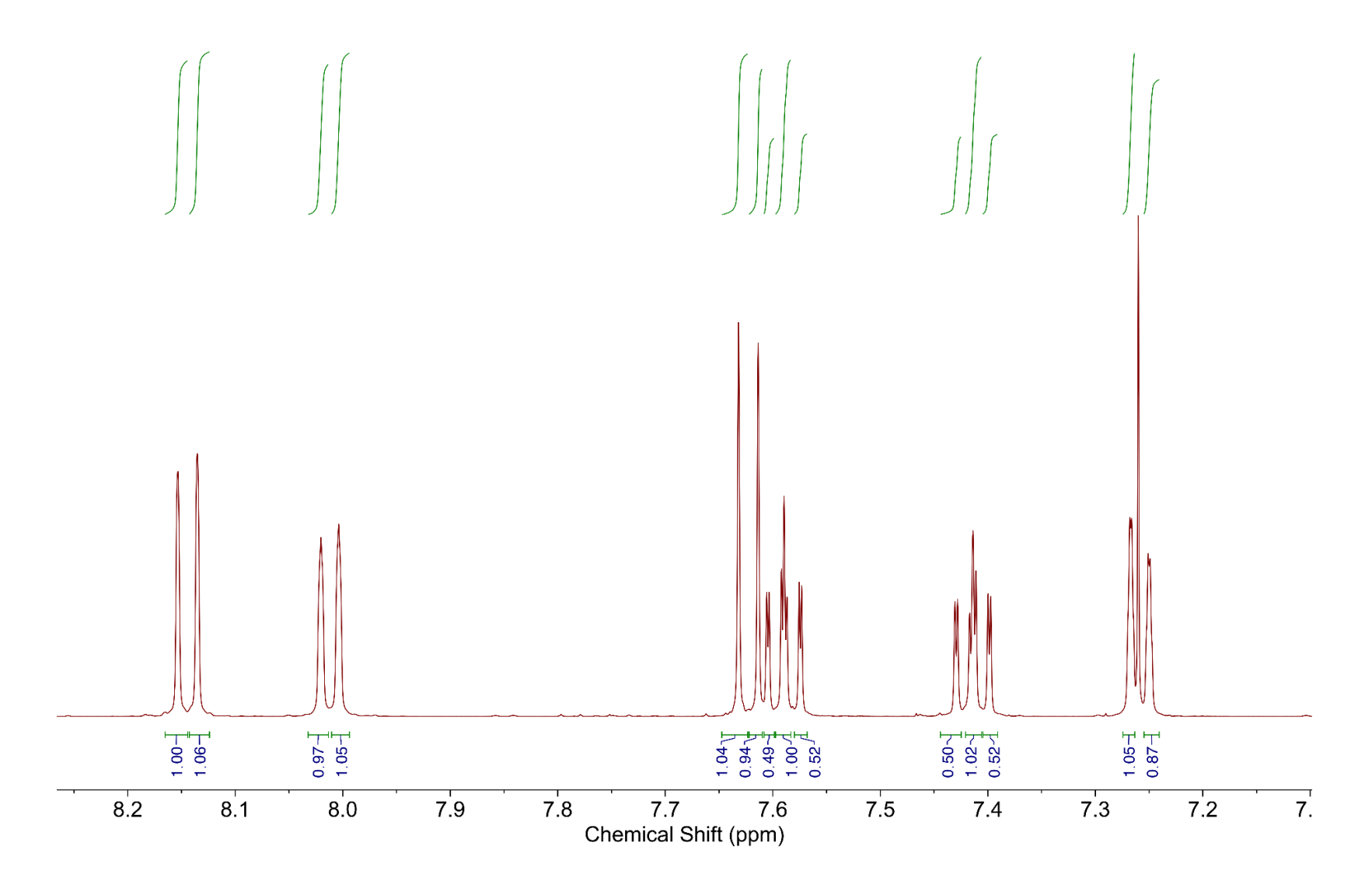


Figure 16 - 1 H NMR spectrum of (R)-2,2'-bistriflate-1,1'-binaphthyl, **52**.

The six environments identified in Figure 16 correspond to the six unique aromatic protons of **52**, the labelling scheme for which is shown in Figure 17.

$$H_d$$
 H_e
 H_f
 R
 H_b
 H_a
 OTf

Figure 17 - ¹H environments of compound **52**.

The aromatic signals correctly integrate to 12 protons, with H_b being the most deshielded, and hence, downfield at δ 8.15. H_b is observed as a doublet with a 3J coupling of 5 Hz. From the 1H - 1H COSY NMR spectrum obtained, Figure 18 shows a cross peak is observed that links this environment to a signal at δ 7.62. This signal is H_a ,and is observed as a doublet. The coupling is reciprocal to that of H_a . H_b is more deshielded than H_a because of the mesomeric effect of the triflate, which results in H_a being more shielded than H_b .

Further evidence for these assignments is obtained from the 1H NMR NOESY spectrum, Figure 19. H_b possesses two through-space cross peaks to H_a and to another signal at δ 8.01. The latter is H_c . H_c presents as a doublet with 3J coupling of 10 Hz. The doublet multiplicity results from the coupling that exists with the protons in the adjacent environment. It possesses a cross peak in the 1H - 1H NMR COSY to a signal at δ 7.59, which is assigned as H_d . H_d possess a cross peak to another signal at δ 7.40 (H_e), with this signal showing a further cross peak to a doublet at δ 7.26 (H_f). The two triplets at δ 7.59 and δ 7.40 are indicative of protons in the environments H_d and H_e and are due to the similar 3J coupling

magnitudes to the two nuclei adjacent to them. The cross peaks observed in the $^1\text{H-}^1\text{H}$ COSY and ^1H NOESY NMR data obtained, Figure 18 and Figure 19 respectively, enabled the assignment of similar proton environments, such as the triplets for H_d and H_e , to be distinguished.

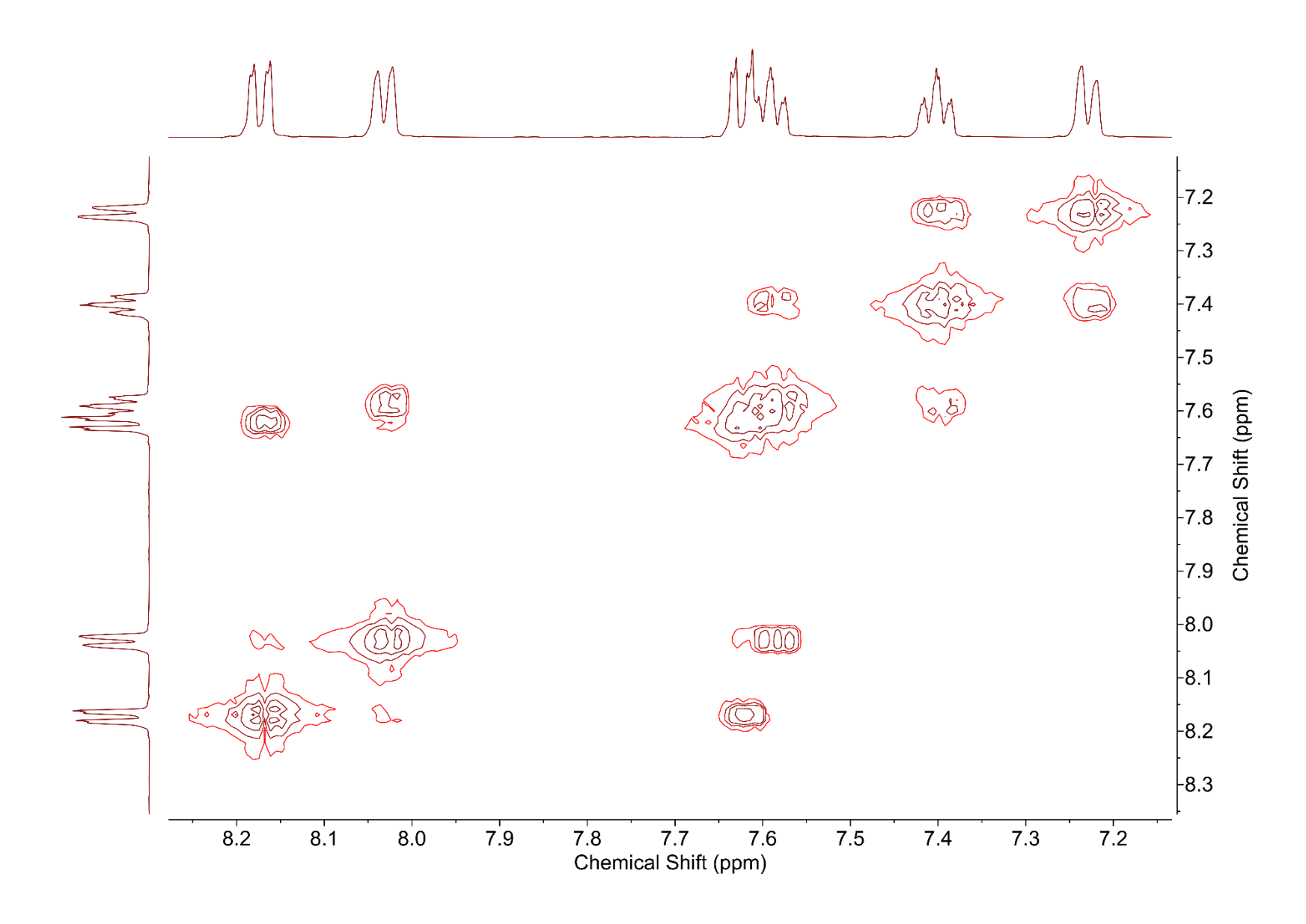


Figure 18 - ¹H-¹H COSY NMR spectrum of compound **52**.

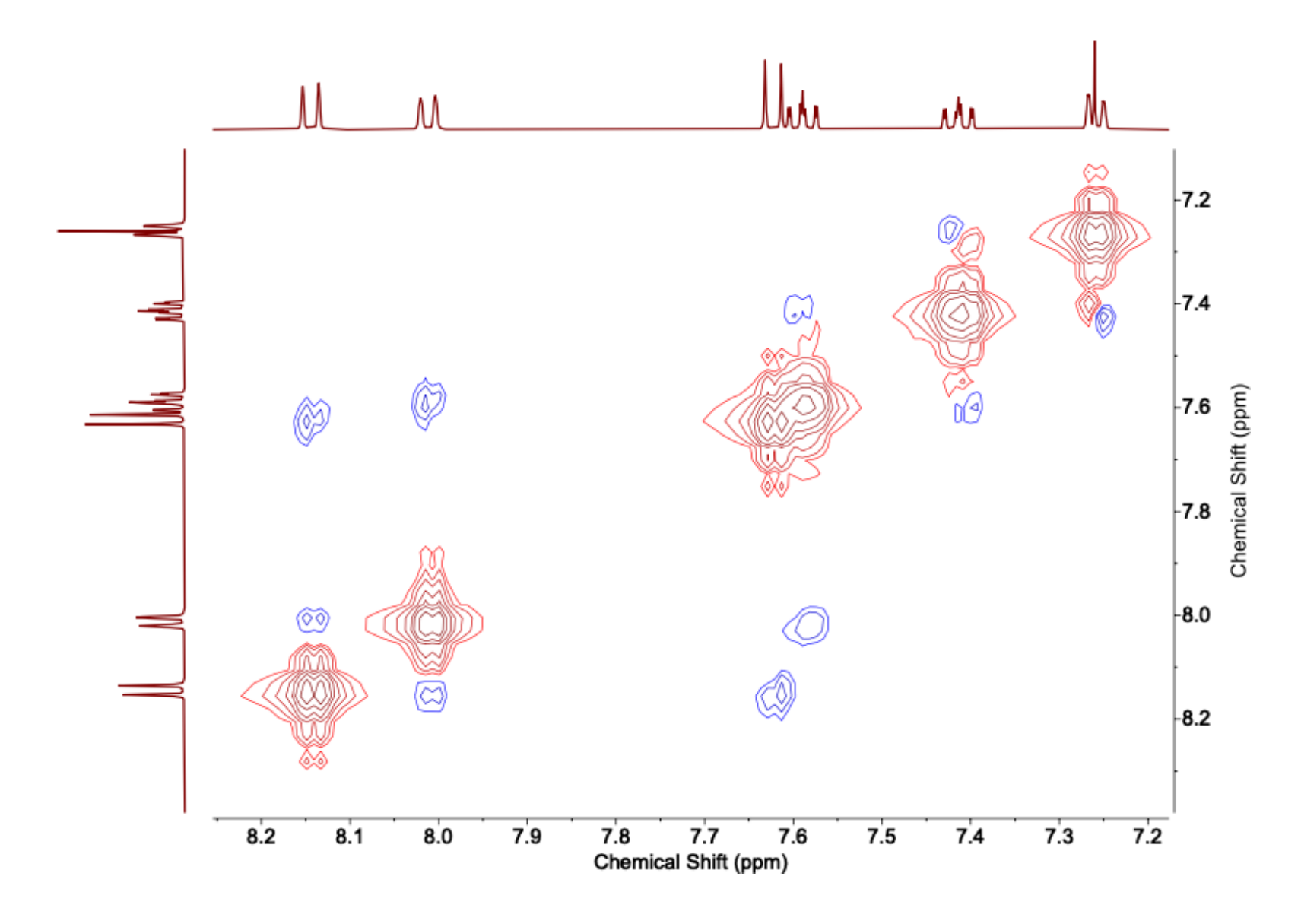


Figure 19 - ¹H NOESY NMR spectrum of compound **52**.

The doublet signal at δ 7.25 shows spatial coupling to the triplet at δ 7.42, indicative of the protons H_f to H_e . That triplet representing H_e also spatially couples to the triplet at δ 7.59, showing the protons in the H_d environment. The cross peak environment seen between the δ 7.59 triplet and the δ 8.01 doublet shows the H_d and H_c coupling. Crucially, the doublet at δ 8.01 is confirmed to be representative of the protons in H_c due to the spatial coupling to the doublet at δ 8.14, environment H_b , that cannot be seen from the $^1H_-^1H$ COSY data obtained. The H_b environment itself also couples spatially to H_a at δ 7.62, which shows no further spatial homonuclear coupling thus confirming the specific peak assignments.

The synthesis of compound **52** was determined to be successful as the data obtained all correlated to the literature.⁵²

2.8.2 Synthesis of (R)-2,2'-dimethyl-1,1'-binaphthyl, 3

Compound **52** was converted to the compound (*R*)-2,2'-dimethyl-1,1'-binaphthyl, **53**, *via.* a Kumada cross-coupling reaction, following an adaptation of the literature procedure, Scheme 4.²⁵

Scheme 4 - The synthetic route towards (R)-2,2'-dimethyl-1,1'-binaphthyl, 53.

The triflate substituents of **52**, at the 1,1' positions, were employed as they are relatively good leaving groups for this conversion. Following the reaction of **52** with methyl magnesium iodide/bromide (MeMgI/Br), catalysed by Ni(dppp)Cl₂ (dppp = (diphenylphosphino)propane), a white solid was obtained (100%) from which single crystals were grown, using a minimum amount of ethyl acetate. The ¹H NMR spectrum for compound **53**, Figure 20, provides evidence that the synthesis of **53**, was successful.

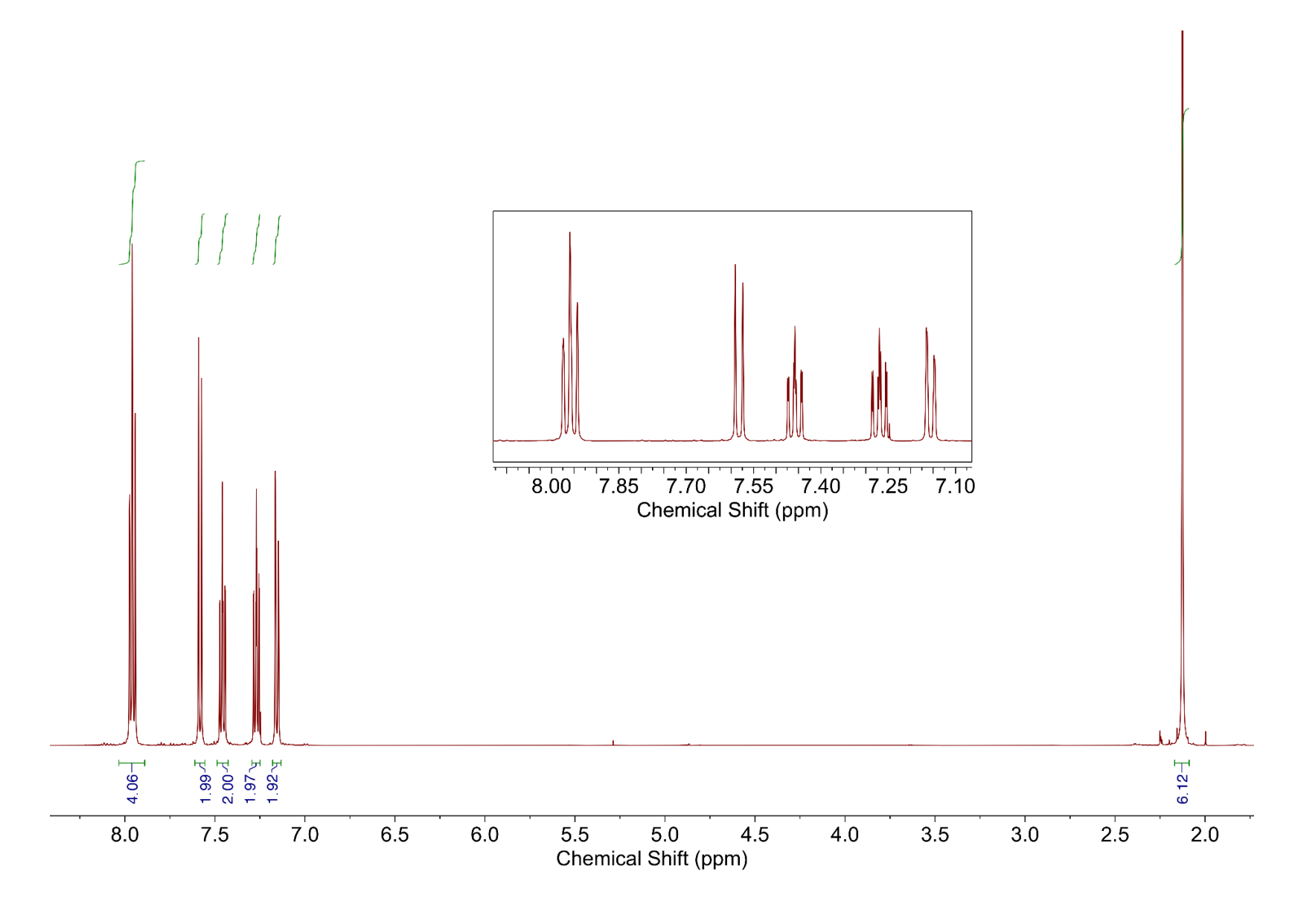


Figure 20 - 1 H NMR spectrum of (R)-2,2'-dimethyl-1,1'-binaphthyl, **53**.

The 1 H NMR spectrum for compound **53**, Figure 20, shows a sharp singlet at δ 2.13, integrating to six protons against the 12 in the aromatic region. This sharp singlet represents the six protons in the two methyl groups, H_g Figure 21, below.

Figure 21 - Proton environment labelling for compound 53.

The aromatic region of the spectrum, Figure 20, correctly integrates to 12 protons and has been shown as an insert to better showcase the chemical shift changes of these proton environments relative to those shown in Figure 16 for compound **52**. The aromatic environments responsible for the most downfield singlet at δ 7.96 are H_b and H_c. The ¹H NMR spectrum aromatic peaks for compound **53** follow the same chemical shift order as compound **52**, though they are more up-field in comparison as they are not as deshielded. Interestingly, the most down-field peak at δ 7.96 is a triplet, despite other examples in literature quoting multiplets.^{25, 49} Theoretically, this environment should exist as a doublet of doublets since ³Jhh and ⁴Jhh coupling is possible. Since the ⁴Jhh coupling may be too small to be observed, it presents as a multiplet. The triplet environment does, however, match other examples in the literature.⁵²

The crystal structure for compound **53** was obtained by growing crystals from the crude material by slow evaporation from CH₂Cl₂. The ball and stick representation of **3** is shown in Figure 22 and Figure 23.

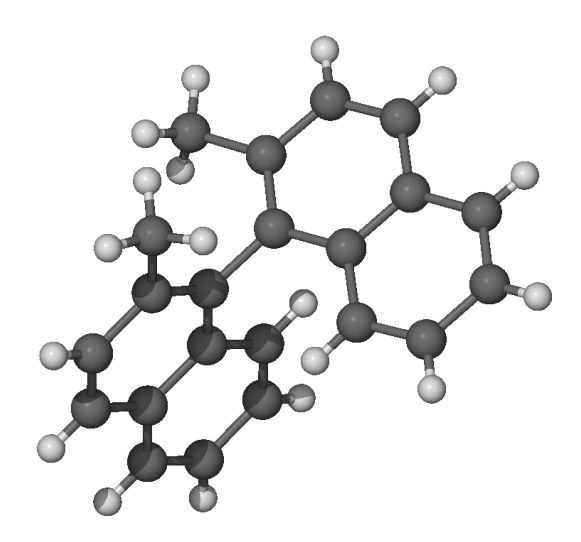


Figure 22 - Crystal structure obtained of compound **53**.

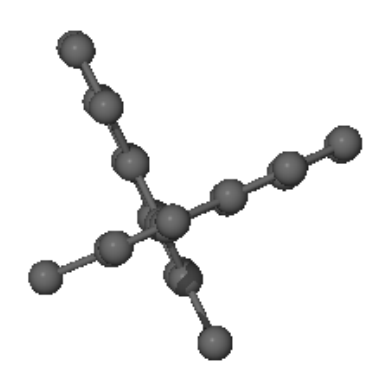


Figure 23 - Different perspective of compound **53** showing emphasis on angles of atropisomer.

Although reported previously in the literature,⁷ the crystal structure obtained herein has crystallised in a different space-group ($C_2/_c$ instead of $P2_1$) and consists of eight molecules in the unit cell (instead of four). The two naphthalene rings are almost at 90 degrees to one another, with the torsion angle between the two rings being measured at -92.9 degrees. The increased torsion angle, relative to **56** and

59 is due to the lack of a seven membered ring constraining the aromatic rings. As such, the naphthalene rings are almost perpendicular to one another.

The crystal structure, alongside the other data obtained, provides sufficient evidence that compound **53** was successfully synthesised and isolated for use in the novel synthetic reaction trials towards compound **56**.

2.8.3 Novel synthetic step towards (*R*)-ethyl-2,2'-bis(methylene)-1,1'-binaphthyl phosphinic acid.

The synthesis of (*R*)-ethyl-2,2'-bis(methylene)-1,1'-binaphthyl phosphinic acid recently published consists of multiple steps with low atom economies and utilises combinations of explosive and restricted reagents.²⁵ To circumvent three of these steps, a novel reaction is proposed, indicated by the red arrow in Scheme 2 and showcased in Scheme 5.

Scheme 5 - Proposed novel synthetic step of (*R*)-ethyl-2,2'-bis(methylene)-1,1'-binaphthyl.

The initial deprotonation step builds on the *n*-BuLi (*n*-butyllithium)

/TMEDA(*N*,*N*,*N*',*N*'-tetramethylethylenediamine) -mediated lithiation work by

Collum *et al.* in 2000.⁵³ Though the group have published multiple single crystal structures of the *n*-BuLi/TMEDA complexes that can be isolated, one of the simplest complexes isolated is shown in Figure 24.

Figure 24 – Reported structure of the n-BuLi/TMEDA dimer isolated as a single crystal by Collum *et al.* in 2000.⁵³

Though Collum *et al.* isolated single crystals of the *n*-BuLi/TMEDA complexes, Engelhardt and co-workers went on to report the use of these complexes to deprotonate (*S*)-53, and successfully isolated single crystals of the complexes depicted in Figure 25.⁵⁴ The novel synthetic reaction from compound 53 to 56, builds on this work by initially synthesising the *n*-BuLi/TMEDA deprotonated complexes of 53 (compound 61, Figure 25), prior to the *in-situ* formation of the seven-membered phosphorous containing ring of compound 56, using ethyldichlorophosphate, Scheme 5.

Figure 25 - Dilithiated (*S*)-binaphthyl intermediate complexes previously published by Engelhardt *et al*.⁵⁴

The *in-situ* reaction proposed (Scheme 5), avoided the isolation of the complexes $\bf 61-62$ as crystals under inert conditions. Following the deprotonation step, it was hypothesised that an S_N2 reaction would then occur between the dilithiated binaphthyl intermediate $\bf 61$ and the electrophile ethyldichlorophosphate $\bf 63$ to obtain the heterocycle $\bf 56$, as shown in Figure 26.

Figure 26 - The proposed mechanism for the novel, direct conversion of compound **53** to **56**.

The proposed reaction required completely dry, inert conditions to avoid the reprotonation of **61** back to the starting compound **53** with the contamination of water. The initial reaction trials and recordings are summarised in Table 1.

Table 1 - Initial trials of novel esterification reaction for compounds 53 to 56.

Entry	Chirality	Scale	Reactant order	Equivalence	Solvent	Temperatures and timings	Observations	Result
1	Racemic	7.4 mg	i.) <i>n-</i> BuLi to THF, 5 3 in THF followed	2.4 eq. <i>n</i> -BuLi to 53	1 mL THF (from cabinet)	i.) 0 C for 18 hrs	Yellow solution throughout	No correct ³¹ P NMR peak
			by TMEDA	2.4 eq. TMEDA		ii.) -68 C to 0 C 10 hrs	reaction	¹ H NMR contaminated
			ii.) 63	1.1 eq. 63				5 3
2	(R)	5.4 mg	1.) <i>n-</i> BuLi to	2.4 eq. <i>n-</i> BuLi	1 mL THF	i.) 0 C for 3 hrs	Yellow	No correct ³¹ P
			THF	to 5 3	(bottled)	ii.) -68 C for 10	solution throughout	NMR peak
			2.) R)-5 3 in THF	2.4 eq. TMEDA.		minutes before room temp. 12 hrs	reaction	¹ H NMR indicates 5 3 remained
			3.) TMEDA	1.1 eq. 63		1115		remained
			4.) 63					
3	Racemic	65.3 mg	i.) <i>n</i> -BuLi to THF, 5 3 in THF followed	2.4 eq. <i>n</i> -BuLi to 5 3	THF (12 mL) (bottled)	i.) 0 C 1.75 hrs ii.) -68 C to	Orange solution turned yellow on	New ³¹ P NMR peak at 58 and 46 ppm.
			by TMEDA	2.41 eq. TMEDA		room temp. for 12 hrs	addition of TMEDA	¹ H NMR
			ii.) 63					mostly
				1.1 eq. 63				contaminated 5 3
4	Racemic	74.4 mg	i.) <i>n-</i> BuLi to THF, 5 3 in THF, TMEDA	2.4 eq. <i>n</i> -BuLi to 5 3	6 mL THF (bottle stored over mol	i.) 0 C 10 mins, TMEDA 3 hrs, 0 C	Very deep red to colourless on addition of	Many new ³¹ P NMR peaks between 10
			ii.) 63	2.41 eq. TMEDA	sieves)	ii.) -78 C addition of 63 ,	TMEDA. Cloudy yellow ppt. produced.	and 17 ppm (possible

				1.1 eq. 63		room temp. 18 hrs		mono substitution)
								¹ H NMR showed mostly contaminated 5 3
5	Racemic	77.1 mg	i.) <i>n-</i> BuLi to THF, 5 3 in THF, TMEDA	2.4 eq. <i>n</i> -BuLi to 5 3	6 mL THF (cabinet)	i.) 0 C for 10 mins, TMEDA 0 C 2 hrs, 20	Colourless to deep red in 10 mins. Pale	³¹ P NMR peaks at 4 and 8 ppm (63)
			ii.) 63	2.41 eq. TMEDA		C for 1 hr.	yellow on addition of 63 .	¹ H NMR
			11. / 00	TWEDA		ii.) -78 C	addition of oo.	shows mostly
				1.1 eq. 63		addition of 63 , RT 15 hrs		5 3 .

The initial reaction trials were conducted using both racemic and chiral compound **53**, on a very small scale, 5-7 mg. Though the dilithiation step was based on the work of Engelhardt *et al.*,⁵⁴ changes were made to the method to improve the safety of this procedure. A notable change to the method⁵⁴ was to not remove the hexane from the *n*-BuLi, as this avoided heating the pyrophoric compound and is more recently the set precedent in the literature. Scaling up the reaction ten-fold appeared to provide a more successful deprotonation step, indicated by the colour changes of the reaction mixtures; which were more closely correlated with the crimson red dilithiated crystals synthesised by Engelhardt *et al.*⁵⁴ The most promising result from these initial trials, Table 1, was entry 3, as the crude product showed a peak at 58 ppm in the ³¹P NMR spectrum, which is in an appropriate region expected for binaphthyl-based phosphinic esters.^{25, 49} This could have resulted from using a slight excess of TMEDA to *n*-BuLi. Further reaction trials are summarised below in Table 2.

Table 2 - Further reaction trials of the novel esterification reaction from racemic compound **53** to **56**.

Entry	Reagent preparations	Scale	Reactant order	Equivalence	Solvent	Temperatures and timings	Observations	Result
1	n-BuLi titrated TMEDA and 63 distilled	79.4 mg	i.) <i>n</i> -BuLi to THF, 5 3 in THF, TMEDA ii.) 63	2.4 eq. <i>n</i> -BuLi to 5 3 2.41 eq. TMEDA 1.1 eq. 63	12 mL THF (cabinet)	i.) 0 C for 4.5 hrs ii.) -78 C overnight	i.) Yellow solution ii.) White ppt. formed.	³¹ P NMR 2.5-5 ppm peaks only. ¹ H NMR mostly 5 3
2	TMEDA and 63 distilled	67.8 mg	i.) 5 3 in THF, <i>n</i> -BuLi, TMEDA ii.) 63	2.4 eq. <i>n</i>-BuLi to 53,2.41 eq. TMEDA63 1.1 eq.	12 mL THF (cabinet)	53 dissolved in THF,15 min stir. n-BuLiadded at -78 C stirred1 hr.TMEDA 0 C to RTovernight63 at 0 C for 4 hrs	i.) Deep red until TMEDA added, changed to pale yellow for remainder of reaction.ii.) White ppt. formed.	Starting material only recovered.
3	TMEDA refluxed over greying LiAlH ₄ , distilled immediately before use 63 distilled before use	70.5 mg	i.) 53 dissolved in THF, <i>n</i> -BuLi, TMEDA ii.) 63	2.4 eq. <i>n</i> -BuLi to 5 3 , 2.41 eq. TMEDA 1.5 eq. 63	THF (12 mL, cabinet)	i.) -78 C for <i>n</i> -BuLi addition, 5 hrs, 0 C for TMEDA addition, 6 hrs. ii.) 0 C 63 addition, overnight	 i.) Solution pink on <i>n</i>-BuLi addition, deep red with TMEDA. ii.) Yellow solution prior to addition of 63. 	³¹ P NMR peaks at -13 to -8.5 ppm ¹ H NMR starting reagents
4	THF over mol sieves overnight. n-BuLi & TMEDA (new stock)	74.5 mg	i.) 53 in THF, n-BuLi followed by TMEDA (×2) ii.) 63	2.4 eq. <i>n</i> -BuLi to 5 3 , 4.85 eq TMEDA 1.1 eq. 63	THF (12 mL)	i.) -78 C ii.) -78 C for 63 addition. Left to reach RT overnight.	Yellow solution to deep red on addition of TMEDA. Yellow solution prior to 63 addition. White ppt. produced.	³¹ P NMR peaks at -8.5 to -4. ¹ H NMR shows contaminated starting material.

5	THF over mol sieves overnight.	78.8 g	i.) 5 3 in THF, <i>n</i> -BuLi, TMEDA.	2.4 eq. <i>n</i> -BuLi to 5 3 , 2.41 eq. TMEDA	THF (12 mL)	i.) -78 C until TMEDA added, warmed to 0 C.	i.) Yellow solution to deep red as temp. increased from -78 C to	³¹ P NMR peak at 49.4 ppm
	<i>n</i> -BuLi & TMEDA (new stock)		ii.) 63	1 eq. 63		ii.) 63 added at 0 C	0C.	¹ H NMR shows mostly 5 3
	(o., etcok)		, ••	. 54. 🕶		, 55 44454 41 6 6	ii.) Orange to deep yellow solution.	recovered.

The results summarised in Table 2 show the reaction trials in which both the reactant order and preparations were altered. To avoid the use of a secondary vessel, in which the dimethyl substituted compound **53** was dissolved in THF prior to addition, and potential air exposure during transfer, the reaction vessel was initially charged with compound **53** under an argon atmosphere. This resulted in an accelerated colour change of the solution to deep red instantaneously. This suggested that the deprotonation of **53** was initially more successful, before the addition of TMEDA which immediately turned the solution yellow, indicative of reprotonation, since the reaction trial resulted merely in starting material recovery.

The negative result of the reaction trial, Table 2, entry 2, suggested that the TMEDA utilised was potentially contaminated with water. Therefore the TMEDA was heated to reflux over the drying agent LiAlH₄ (lithium aluminium hydride) and distilled immediately prior to use for the remaining reaction trials. Adjustments to the equivalence of ethyldichlorophosphate 63 were also made, as shown for Table 2, entry 3, from 1.1 eq. to 1.5 eq. Although this reaction trial resulted in the recovery of starting material, this may also have been due to the reaction mixture becoming contaminated with water, as the solution had returned to yellow prior to the addition of ethyldichlorophosphate. Further novel cyclisation reaction trials testing reaction concentrations are summarised in Table 3.

.

Table 3 - Novel cyclization esterification reaction trials in which reaction concentrations were altered

Entry	Reagent preparations	Scale	Reactant order	Equivalence	Solvent	Temperature and timings	Observations	Result
11	As previous	77.9 mg	i.) 5 3 in THF, <i>n</i> - BuLi, TMEDA ii.) 63	2.4 eq. <i>n</i> -BuLi, 2.41 eq. TMEDA, 1 eq. 63	THF (12 mL)	i.) -78 C and 10 min stir prior to TMEDA. 45 mins before warmed to 0 C. ii.) 0 C addition of 63, 3hrs 10mins.	Solution pink with <i>n</i> -BuLi, deep red as warmed to 0 C with TMEDA. Orange on addition of 63 to yellow solution as quenched.	³¹ P NMR peaks at 58.45, 49.53, 35.70, 33.34. ¹ H NMR shows mostly 5 3 . Isolation unsuccessful
12	As previous	74.4 mg	i.) 5 3 in THF, <i>n</i> - BuLi, TMEDA ii.) 63	2.4 eq. <i>n</i> -BuLi, 2.41 eq. TMEDA, 1 eq. 63	THF (6 mL)	i.) -78 C and 10 min stir prior to TMEDA. 45 mins before warmed to 0 C. ii.) -78 C addition of 63, left overnight at room temperature.	Pink solution with <i>n</i> -BuLi, deep red as warmed to 0 C with TMEDA. Orange on addition of 63 to yellow solution as quenched.	³¹ P NMR peaks at 58.47 and 33.34 ppm ¹ H NMR shows mainly starting material recovery and minor evidence of peaks between 3 & 4 ppm.
13	<i>n</i> -BuLi titrated. Conc. 2.23 M	59 mg	i.) 53 in THF, <i>n</i> - BuLi, TMEDA ii.) 63	2.4 eq. <i>n</i> -BuLi, 2.5 eq. TMEDA, 1.1 eq. 63	THF (2 mL)	i.) 10 mins stir at - 77 C prior to TMEDA. 30 mins stir before warmed to 0 C. ii.) 63 added at 0 C, 15 hrs	Orange solutions that turned yellow upon addition of 63 .	¹ H NMR starting material only
14 (<i>R</i>)	As entry 13	65.3 mg					Orange solutions that turned yellow upon addition of 63 . Formed white ppt	³¹ P NMR 58.46, 49.56 and 33.34 major peaks. ¹ H NMR .contaminated 63 (3 to 4 ppm).

The ³¹P{¹H} NMR spectra of the crude material from the reaction trials, Table 3, resulted in mixtures of compounds consisting of multiple phosphorous environments. These may have been caused by side reactions such as monosubstitutions, or multiple substitutions at the same carbon site. Due to the ¹H NMR spectra providing evidence of significant amounts of starting material remaining present, the reaction trials were amended in order to attempt to push the desired novel reaction to completion. The concentration of the reaction mixture was increased by using less solvent, from 12 mL to 2 mL. The more concentrated reaction mixtures appeared to show more frequent signs of cyclisation success in comparison with the more dilute trials.

To also ensure that the correct amount of *n*-BuLi was utilised for sufficient deprotonation, the accurate concentration was determined by titrating the solution against *n*-benzylbenzamide, following a procedure adapted from the literature.⁵⁵ The concentration was found to be 2.23 M instead of the 2.5 M stated by the manufacturer and so the amounts used were required to be altered. The *n*-BuLi was titrated regularly to avoid this in future reaction trials. The *n*-BuLi equivalence used was also increased to 2.5 eq. and the TMEDA equivalence was adjusted accordingly. The reaction trials summarised in Table 3 indicated that more concentrated reaction mixtures produced better results as more trials resulted in phosphorous environments in the expected chemical shift region in the ³¹P NMR spectra and had TLC spots with the expected R_f of 0.4 in EtOAc.⁴⁹ Isolation attempts from these crude materials by manual column chromatography; automated chromatography and dry flash column chromatography, ⁵⁴ eluting with EtOAc was unsuccessful and resulted in loss of the desired product.

Another example of the dillithiation of compound **53** in literature⁵⁴ utilised diethyl ether (Et₂O) as the reaction solvent. This was incorporated into reaction trials carried out in duplicate for both the racemic and chiral **53** and are summarised in Table 4.

Table 4 – Reaction conditions for using Et₂O as a reaction solvent for the novel cyclisation esterification step.

Entry	Scale	Equivalence	Solvent	Reactant Order	Temperature and timings	Observations	Results
14 (rac)	17.2 mg	2.4 eq. <i>n</i> -BuLi, 2.41 eq. TMEDA, 1.1 eq. 63	THF (2 mL)	i.) 5 3 , solvent, <i>n</i> - BuLi, TMEDA ii.) 63	i.) -78 C for addition of <i>n</i> -BuLi to vessel, warmed to 0 C after TMEDA addition for remainder of reaction.	Yellow solution to red with n-BuLi, to dark brown with TMEDA Dark yellow after 63 . White ppt. formed	³¹ P NMR many peaks from 58 ppm to 0 ppm ¹ H NMR possesses starting material signals and evidence of reaction success with peaks between 4 & 3 ppm
15 (<i>R</i>)	12.9 mg	2.4 eq. <i>n</i> -BuLi, 2.41 eq. TMEDA, 1.1 eq. 63	THF (2 mL)	i.) 5 3 , solvent, <i>n</i> - BuLi, TMEDA ii.) 63	i.) -78 C for addition of <i>n</i> -BuLi to vessel, warmed to 0 C after TMEDA addition for remainder of reaction.	Yellow solution to orange with <i>n</i> -BuLi to deep red with TMEDA. White ppt. formed.	³¹ P NMR peak at 58.51 ppm ¹ H NMR shows mostly starting material but some peaks between 3 & 4 ppm.
16 (rac)	11.1 mg	2.4 eq. <i>n</i> -BuLi, 2.41 eq. TMEDA, 1.1 eq. 63	Et ₂ O (2 mL)	i.) 53, solvent, <i>n</i> - BuLi, TMEDA ii.) 63	i.) -78 C for addition of <i>n</i> -BuLi to vessel, warmed to 0 C after TMEDA addition for remainder of reaction.	Yellow solutions to orange with <i>n</i> -BuLi and TMEDA. Slower for Et ₂ O	³¹ P NMR many peaks from 58.46 to -5 ppm. ¹ H NMR shows mainly starting material recovered and peak at 3 ppm missing.
17 (<i>R</i>)	12.9 mg	2.4 eq. <i>n</i> -BuLi, 2.41 eq. TMEDA, 1.1 eq. 63	Et ₂ O (2 mL)	i.) 53, solvent, <i>n</i> - BuLi, TMEDA ii.) 63	i.) -78 C for addition of <i>n</i> -BuLi to vessel, warmed to 0 C after TMEDA addition for remainder of reaction.	Yellow solutions to orange with <i>n</i> -BuLi with TMEDA. Slower deep orange colour change for Et₂O.	 31P NMR no product peaks 1H NMR starting material recovered only.

The reaction trials utilising Et₂O as solvent, entries 3 and 4 in Table 4, proved to be less successful in comparison to the reaction trials using THF, entries 1 and 2 in Table 4. Not only was the second cyclisation step unsuccessful, resulting in mostly starting material recovery, the initial deprotonation step was also significantly slower than the deprotonation step using THF. This was indicated by the lack of colour change from yellow to deep crimson red. The Et₂O trials changed to deep orange for the deprotonation step, despite being left overnight, in comparison to the THF trials which turned deep crimson over 2-3 hours.

Therefore, THF was deemed the best solvent to continue with due to the much faster deprotonation indication from this deep red colour change during the deprotonation step.

For the following final reaction trials, summarised in Table 5, the order of reactants added were altered to add TMEDA to the reaction vessel prior to the addition of n-BuLi, as this has shown precedence in the literature. Table 5 shows the increase of reaction scale from 85 mg, entry 1, to over 1 gram, entry 6. The results summarised below show more successful results as the scale was increased from 85 mg to 476 mg, entries 1 to 4, though on a 1 g scale, the ¹H NMR spectrum did not have the necessary signals at 3 ppm and 1.39 ppm, representative of successful cyclisation.^{25, 49}

Table 5 – Reaction scale, and order of addition, for the novel cyclisation step towards compound **56**.

Entry	Scale	Reactant order	Equivalence	Temperatures and timings	Observations	Results
1 (racemic)	85.5 mg	53 in THF (0.4 mL), TMEDA, <i>n</i> -BuLi	2.4 eq. TMEDA, 2.4 eq. <i>n</i> -BuLi, 1.1 eq. 63	i.) 53, TMEDA in THF stirred for 30 mins. Cooled to -78 C for addition of <i>n</i> -	i.) Yellow solution turned deep red on addition of <i>n</i> - BuLi	³¹ P NMR shows peaks from 59.2 to -12.33 ppm
		followed by 63		BuLi, 4 hrs.	:: \ \ \ \ \ \ \ \ \ \ \ \ \ \ \ \ \ \	¹ H NMR shows mostly 5 3
				ii.) 63 added and left overnight to stir and reach	ii.) Yellow solution on addition of 63 and creamy white ppt. formed.	TLC spot at Rf 0.4
				room temp.		Column hex to EtOAc (100-0)
						Degraded.
2 (<i>R</i>)	163.4	As entry 1 but	As entry 1	i.) 5 3 & TMEDA in THF	As entry 18	³¹ P NMR 58.39 to -8 ppm
	mg	0.45 mL THF		stirred for 1 hr 20 mins. <i>n</i> -BuLi added and stirred 1 hr prior to 63		¹ H NMR shows 3-4 ppm peaks and TLC spot at 0.4 but degraded on column.
3 (<i>R</i>)	242.0	As entry 1 but 0.5 mL THF	As entry 1	i.) 5 3 in THF, TMEDA, stirred for 1 hr, <i>n</i> -BuLi	Orange solution turned deep red on addition of n-BuLi.	³¹ P NMR 58.39 to -8 ppm
	mg	0.5 IIIE IIII		added and stirred 7 hrs prior to 63	Solution turned yellow with white ppt. formed after addition of 63 .	¹ H NMR shows 3-4 ppm peaks and correct Rf TLC spot but degraded after column 7/1 CH ₂ Cl ₂ /EtOAc.
4 (R)	475.9 mg	53 in THF (1.5 mL), TMEDA, n-BuLi followed by 63	As entry 1	i.) 5 3 , TMEDA in THF 1 hr - 78 C. i.) <i>n</i> -BuLi at -78 C to room temp. for 6 hrs 15 mins.	Deep red solution on addition of <i>n</i> -BuLi, crimson crystals formed before 63 added. White ppt. formed.	³¹ P NMR 64.62 ppm, ¹ H NMR showed 3-4 ppm product peaks before degradation on column. (CH ₂ Cl ₂ /EtOAc 7/1 to EtOAc 100%).
				ii.) 63 added at -78 C and left to reach RT overnight.		

5 (<i>R</i>)	1.029 g	i.) 53 in THF (2 mL) TMEDA, n-BuLi ii.) 63	2.4 eq. TMEDA, 2.41 eq. <i>n</i> -BuLi, 1.1 eq. 63	i.) 53 in THF 10 mins. TMEDA at -78 C, for 1 hr. <i>n</i> -BuLi added and stirred for 6.5 hrs at RT before addition of 63 .	 i.) Red solution turned crimson on addition of <i>n</i>-BuLi. ii.) Solution slowly went yellow and white ppt. 	 ³¹P NMR peak at 64.58 ppm and crude TLC spot at 0.4. ¹H NMR crude missing 3 ppm and 1.39 ppm peaks.
				ii.) 63 added at -78 C and left to reach RT overnight.	formed.	

The most successful trials in these scaling experiments were entries 3 and 4 at 242 mg and 476 mg, respectively. These trials showed signals in the ³¹P and ¹H NMR spectra in the expected region for compound **56**, as well as a spot with an R_f of 0.41 by TLC analysis using EtOAc as eluent. Notably, entry 4 formed the deprotonated crimson red crystals, similarly to Engelhardt *et al.*⁵⁴ *in-situ*. Unfortunately, all attempts to isolate **56** from these crude mixtures were unsuccessful. The trials summarised in Table 5 provide evidence that this novel cyclisation has the potential to be scaled up further.

The final trials of the novel cyclisation step toward compound **56**, testing the equivalences of reactants and reaction method, on the more successful scale of around 0.5 g, are summarised in Table 6.

Table 6 – Summary of the final novel cyclisation reaction trials.

Entry	Scale	Reactant order	Equivalence	Temperatures and timings	Observations	Results
1	500 mg	53 in 2.5 mL THF, TMEDA followed by <i>n</i> -BuLi then 63 .	2.4 eq TMEDA, 2.41 eq <i>n</i> -BuLi, 3.3 eq 13	53 in THF, TMEDA, 1 hr stir prior to <i>n</i> -BuLi addition. 63 added and stirred overnight. Second bigger portion 2.2 eq 63 added.	Orange solution turned deep red on addition of <i>n</i> -BuLi. Creamy white ppt. formed after all portions of 63 added.	Crude 1H NMR spectrum of 56 showcased, Figure 27
2	500 mg	53 in 2.5 mL THF, TMEDA followed by <i>n</i> -BuLi then 63 .	5 eq TMEDA, 5.2 n-BuLi, 5.5 eq (excess) 13	As entry 1	As entry 1 but excess 63 added as remained dark redblack overnight	³¹ P NMR peaks from 64.58 ppm -35 ppm. ¹ H NMR shows mixture of 5 3 and 5 6 .
3	500 mg	53 in 2.5 mL THF, TMEDA followed by <i>n</i> -BuLi then 63 .	10 eq TMEDA, 10.2 eq <i>n</i> -BuLi, 11.1 eq (excess) 13)	As entry 1	As entry As entry 1 but excess 63 added as remained dark red-black overnight.	³¹ P NMR peaks from 64.58 ppm -35 ppm. 1H NMR shows mixture of 5 3 and 5 6 .
4	100 mg	Hexane stripped from <i>n</i> -BuLi, TMEDA added neat, 5 3 in THF 1.5 mL)	2.4 eq TMEDA, 2.41 eq <i>n</i> -BuLi, 3.3 eq (excess) 63	<i>n</i> -BuLi stripped of hexane by heating under vacuum. TMEDA added at -78 C neat and 53 dissolved in minimum THF	White fume from red solution on addition of 63 . Yellow solution formed with lots of white ppt.	No TLC spot at Rf 0.4 in EtOAc No ³¹ P NMR peaks in correct ppm region. ¹ H NMR spectrum of 5 3 recovered.
5	100 mg	Hexane stripped from <i>n</i> -BuLi, TMEDA added neat, 5 3 in THF (2 mL)	5 eq TMEDA, 5.2 <i>n</i> -BuLi, 5.5 eq 63	n-BuLi stripped of hexane by heating under vacuum. TMEDA added at -78 C neat and 53 dissolved in minimum THF	Deep red solution turned peachy with white ppt. on addition of 63	No TLC spot at Rf 0.4 in EtOAc or ³¹ P NMR peaks in expected region. ¹ H NMR shows peaks at 3 and 4 ppm.
6	100 mg	Hexane stripped from <i>n</i> -BuLi, TMEDA added neat, 5 3 in THF (2 mL)	10 eq TMEDA, 10.2 eq <i>n</i> -BuLi, 5.5 eq 63	n-BuLi stripped of hexane by heating under vacuum. TMEDA added at -78 C neat and 53 dissolved in minimum THF	Extremely reactive on addition of 63, yellow solution turned dark brown.	No TLC spot at Rf 0.4 in EtOAc or ³¹ P NMR peaks in expected region. ¹ H NMR shows minor peaks at 3 and 4 ppm.

Table 6 shows the final and most successful trials of the novel cyclisation reaction of compound 53 to compound 56. On a 500 mg scale, the equivalences of compound **53** to TMEDA were trialled at 1:2.4, 1:5 and 1:10, with other reagents amended accordingly, shown by entries 1 to 3 respectively. These experiments resulted in a crude mixture consisting of compound 56 and compound 53. Unfortunately, the desired product could not be isolated therefore the crude data for Table 6, entry 1, is shown in Figure 27 and Figure 29. The final reaction trials in Table 6 followed the methodology by Engelhardt et al.⁵⁴ more closely, while still maintaining the novelty of carrying out the full cyclisation reaction with compound **63** *in-situ*. These reaction trials consisted of taking the extra preparation step to remove the hexane solution from *n*-BuLi prior to the reaction starting. These trials were carried out at a slightly smaller scale due to the safety risks of heating n-BuLi. After the hexane solution was removed under vacuum very carefully with heat, TMEDA solution was added neat to the remaining residue at −78°C; immediately after distillation from LiAlH₄. Compound **53** was dissolved separately in a minimum amount of THF, prior to the dropwise addition to the strongly basic solution of *n*-BuLi and TMEDA. The deprotonation steps were successful as indicated by the colour changes to the dark crimson reds, however, the cyclisation steps were not as successful as the other reaction trials following the safer methodology, since no TLC spot with R_f of 0.41 or ³¹P NMR peaks in the correct chemical shift regions could be seen from these trials. This may have been due to the extreme reactivity observed on the addition of 63, even at temperatures of -78°C, the reaction was violently exothermic and appeared to visibly degrade the reaction mixture.

2.8.3.1 The isolation trials towards pure compound 56

Following work ups consisting of a saturated ammonium chloride quench at 0°C and multiple extractions into CH₂Cl₂, isolation of **56** was attempted utilising multiple silica column chromatography and recrystallisation techniques.

Previous work by the Caffyn group⁴⁹ isolated the racemic cyclised ethyl ester **56** utilising flash silica chromatography, eluting with EtOAc, however, this could also not be replicated without the ester degrading on the silica. Short columns, dry flash columns and automated columns were trialled, using many combinations of eluents and eluent gradients in attempts to isolate the desired compound. A gradient of CH₂Cl₂/EtOAc (7/1 to 4/1) was also tested following work by Mikami *et al.*²⁵ who successfully isolated the similar methyl ester **18**. Unfortunately, this also did not result in the purified ethyl ester **56**. Following numerous unsuccessful purification attempts utilising multiple different silica gel chromatography techniques, all resulting in the degradation **56**, recrystallisation techniques were trialled.

The crude white powder from successful reaction trials were dissolved in minimum amounts of different solvents and different miscible solvent mixtures such as hexane, EtOac, CHCl₃, CH₂Cl₂, MeOH. The most successful techniques resulted in white solid being re-obtained and utilised minimum amounts of CH₂Cl₂ before the addition of hexane. Although the white solid was grown using this mixture of eluents, the two compounds **53** and **56** grew out of solution simultaneously, despite the difference in polarities. Washing the white crude solids with pentane afforded the cleanest, though impure, spectral data and single spots by TLC analysis with R_f of 0.41 in EtOAc. The ¹H and ³¹P NMR spectra from the reaction

trial summarised by entry 1, Table 6, are showcased in Figure 27 and Figure 29, below.

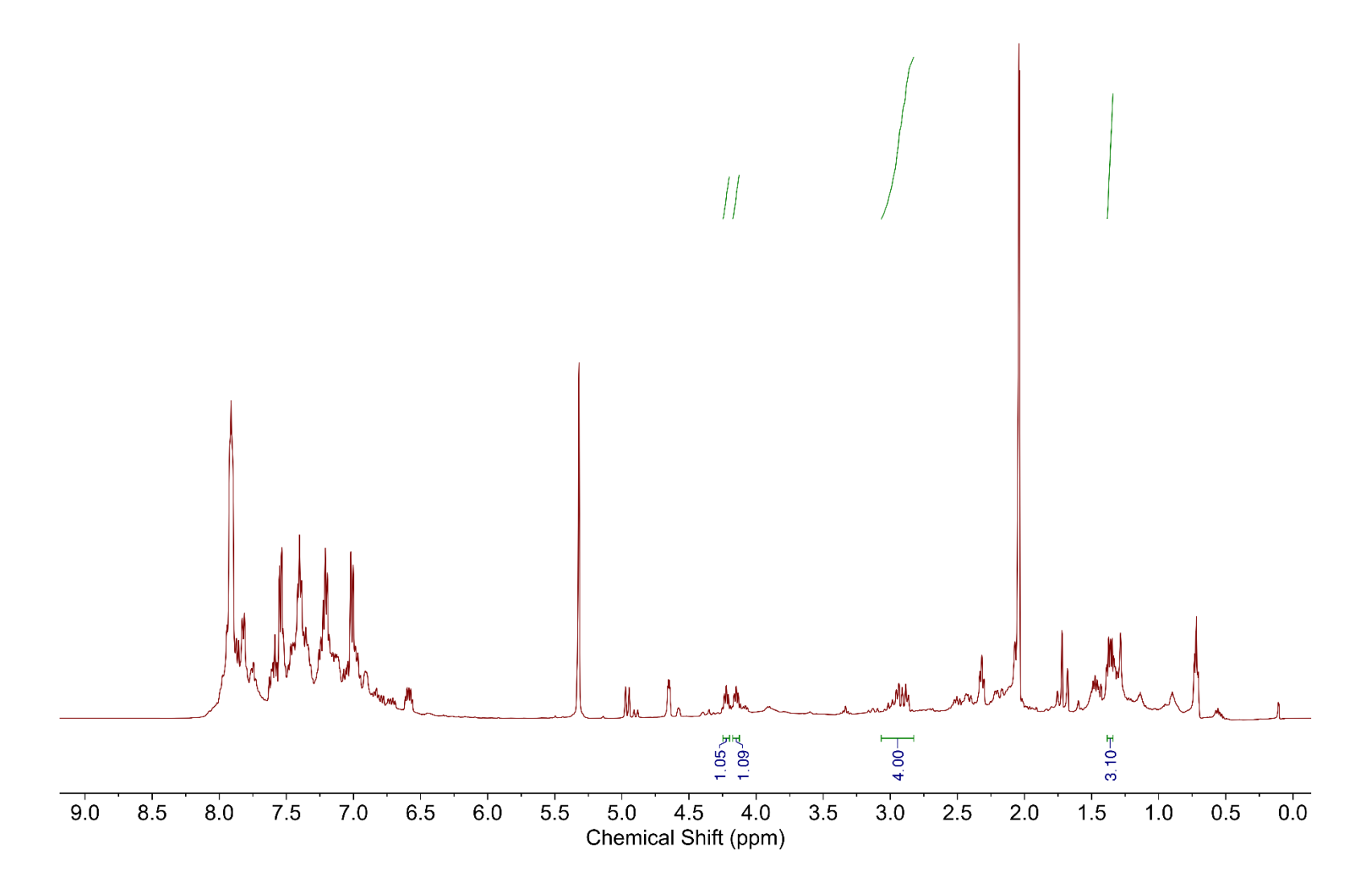


Figure 27 - ¹H NMR spectrum of (R)-2,2'-bis(methylene)-1,1'-binaphthyl phosphinic acid via novel synthetic step.

The ¹H NMR spectrum of chiral compound **56**, in CD₂Cl₂, Figure 27, provides evidence that the novel synthetic step was a success, despite the isolation being unsuccessful. The peaks of particular interest of the crude material are the integrated multiplets at δ 2.97 and δ 4.18, which are representative of the four protons in environment H_g and two ethyl protons at H_h respectively and correlate to the literature for the racemic counterpart.⁴⁹ In comparison to the ¹H NMR spectrum of the starting material for this novel step, compound 53 (Figure 20), in which there are no signals between the aromatic region and the methyl groups at δ 2.31, other than a minor one at δ 5.32 of residual CH₂Cl₂, it is evident from the existence of the multiplet at 2.97, correctly integrated to 4 protons, that the chiral compound **56** had been synthesised *via*. the novel *in-situ* cyclisation step. The methylene protons, H_g and H_h, are non-equivalent due to the restricted rotation imposed by the seven-membered ring of which both methylene carbons are part of. This results in H_g and H_h being diastereotopic and can be considered to each consist of protons in endo- and exo-orientation. These non-equivalent protons form unique couplings with protons in the spin system, namely H_a (⁴J_{HH}) and to each other due to a geminal coupling, resulting in complex coupling patterns being observed which also overlap due to the difference in chemical shift of the endoand exo-orientated protons. The methylene protons of the ethyl group (H_i) are similarly affected. However, this is not due to restricted rotation but because of the chiral centre within the molecule to which they are attached, leading to inequivalent protons being observed for this environment also.

Further evidence of the success of the novel reaction is shown by the ^{31}P NMR spectrum, Figure 29, with a sharp peak at δ 64.6, which correlates to the previously synthesised⁴⁹ racemic ester **56** at δ 64.5. Although this spectrum is particularly contaminated for a ^{31}P NMR spectrum, it disproves any queries that

the signal in the 1 H NMR spectrum at δ 4.18 is residual ethyldichlorophosphate, **63**, since there is no broad singlet at δ 6.75. Notably, this signal is representative of H_h in the 1 H NMR spectrum, which is at a different chemical shift than those for the ethyl protons of **63** (δ 4.18 compared to δ 4.44), further proving that the novel step towards chiral compound **56** was a success.

Figure 28 - Proton environments of phosphinic ester 56.

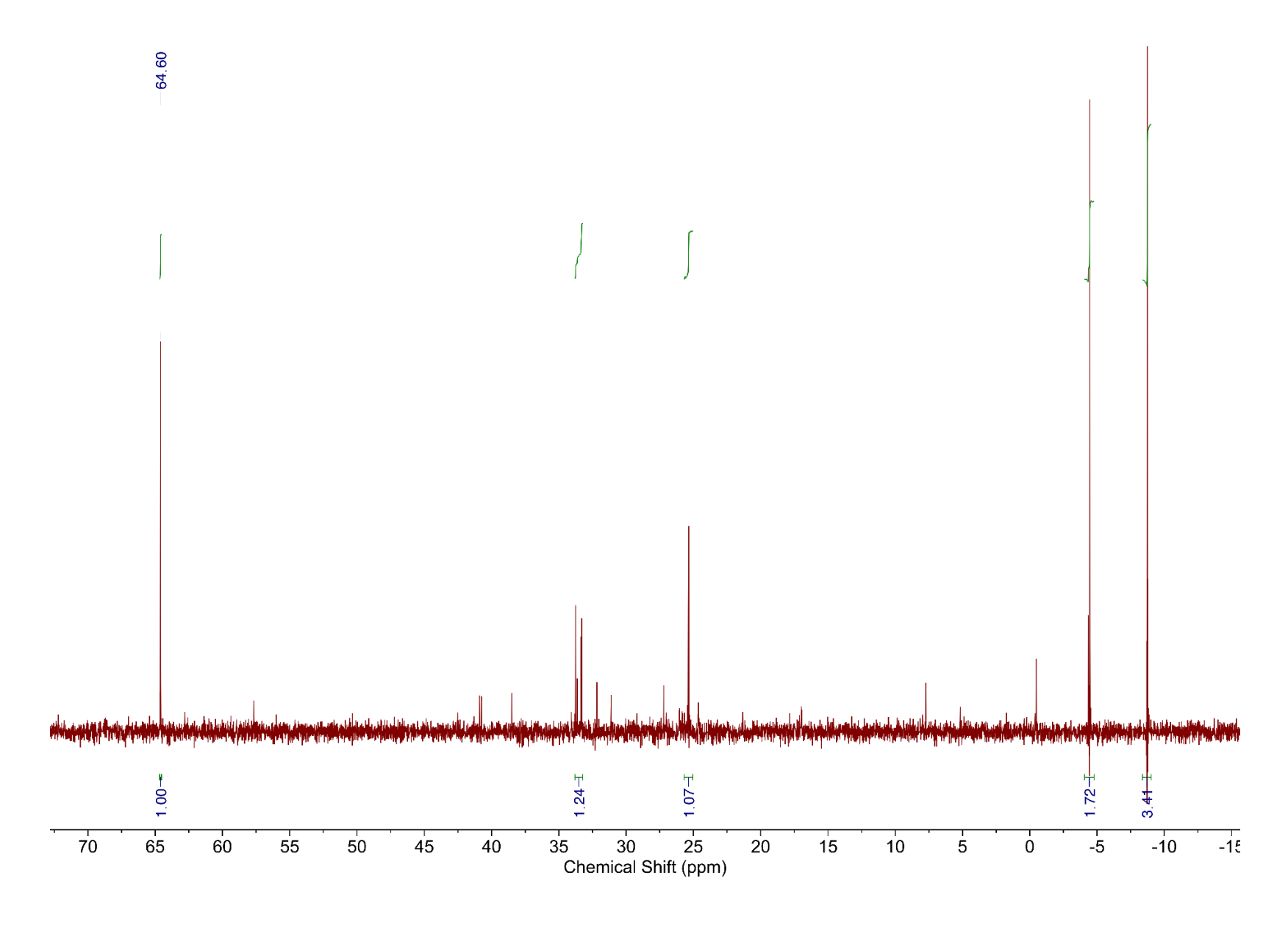


Figure 29 - ³¹P{¹H} NMR spectrum of crude (*R*)-ethyl-2,2'-bis(methylene)-1,1'-binaphthyl phosphinate **56** via novel synthetic step.

The $^{31}P\{^{1}H\}$ NMR spectrum impurity signals between δ 34 and δ 25 are in the region for phosphonate compounds, 54 suggesting that some side reactions may have occurred resulting in the formation of phosphonates. The minor impurity signals between δ 10 and δ 0 are in the region of phosphate monoesters 54 and the larger signals at δ –4 to δ –8.5 are in the regions of phosphate diesters, 54 halophosphate esters and phosphoric/phosphonic amides respectively. 56 This suggests that multiple side reactions may have occurred to produce multiple phosphorous containing biproducts, contributing to the complications of isolation.

2.8.4 Synthesis of (*R*)-2,2-bis(bromomethyl)-1,1'-binaphthyl

Due to the purification complications of the novel cyclisation reaction towards chiral ester **56**, the synthesis towards novel Brønsted acid catalysts was carried out following an amended synthetic route, based on the previously reported synthetic routes, Scheme 2.^{25, 49} *N*-bromosuccinimide (NBS) was utilised for the bromination of compound **53** and the reaction was radically initiated using AlBN. Although this step has previously been reported to be both high yielding and fast, 81% over 2 hours on a 2 g scale; this could not be replicated and yields of up to 69% were obtained over five days, on a similar scale to Mikami *et. al.*²⁵ This may have been due to the group using the restricted chemical carbon tetrachloride (CCl₄) as a solvent for the conversion as opposed to CH₂Cl₂. The yield obtained using CH₂Cl₂ was an improvement on the previously reported yield for this synthesis using tetrachloroethylene (C₂Cl₄), which was 47%, ⁴⁹ though multiple portions of AlBN were required to initiate this step, CH₂Cl₂ was used as the solvent for this step as it is less regulated in the UK and thus more readily accessible in synthetic laboratories. The work up of the crude material was also

amended as more washes using water were required to quench and remove the extra portions of AIBN utilised. Yellow crystals were grown from the crude material using CH₂Cl₂ and hexane to afford isolated compound **54** for use in the next synthetic step without further purification. Furthermore, this step afforded improved atom economy and environmental impact compared to previous reports.^{25, 49}

2.8.5 Synthesis of (R)-2,2'-bis(methylene)-1,1'-binaphthyl phosphinic acid 55

(*R*)-2,2'-bis(methylene)-1,1'-binaphthyl phosphinic acid, compound **55**, was synthesised from **54** *via*. a synthetic step amended from the literature.^{25, 49} The reaction towards phosphinic acid **55** builds on previous work by Boyd *et al*. in the synthesis towards phosphorus containing heterocycles.³³ Though previous literature^{25, 33, 49} utilises ammonium hypophosphite (NH₄H₂PO₂) as the source of phosphorous for the cyclisation reaction, compound **55** was successfully isolated using anilinium hypophosphite for the formation of the phosphorous heterocycle. The anilinium hypophosphite was prepared following the literature procedure.⁹ The phosphinic acid **55** was successfully synthesised and isolated in yields of up to 64 %, an improvement in the atom economy of the reaction towards the racemic acid, previously reported by the Caffyn group from 42%.⁴⁹ Following a trituration of the cream material using CH₂Cl₂ and pentane, a white solid was obtained and protected as the ethyl ester **56** without further purification.

2.8.6 Synthesis of (*R*)-ethyl-2,2'-bis(methylene)-1,1'-binaphthyl phosphinate

Prior to the fluorination reaction, phosphinic acid **55** required protection to ensure there were no direct fluorination reactions of the phosphorous acid moiety. As phosphinic acid groups are susceptible to fluorination, they can rapidly produce

phosphorous(V) fluoride (P(V)-F) bonds, with reaction times as fast as 60 seconds.⁵⁷ An example of a rapid organophosphorous(V) fluorination of the diphenyl acid, **65**, using a sulfone iminium fluoride (SIF) reagent, reported by Melvin *et al.*,⁵⁷ is shown in Scheme 6.

Scheme 6 - An example from the extensive scope of rapid fluorinations of organophosphorous acids by Melvin and co-workers.⁵⁷

The deoxyfluorination reaction shown highlights the susceptibility of aromatic phosphinic(V) acids to fluorination, even under mild conditions. Though more recently organophosphorous(V) fluorides have found significant relevance in the pharmaceutical industry, ^{57, 58} historically they have been utilised in chemical warfare as toxins and nerve agents due to their biological activity. ⁵⁹⁻⁶¹ As such, undesired side fluorination reactions were avoided through the protection of the aromatic phosphinic acid **55** as an ester. Mikami and co-workers previously reported the protection of **55** as the chiral methyl ester **49**, as outlined in Scheme 7 below. ²⁵

Scheme 7 - Synthesis of methyl ester **68** by Mikami *et al.*²⁵ in a two-step esterification of the chiral phosphinic acid **55**.

Despite this reaction reporting a relatively high atom economy, the second step was avoided due to the use of methyl iodide, a category 2 carcinogen. In order to circumvent this, a one-pot reaction was carried out; following the racemic work previously undertaken by the Caffyn group.⁴⁹ This step is shown in Scheme 8.

Scheme 8 - The one-pot reaction to convert racemic phosphinic acid **55** to phosphinic ester **56**, via. the phosphonochloridate intermediate **69** reported by the Caffyn group.⁴⁹

The aromatic phosphonochloridate **69** was prepared employing thionyl chloride as both solvent and reagent.^{49, 62} The solvent was removed *in vacuo* and the ethyl phosphinic ester **56** was synthesised by reacting **69** with absolute ethanol.

Chiral phosphinic acid **56** was successfully synthesised and isolated following an automated silica gel column, eluting with 100% EtOAc. Isolating this ester proved to be paramount for successful fluorination in the next step.

2.8.7 Synthesis of (*R*)-ethyl-2,2'-bis(difluoromethylene)-1,1'-binaphthyl phosphinate **7**.

To potentially enhance the Brønsted acid catalytic ability of the targeted phosphinic acids, fluorine atoms were introduced at the α , α' positions^{25, 48} of the phosphorous atom. Since Mikami *et al.* synthesised the methyl fluorinated phosphinic ester **68** and previous work by the Caffyn group synthesised the racemic fluorinated phosphinic ester **57**, Scheme 9 showcases the step towards the first synthesis of the chiral compound **57**.

Scheme 9 - Synthesis of the novel chiral (*R*)- enantiomer of fluorinated phosphinic acid **57**.

NaHMDS was utlised to deprotonate the methyl linkages of the aromatic heterocyclic phosphinic ester **56** at −78°C in THF for one hour. After the reaction mixture had a clear colour change to deep red, NFSI was added dropwise over a 3 minute period and stirred at the same temperature for 8 hours. Following a mildly acidic quench using HCI and extraction into EtOAc, a cream solid of crude **57** was

obtained. The novel (*R*) enantiomer of chiral compound **57** was isolated in 53% yield and purified using an automated silica gel column, eluting with CHCl₃.

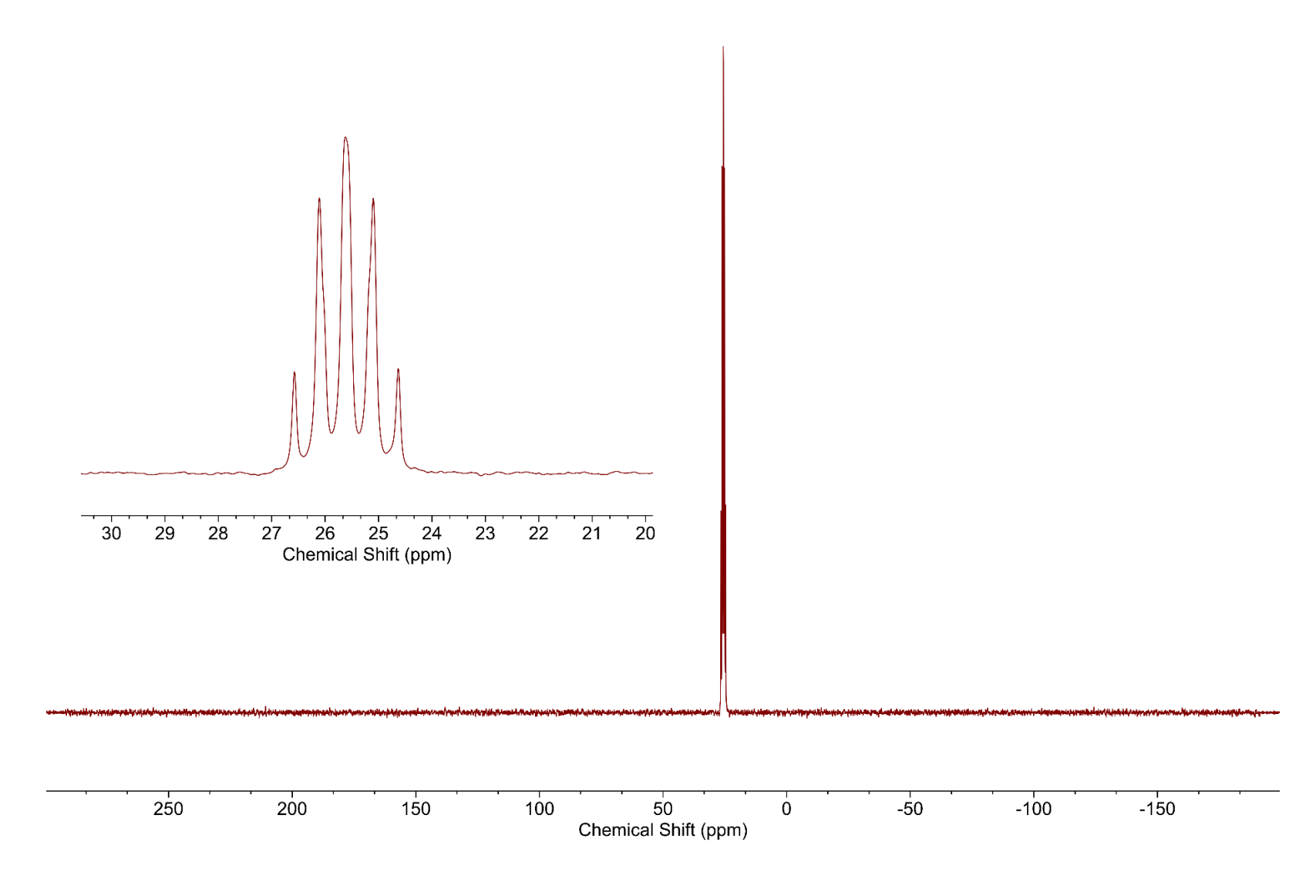


Figure 30 - $^{31}P\{^{1}H\}$ NMR spectrum of novel (R)-ethyl-2,2'-bis(difluoromethylene)-1,1'-binaphthyl phosphinate **57**.

The ${}^{31}P\{{}^{1}H\}$ NMR spectrum, Figure 30, shows a single quintet peak at δ 25.61 (J=95 Hz), a significant difference in chemical shift in comparison to the starting compound, phosphinic acid 55. The quintet splitting of the peak is caused by the coupling of the phosphorous atom to the four non-equivalent fluorine atoms; attached to the adjacent carbon in the heterocycle of compound 57, Scheme 9. The non-equivalence of the heterocycle CF₂ group fluorine atoms is caused by the fixed position of the phosphinic ester group. This moiety of **57** cannot tautomerise. unlike phosphinic acid 55, and as such, introduces inequivalence to the fluorine atoms. The carbon atoms of the two CF₂ groups are also at fixed positions within the heterocycle and cannot rotate, contributing to the inequivalence of the four fluorine atoms as well. The non-equivalence of the fluorine atoms is further emphasised by the four separate environments observed in the ¹⁹F NMR spectrum Figure 33. Each fluorine atom is represented by a doublet of doublets. These peaks are caused by the coupling of the fluorine atoms to each other as well as to the phosphorous atom. Fluorine environment assignments are highlighted, Figure 31. The most downfield signal at δ -91.36 gave the coupling constants ${}^2J_{F-F}$ = 194 Hz and ${}^2J_{F-P}$ = 87 Hz; the environment at δ –93.37 gave ${}^2J_{F-F}$ = 182 Hz and ${}^2J_{F-P}$ = 100 Hz. The more upfield signals gave coupling constants of ${}^2J_{F-F}$ = 182 Hz and $^{2}J_{F-P} = 100 \text{ Hz}$ at $\delta = 121.54$ and $^{2}J_{F-F} = 200 \text{ Hz}$ and $^{2}J_{F-P} = 94 \text{ Hz}$ at $\delta = 123.69$. The most downfield environment is representative of the fluorine F_d, whereas the peak at $\delta - 93.37$ represents F_c. The F_a environment is shown by the signal being more upfield at δ –121.54 than F_b at δ –123.69 due to the former being axially orientated whereas the latter is equatorially orientated relative to P=O.

57

Figure 31 - Fluorine environments for novel fluorinated ester 57.

The successful synthesis of phosphinic ester **57** was reinforced from the ¹H NMR spectrum obtained, Figure 34. The labelled proton environments are shown in Figure 32.

Figure 32 – Labelled proton environments for novel fluorinated ester 57.

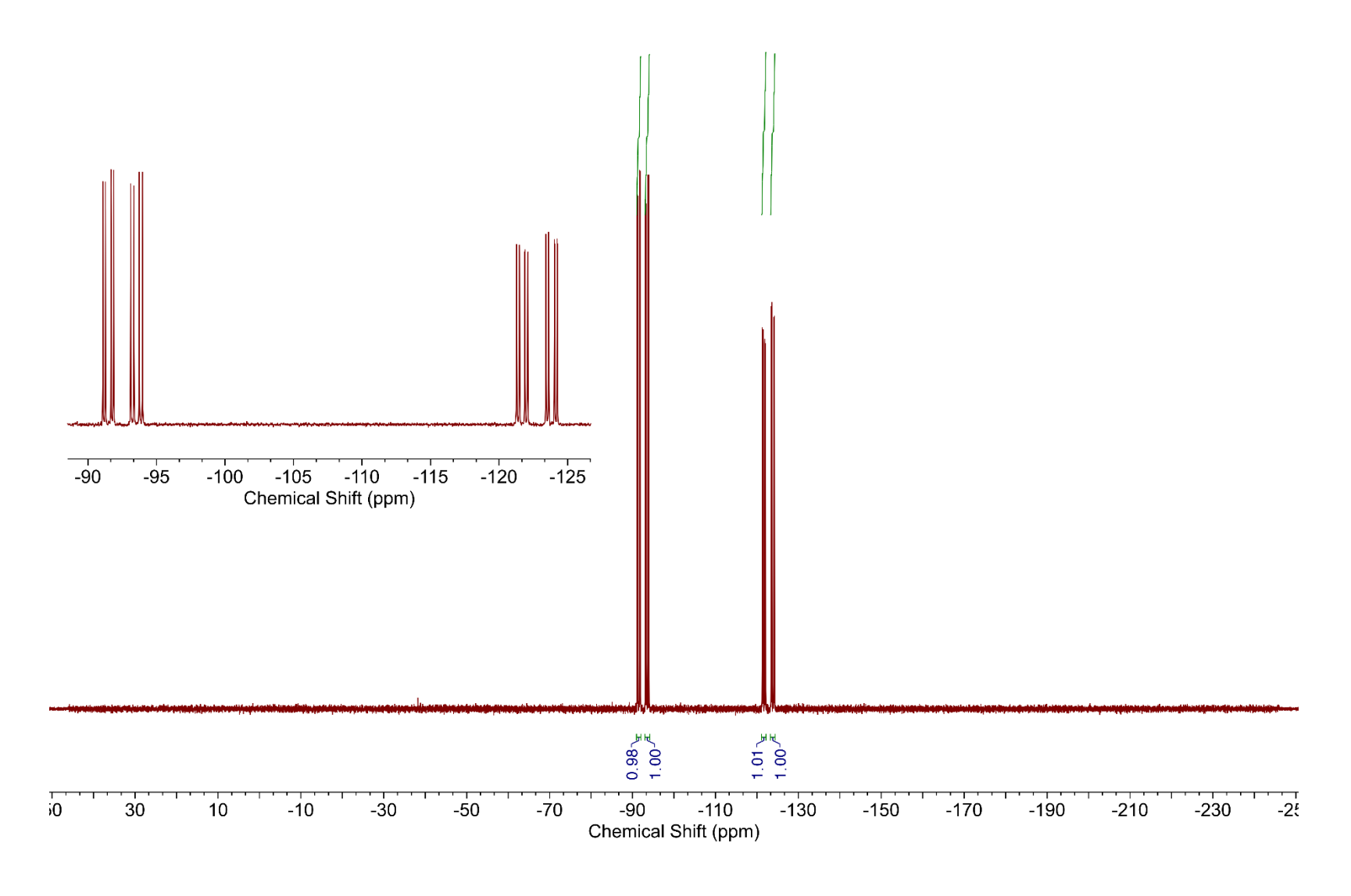


Figure 33 - ¹⁹F NMR spectrum of novel (*R*)-ethyl-2,2'-bis(difluoromethylene)-1,1'-binaphthyl phosphinate **57**.

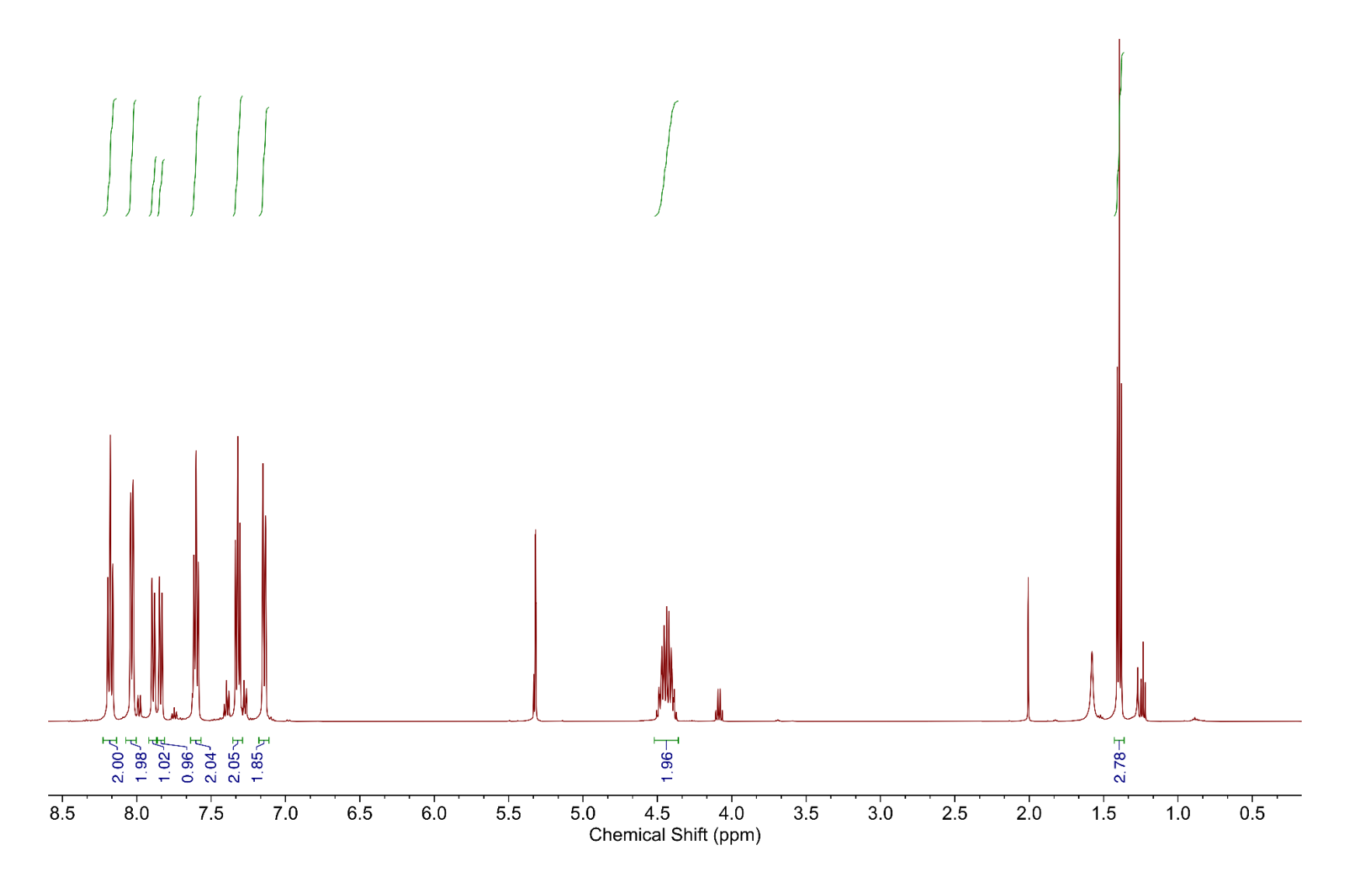


Figure 34 - ¹H NMR spectrum of novel (*R*)-ethyl-2,2'-bis(difluoromethylene)-1,1'-binaphthyl phosphinate **57**

The 1 H NMR spectrum of phosphinic ester **57** in CD₂Cl₂ provides further evidence that the synthesis of the chiral ester was a success. The triplet at δ 1.39 and the multiplet at δ 4.44 represent the OEt protons of the ester. The lack of methylene protons at δ 3.10 shows that **57** was successfully isolated from any remaining starting material **56** from the crude mixture, despite the aromatic region showing slight contamination.

The $^1\text{H-}^1\text{H}$ COSY data obtained is shown in Figure 35. Crucially, the coupling of the ethyl ester protons, H_g and H_f can be seen from the cross peaks at δ 4.41 and δ 1.37. The aromatic regions remain consistent with correlating coupling to that of compound **52** and has not been reassigned.

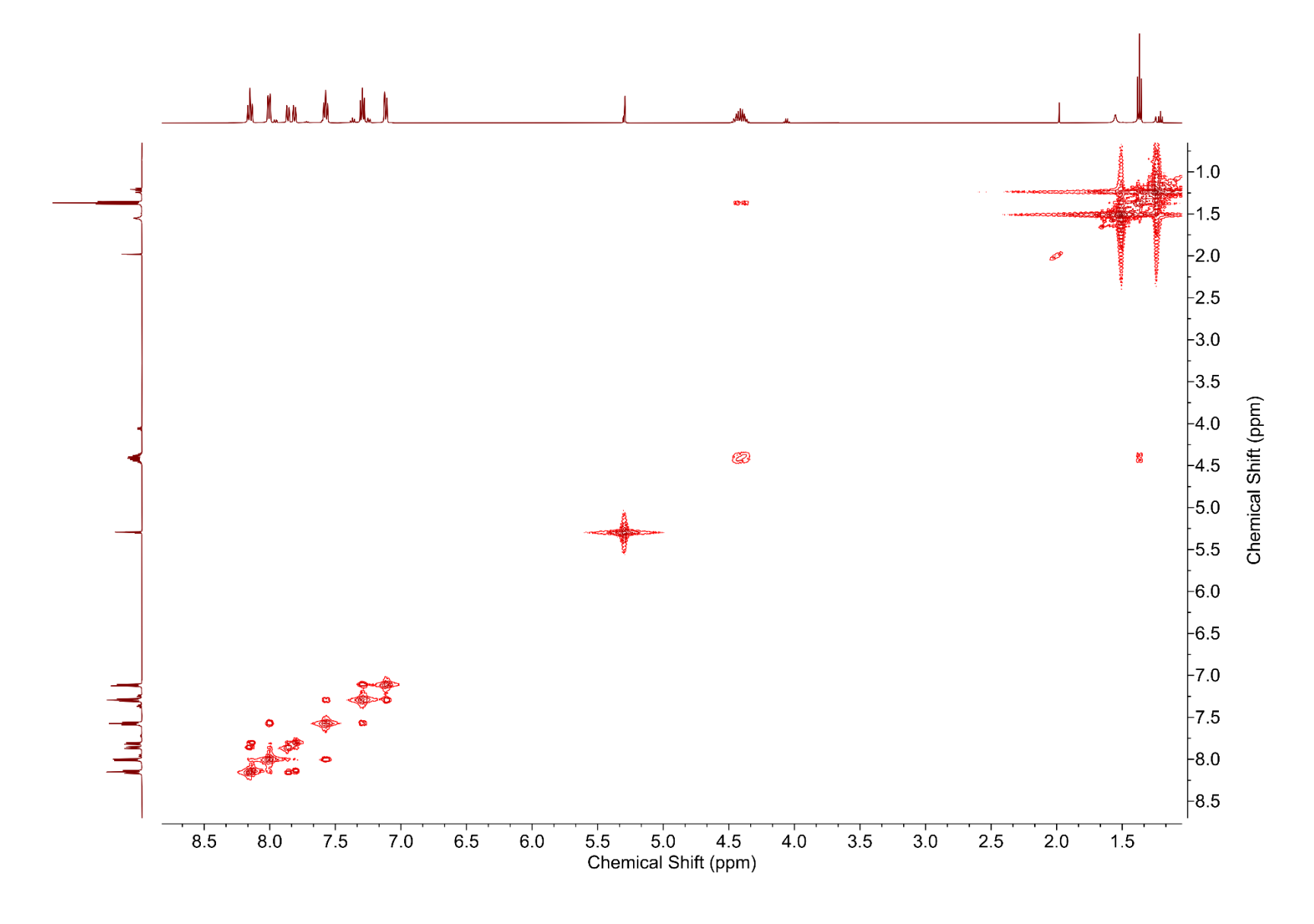


Figure 35 - ¹H-¹H COSY NMR spectrum of novel fluorinated ester **57**.

The mass spectrum, Figure 36, eluted with a retention time of 6.653 minutes and shows the ion peak for the parent ion $[M+H]^+$ with m/z = 445.1. Peaks $[M+Na]^+$ at m/z = 467.2, $[2M+H]^+$ with m/z = 889.4 and $[2M+Na]^+$ with m/z = 911.4 were also observed. The data obtained provided substantial evidence that the synthesis of **57** was successful.

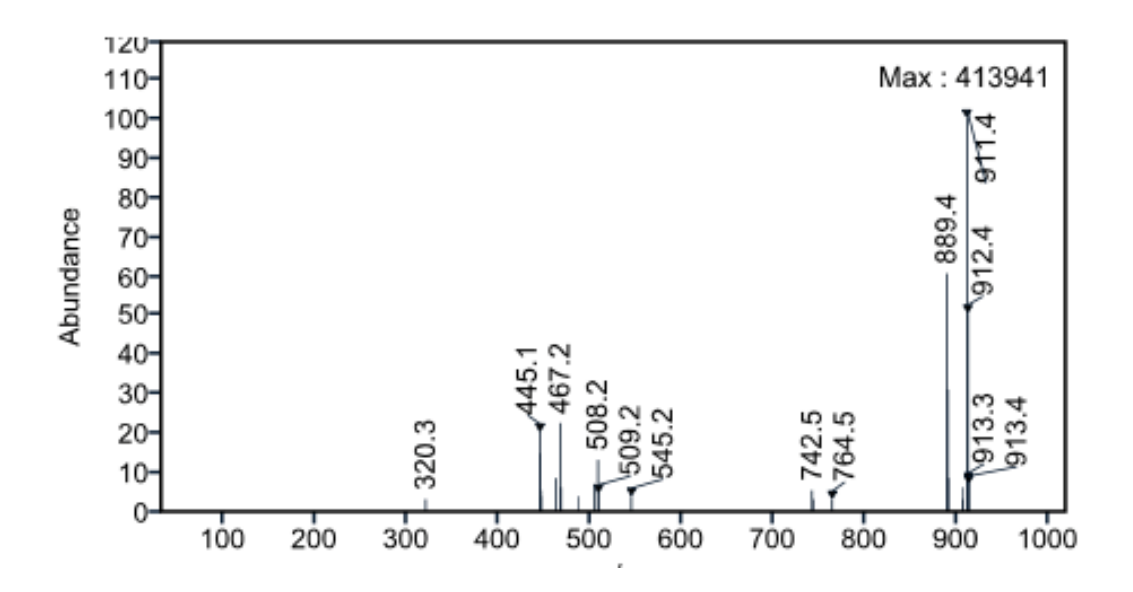


Figure 36 - Mass spectrum obtained for novel chiral fluorinated ester 57.

2.8.8 Synthesis of 3,3'-substituted phosphinic acid atropisomers

The new chiral ester **57** was then deprotected using MeOH and NaOH (2 M) in CH₂Cl₂ and compound **59** was used without further purification. Following the successful synthesis of the fluorinated phosphinic acid **59**, a novel reaction was trialled with the aim of substituting at the 3,3'-positions with large groups to enhance steric hinderance to the catalyst. Though the ideal target substituted phosphinic acids would have structures similar to that of TRIP (**8b**) substitution of

a smaller halide and aldehyde or group, using dimethylformamide (DMF), was tested for reaction proof of concept (Figure 37).

Figure 37 - Synthesis of 3,3'-substituted BINOL derived phosphorous esters.

The novel reaction shown in Figure 37, was trialled using the four compounds highlighted. Similarly to the novel reaction previously discussed in this chapter, from compound **53** to **56**, a strong base is utilised for the deprotonation of the aromatic back bone at the 3,3'-positions, prior to the addition of the substituents. In this instance, Schlosser's superbase "LICKOR",²³ a combination of *n*-BuLi and potassium tert-butoxide was used for the deprotonation step and DMF as the source of the aldehyde moiety. To make the superbase, the hexane was removed from *n*-BuLi and potassium tert-butoxide was added dropwise at −78°C. Although the dilithium salt was observed from the distinctive brown precipitate that formed,⁶³ these reaction trials were unsuccessful and the 3,3'-substituted esters were not

obtained following the addition of bromine or DMF. Following these unsuccessful proof-of-concept reaction trials, the work towards catalysts with bulkier substituents was ceased.

2.9 Conclusions

The chiral phosphinic acid **59** was successfully synthesised from seven steps, with an overall yield of 78%, for later applications in asymmetric catalysis. A novel synthetic step was extensively trialled to improve the originally published synthetic route. The novel step circumvented three steps with low atom economies and avoided the use of restricted reagents with negative environmental impacts. The targeted ester **56** of this new reaction was successfully synthesised, however, isolation of the product was unsuccessful. A novel chiral fluorinated ester **57** was synthesised and isolated following the amended synthetic route. The chiral target fluorinated phosphinic acid **57** was synthesised following the deprotection of the novel chiral ester for later applications in asymmetric catalysis. A small library of fluorinated phosphinic esters with 3,3'-position substituents were targeted *via*. a novel "LICKOR" reaction, for deprotection to the corresponding phosphinic acids. Four esters were successfully deprotonated using Schlosser's base, however, the target esters were not obtained from the second step of the reaction trials.

2.10 Future Work

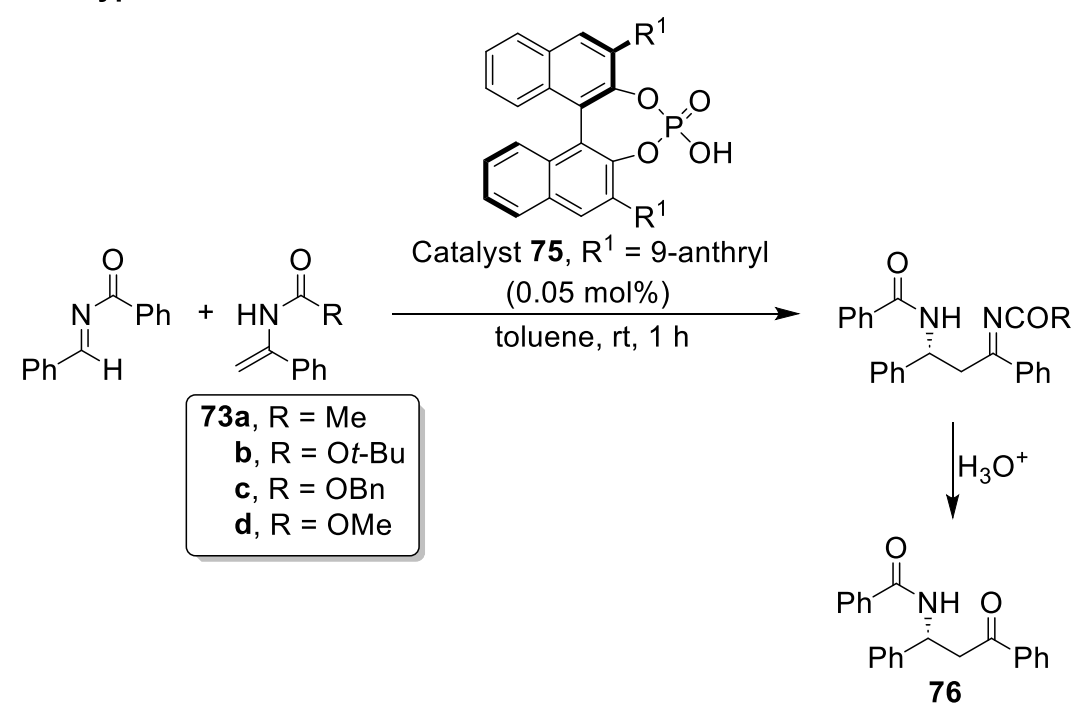
The targeted ester **56** of the novel synthetic step has the potential to be isolated using different isolation techniques not previously trialled, such as by reverse phase column chromatography. Successful isolation of this compound would have led to an improved synthetic route towards the novel fluorinated phosphinic acids, for later use as asymmetric catalysts, eradicating three low yielding, hazardous steps. The novel step may have proven more successful by utilising a different base for the deprotonation of the demethylated compound **53**. While *n*-BuLi was used throughout, a stronger base like *tert*-BuLi could be employed.

3. The synthesis of sulfonamides for the pK_a determination of the Brønsted acid 2,2'-bis(difluoromethylene)-1,1'-binaphthyl phosphinic acid

Initially, chiral Lewis acids were predominantly employed as asymmetric catalysts for carbon-carbon bond formations, providing excellent enantioselectivity. 42 More recently, chiral Brønsted acids have been investigated for use as a new class of organocatalysts for asymmetric reactions.^{42, 64} Unlike chiral Lewis acid catalysts, which are formed in situ by reacting with a chiral ligand, Brønsted acids are catalytically active in their native form. Brønsted acids are also easier to handle, being mostly stable to oxygen and water, meaning that they can be synthesised in large quantities and stored for long periods of time. These features make them both more environmentally friendly and preferential for use on an industrial scale when compared to Lewis acid catalysts. The application of 1,1'-bi-2-naphthol (BINOL) derived acids as asymmetric catalysts⁶⁵ has also been favoured due to the high yields and enantioselectivities obtained, even when using relatively low loading concentrations of catalyst comparatively. In 2008, Terada and co-workers reported obtaining yields as high as 99% and enantiomeric excesses greater than 98% for an enantioselective direct Mannich reaction of imines, using a catalytic loading of 2 mol%, Scheme 10. Terada and co-workers also highlighted the effectiveness of BINOL derived acids at even lower loading concentrations, of just 0.05 mol%, for an aza-ene-type reaction of glyoxylate derived imines and enecarbamates, Scheme 10.15 Where Lewis acid catalysts are often stoichiometric, Brønsted acid catalysts can be used with loadings as low as 0.01 mol%.66

Enantioselective Mannich reaction

Aza-ene type reaction



 76 yield and ee from
 73a: 90% 86% ee
 73d: 85% 95% ee

 73b: 94% 60% ee
 73d: 82% 95% ee (0.1 mol% 74, 5 h)

 73c: 55% 83% ee
 73d: 85% 93% ee (0.05 mol% 74, 5 h)

Scheme 10 - Terada *et al.* employed BINOL derived Bronsted acids as catalysts in an enantioselective direct Mannich reaction and an aza-ene type reaction.¹⁵

Chiral Brønsted acids can be categorised into two main classes: neutral hydrogen bonding catalysts and stronger Brønsted acids;⁴² often derived from BINOL. Examples of these Brønsted acid classes are shown in Figure 38.

Hydrogen-Bonding Catalysts ← Stronger Brønsted Acid Catalysts

77, Thiourea

78, TADDOL

79, 3,3'-substituted BINOL

80, 3,3'-diphenyl-1,1'-binaphthyl-2,2'-diyl hydrogen phosphate

Figure 38 - Thiourea and taddol are examples of hydrogen-bonding Brønsted acid catalysts. Stronger phosphoric Brønsted acid catalyst examples derived from BINOL.⁴²

The use of smaller, hydrogen-bonding Brønsted acids as metal (ion)-free catalysts has been extensively investigated by other research groups since the early 2000's, particularly in the search for the smallest "artificial enzymes". 66-69 Many (thio)ureas have proven to be privileged chiral catalysts in a great number of bioinspired organocatalytic asymmetric reactions due to their ability to donate two differing hydrogen-bonds simultaneously. 66 The ability of these Brønsted acids to donate hydrogen bonds *via*. their acidic protons, the more effective they are as catalysts. 20 Therefore, the pK_a values of such hydrogen-bonding Brønsted acids

has been investigated; in 1988 Bordwell published over 300 pKa values in just one publication.⁷⁰

The pK_a of **77**, Figure 39, and similar phosphoric Brønsted acids were determined by O'Donoghue *et. al.* in 2011.⁷¹ They found that by changing the substituents in the 3 and 3' positions to largely alter the electronic and steric effects of the catalysts, little effect on the pK_a values of the acids were observed.

Figure 39 - The structures and pK_a values in DMSO of some of the phosphoric acids determined by O'Donoghue *et. al.*⁷¹

Similarly to many of the pK_a values of the hydrogen-bonding Brønsted acids reported by Bordwell,⁷⁰ these phosphoric Brønsted acid pK_a values were determined using a UV-spectroscopic method. There are now many different techniques established to determine the pK_a of compounds,⁷² though potentiometric and spectroscopic remain the most popular.²² Potentiometric methods of pK_a determination are the simplest to undertake, as the pK_a values are determined from a titration curve. For spectroscopic methods, buffer solutions are used, and a UV-Vis spectrum is taken to measure the absorbance at each point of the titration. The pK_a is then determined from a plot of absorbance against pH.²²

Although popular solvents for the determination of pK_a values *via* these methods were often either H₂O or DMSO, since the 1960's, acetonitrile (MeCN) has been favoured due to it's low basicity. Although DMSO has a lower basicity than MeCN, MeCN is more suitable for the pK_a determination of strong acids due to the low ability of MeCN to solvate anions; it also favours the dissociation of ion pairs into free ions.²¹ For the pK_a determination of BINOL based phosphoric acids, non-aqueous solvents are not suitable as many with structures similar to **80-83**, shown in Figure 39, have very low solubility (< 1mM) in water.

Since the catalytic ability of phosphoric acids varies greatly depending on their acidity, Leito and co-workers published a complete study on the pK_a values of the most readily used Brønsted acids catalysts in 2013.²⁰ The pK_a values were determined in MeCN using a UV-vis spectrophotometric method.²¹ The pK_a values obtained showed distinct groupings of BINOL-derived phosphoric acids, *N*-sulfonyl phosphoramides and sulfonyl imides. The scale developed was later summarised in a review published by Rueping *et al.*; exemplar phosphoric acids are shown in Figure 40.¹⁷

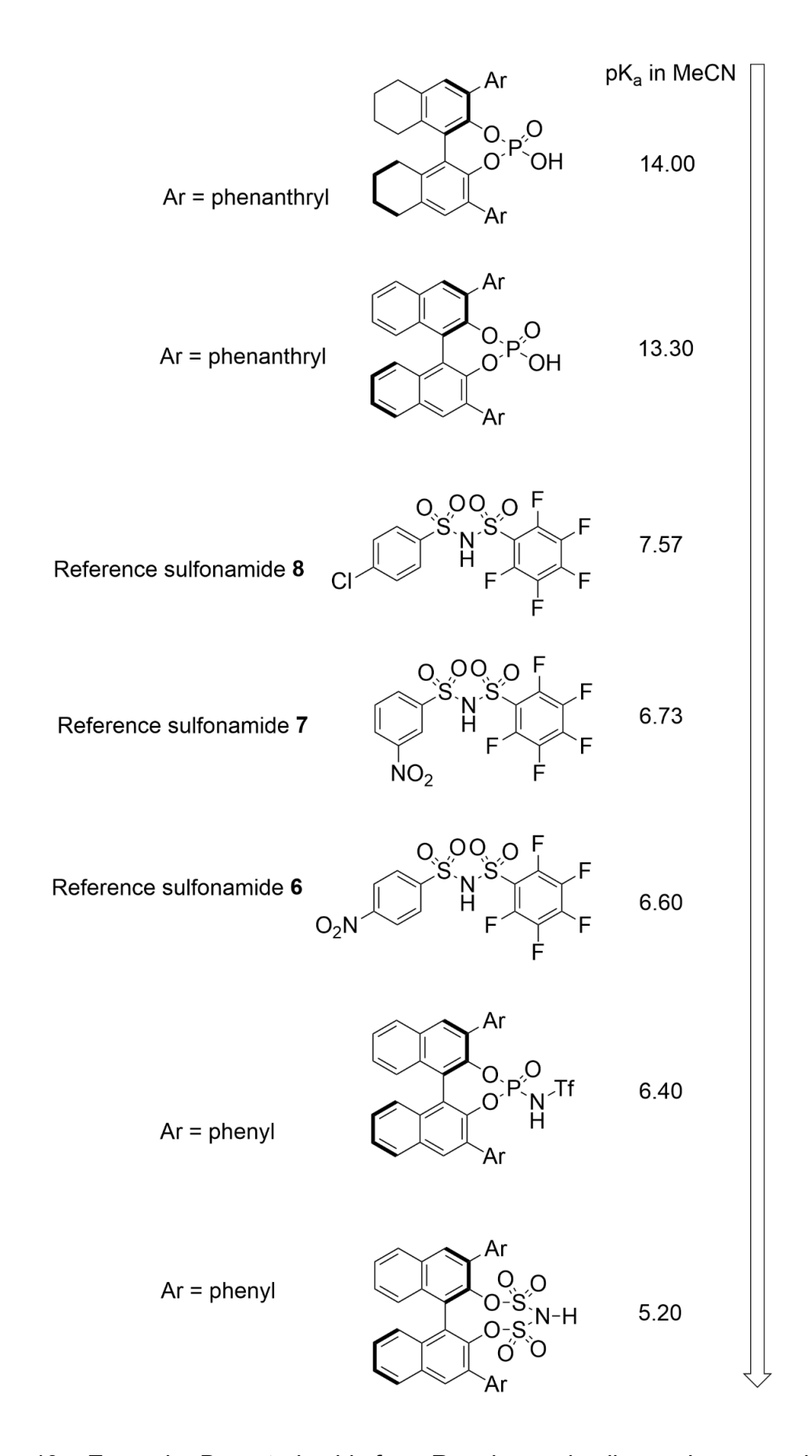


Figure 40 – Exemplar Brønsted acids from Rueping and colleague's summarised scale of pKa values determined in his previous work with Leito *et al.* in 2014.^{17, 20}

Altering solvents for pK_a determination causes a large disparity in the pK_a values obtained for the same molecules, as can be seen by comparison of the values of 80 in Figure 40 and Figure 41. In water, the pKa obtained was 3.86, whereas it was 13.30 in MeCN. As water is more polar, it stabilizes the ionised forms of the acids more effectively, making the acidity of the acids in water significantly higher, correlating to a much lower pKa than in MeCN. The pKa value of hydrochloric acid in MeCN is 10.3, meaning the acidity of both the phosphoric Brønsted acids, shown in Figure 40, are slightly weaker acids than hydrochloric acid, with higher pKa values ranging between 12 and 14. However, these pKa values are indicative of a significantly stronger acid than acetic acid, which possesses a pKa of 23.51 in MeCN.²⁰ In order to test the reactivity of Brønsted acids, and therefore the catalytic ability, some of the catalysts were applied by Rueping et al. in Nazarov cyclizations. 17 The group discovered that not only were there poignant groupings of the Brønsted acids by type as a function of pKa value but they also found a direct correlation between the acidity of the molecule and the catalytic ability of the Brønsted acid. It is, therefore, crucial to consider acidity when designing novel Brønsted acids.

While the pKa values summarised in Figure 40 were determined by the popular UV vis spectroscopic methods previously discussed, the use of NMR spectroscopy to determine pKa values has precendent in the literature. These pKa determinations rely on the observation of peak chemical shifts of both the Brønsted acid in question and a reference compound, both in fully protonated and fully deprotonated environments. Sulfonamides, with similar structures to those grouped in the middle of the scale in Figure 40, make ideal reference compounds for pKa determination by NMR spectrometry. Reference compounds are

particularly advantageous in NMR titrations for pK_a determination and serve a dual purpose. A reference compound is firstly required in order to ensure the chemical shift values obtained from the spectral peaks throughout the titration are accurate. Secondly, a reference compound with a known pK_a value, involved in the NMR titration, enables the determination of absolute pK_a values, as opposed to relative pK_a values. Similarly to determining pK_a values by UV Vis spectrometry, determining pK_a values utilising NMR spectrometry requires performing a titration and collecting an NMR spectrum after addition of each aliquot of acid or base (titration direction dependant). The chemical shifts from the NMR spectra are used in calculating a pK_a value. The calculation pK_a is based on the determination of the ratio of the fully protonated/deprotonated forms of the acid/base pair, where p is the proportion of the protonated form (Equation 1).

$$r = \frac{p}{1-p}$$
 (Equation 1)

The acidity constant, K_a (Equation 2, can be expressed as a function of r, the ratio of protonated against deprotonated forms (Equation 3):

$$K_a = \frac{|B^-||H^+|}{|BH|}$$
 (Equation 2)

$$K_a = \frac{|H^+|}{r}$$
 (Equation 3)

In this case, a reference compound is used and thus the mixture of compounds requires consideration of the equality (Equation 4):

$$K_{a_i}r_i = K_{a_j}r_j$$
 (Equation 4)

This equality holds true for any pair of acids *i* and bases *j* and results in Equation 5:

$$\frac{K_{a_i}}{K_{a_i}} = \frac{\left(\delta_j^{obs} - \delta_j^{B^-}\right) \left(\delta_i^{B-H} - \delta_i^{obs}\right)}{\left(\delta_i^{obs} - \delta_i^{B^-}\right) \left(\delta_j^{B-H} - \delta_j^{obs}\right)}$$
(Equation 5)

The difference in acidity constants provided can then be used to determine the pKa of the potential Brønsted acid catalyst from Equation 6:

$$\Delta p K_{a_{ij}} = \log(\frac{K_{a_i}}{K_{a_j}})$$
 (Equation 6)

The pKa value is determined from ΔpK_a by comparison to the known pKa value of the reference compound utilised throughout the NMR titration. The order of the compounds being protonated or deprotonated, which is titration direction dependant, dictates whether the pKa value of the Brønsted acid is higher or lower than the known pKa of the reference compound used. For titrations that begin with both the reference compound and Brønsted acid in fully protonated forms, the compound that is the first to fully deprotonate is the strongest acid, therefore will have the lowest pKa value. The fully deprotonated forms reached in the NMR titration can be observed when the NMR peaks experience no further chemical shift and are therefore constant. It is pivotal that future Brønsted acids are designed to have high pKa values and therefore greater acidity for applications as catalysts.

Mikami *et. al.* took into consideration acidity and its link to catalytic ability in the design of their perfluoroalkyl phosphinic acid catalysts.²⁵ It has been long established that perfluoroalkyl substituted phosphorus acids are strong acids.²⁴ More specifically, phosphonic acids have been reported to be highly acidic when there is a difluoromethylene (CF₂) group at the α-position to the phosphorus atom.⁷⁷ Mikami *et. al.*²⁵ incorporated this into the design of their novel Brønsted phosphinic acids. An example of one of the BINOL-derived phosphinic Brønsted

acids in particular, 2,2-bis(difluoromethylene)-1,1'-binaphthyl phosphinic acid **59**, Figure 41, consisted of two oxygen atoms substituted by difluoromethylene, CF₂ groups at the phosphorus centre. The CF₂ groups were hypothesised to increase the catalyst acidity and therefore catalytic ability. However, the acidity of the catalysts synthesised was not determined. Thus, the effect of the CF₂ groups on the acidity warrants investigation.

Figure 41 - Structure of 2,2'-bis(difluoromethylene)-1,1'-binaphthyl phosphinic acid (59).

In order to establish the effect the CF₂ groups have on the acidity of Brønsted acid, this chapter will focus on the pK_a determination of **59** by a ¹⁹F{¹H} NMR spectroscopic method in acetonitrile. The value determined will be compared against other Brønsted acids.

To determine the pK_a of the potential Brønsted acid catalyst **59** by ¹⁹F{¹H} NMR spectrometry, a reference compound, containing fluorine, is required. The approach reported by Jeannerat and Shivapurkar.⁷³ requires the chemical shifts of the protonated and deprotonated forms of the acid and reference compound, from a titration monitored by ¹⁹F NMR spectrometry. Three reference compounds were selected for this purpose; their chemical structures are shown in Scheme 11.

The references were chosen based on two key factors: each compound contained multiple fluorine environments to observe using ¹⁹F{¹H} NMR spectroscopy throughout the pK_a determination experiments. Each reference compound also has a known pK_a value in MeCN within one pK_a value⁷³ predicted for the phosphinic acid **59**, which was approximately 6.6 based on previous preliminary data from the Caffyn group.⁴⁹ The pK_a of the potential Brønsted acid **59** is to be determined using ¹⁹F{¹H} NMR. This chapter will detail the synthesis of the reference compounds **81-83**, and their characterisation. Subsequently, the pK_a of **59** will be determined in MeCN using **81-83** as references. A combination of the approaches detailed by Leito, Jeannerat and co-workers^{73, 76} was employed to achieve this aim.

3.1 Results and Discussion

3.1.1 Synthesis of reference compounds

The synthesis of the reference compounds, **84-86**, is shown in Scheme 11. Briefly, the to-step reaction scheme consists of an amination followed by the formation of a sulfonyl amide. Yields of crystalline solids obtained for **84-86** were 5% from the parent sulphonyl chloride.

Scheme 11 - Synthetic route towards reference compounds **84-86** for the p K_a determination by $^{19}F\{^1H\}NMR$ spectroscopic titration.

3.1.1.1 Amination of 4-nitrobenzenesulfonyl chloride

4-Nitrobenzenesulfonamide was obtained from 4-nitrobenzenesulfonyl chloride following a literature procedure.⁷⁸ The product obtained required drying over phosphorous pentoxide to remove the water present. 4-Nitrobenzenesulfonamide was obtained in 80% yield. The ¹H NMR spectrum shown in Figure 42 correlated with the literature.^{76, 79} The doublets at 8.38 ppm and 8.02 ppm, that both integrate to two protons each, represent the aromatic proton environments. Both

environments display second-order coupling. These environments shift by 0.11 ppm and 0.25 ppm compared to the sulfonyl chloride⁷⁹ employed in the synthesis. A broad singlet at 7.70 ppm was also observed and this signal is due to the two protons of the sulfonamide group. The broad singlet was not present in the ¹H NMR spectrum for the sulfonyl chloride, providing evidence that the amination reaction had been successful.

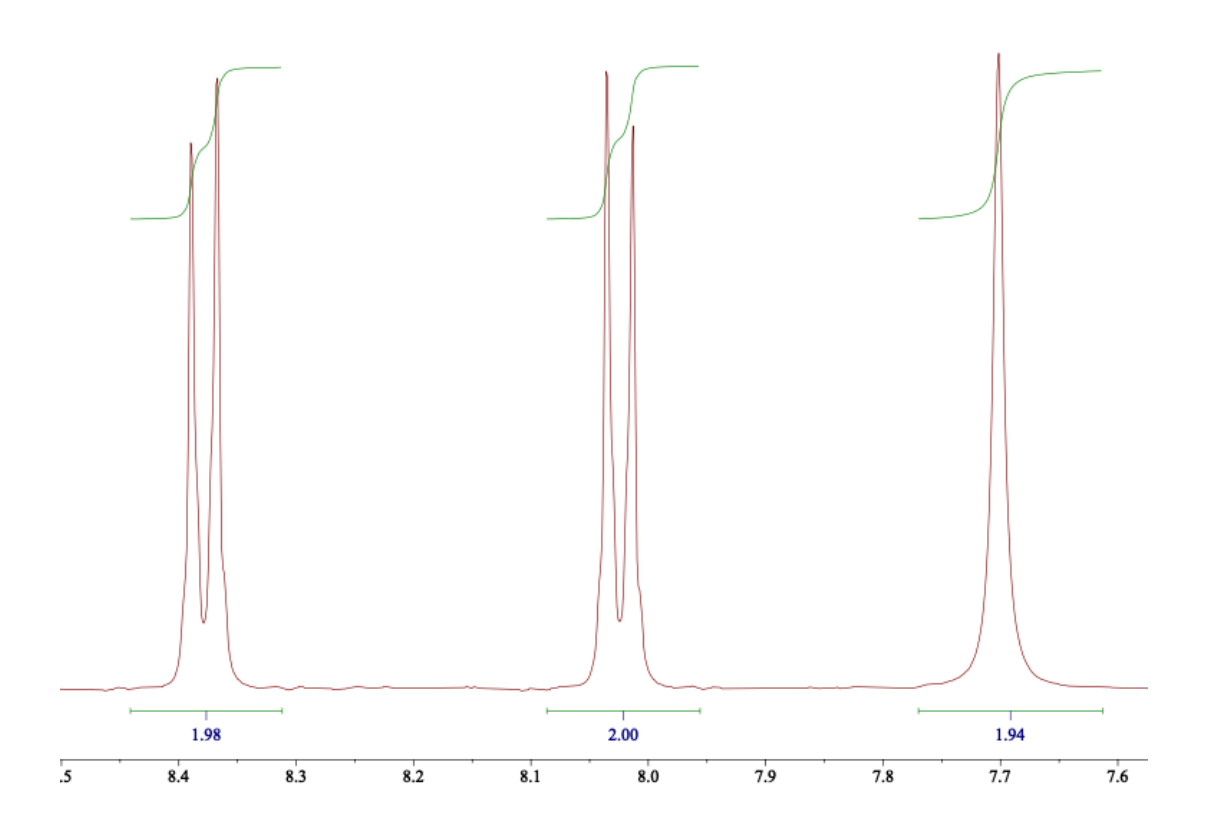


Figure 42 - ¹H NMR spectrum of 4-nitrobenzenesulfonamide. Spectrum collected in DMSO-d₆ at 400 MHz.

3.1.1.2 Amination of 3-nitrobenzenesulfonyl chloride

3-Nitrobenzenesulfonyl chloride was obtained in 94% yield as white crystals, following the literature procedure previously described.⁷⁸ Due to the position of the

nitro substituent, the ¹H NMR spectrum of 3-nitrobenzenesulfonyl chloride is more complex than the 4-isomer. The ¹H NMR spectrum is reported in Figure 43.

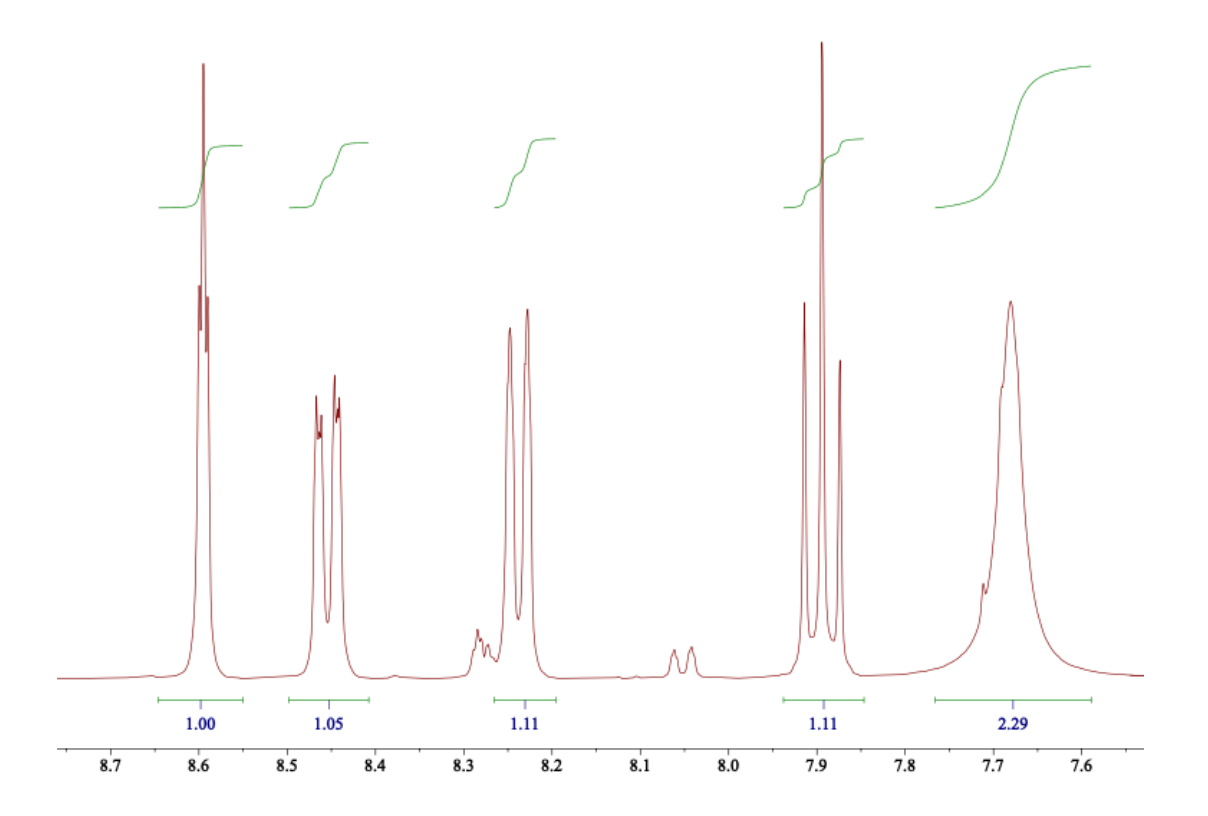


Figure 43 - ¹H NMR spectrum of 3-nitrobenzenesulfonamide in DMSO-d₆. Spectrum acquired at 400 MHz.

The triplet at 8.59 ppm observed in the ¹H NMR spectrum correlates to the proton environment on the aromatic ring that is *ortho* to both electron withdrawing groups (NO₂ and sulfonamide moieties), as it is the proton environment experiencing the greatest de-shielding from the two adjacent electron-withdrawing groups.

Therefore, this proton environment experiences the greatest chemical shift of all the proton environments of 3-nitrobenzenesulfonamide and correlates to the peak furthest downfield at 8.59 ppm. The doublet of doublet of doublets at 8.46 ppm represents the proton environment that is *para* to the NO₂ group. The doublet of

doublet of doublets is caused by the coupling to the three other aromatic protons. This peak is also shifted significantly by the adjacent sulfonamide group. The doublet of triplets peak at 8.24 ppm represents the proton environment that is *para* to the sulfonamide group, which also experiences coupling to the other three aromatic protons. This peak should appear as a doublet of doublet of doublets but the magnitudes of the J-couplings present results in overlap. The triplet peak at 7.89 ppm correlates to the remaining aromatic proton environment, in the *meta*-position to the NO₂ and sulfonamide group. The N-H proton environment is represented by the broad 7.69 ppm doublet peak. These assignments once again accord with those in the literature.^{79,80}

3.1.1.3 Amination of 4-chlorobenzenesulfonyl chloride

Following the synthetic route outlined in Scheme 11, 4-chlorobenzenesulfonamide was synthesised by aminating 4-chlorobenzenesulfonyl chloride with NH₄OH, and was obtained as a white solid in 61% yield. The ¹H NMR spectrum shown in Figure 44 was comparable to the ¹H NMR spectrum collected for 4-nitrobenzenesulfonamide due to the compounds having very similar hydrogen environments; the only observable differences are due to the effects of the more electron-withdrawing chlorine substituent in place of the nitro group, resulting in more up-field chemical shifts for the aromatic proton nuclei.

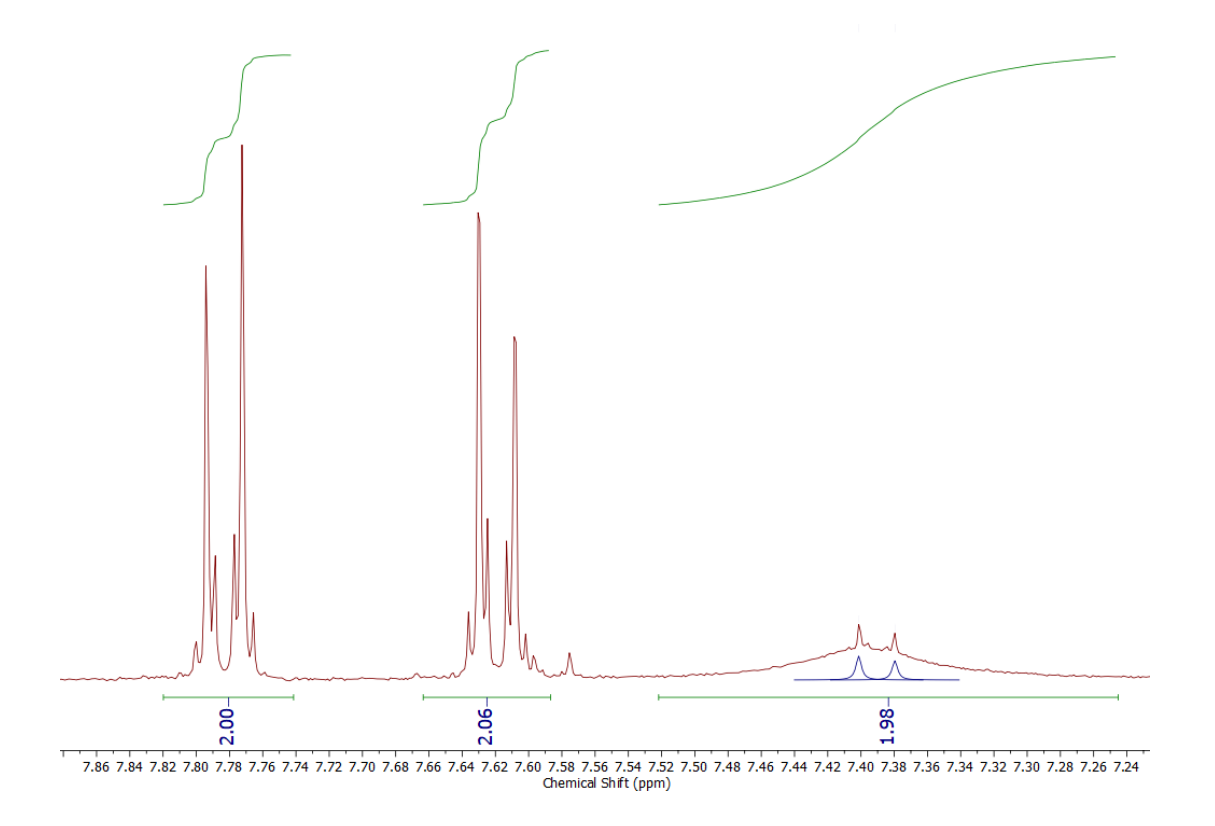


Figure 44 - ¹H NMR spectrum of 4-chlorobenzenesulfonamide in DMSO-d₆, acquired at 400 MHz.

The ¹H NMR spectrum of 4-chlorobenzenesulfonamide consists of two doublets that display second-order coupling. The doublets are at 7.82 ppm and 7.66 ppm, both of which integrate to two protons and correlate to the aromatic proton environments. The doublet at 7.66 ppm integrates a little higher at 2.06 as it could not be completely resolved from a small amount of impurity, which can be seen slightly up-field of the base of the doublet. The very broad peak at 7.43 ppm correlates to the sulfonamide proton environment consisting of two protons.

3.1.1.4 ¹⁹F{¹H} NMR spectra of the reference compounds **81**, **82** and **83** synthesised

The three reference compounds **84**, **85** and **86**, were synthesised using an altered method based on the synthesis previously described.⁷⁸ All were obtained as white solids, either powdered or crystalline. The yields for the reference compounds were up to 13%, an improvement on the 8% reported in the literature.⁷⁵ The stacked ¹⁹F{¹H}NMR spectra of the three compounds are shown in Figure 45.

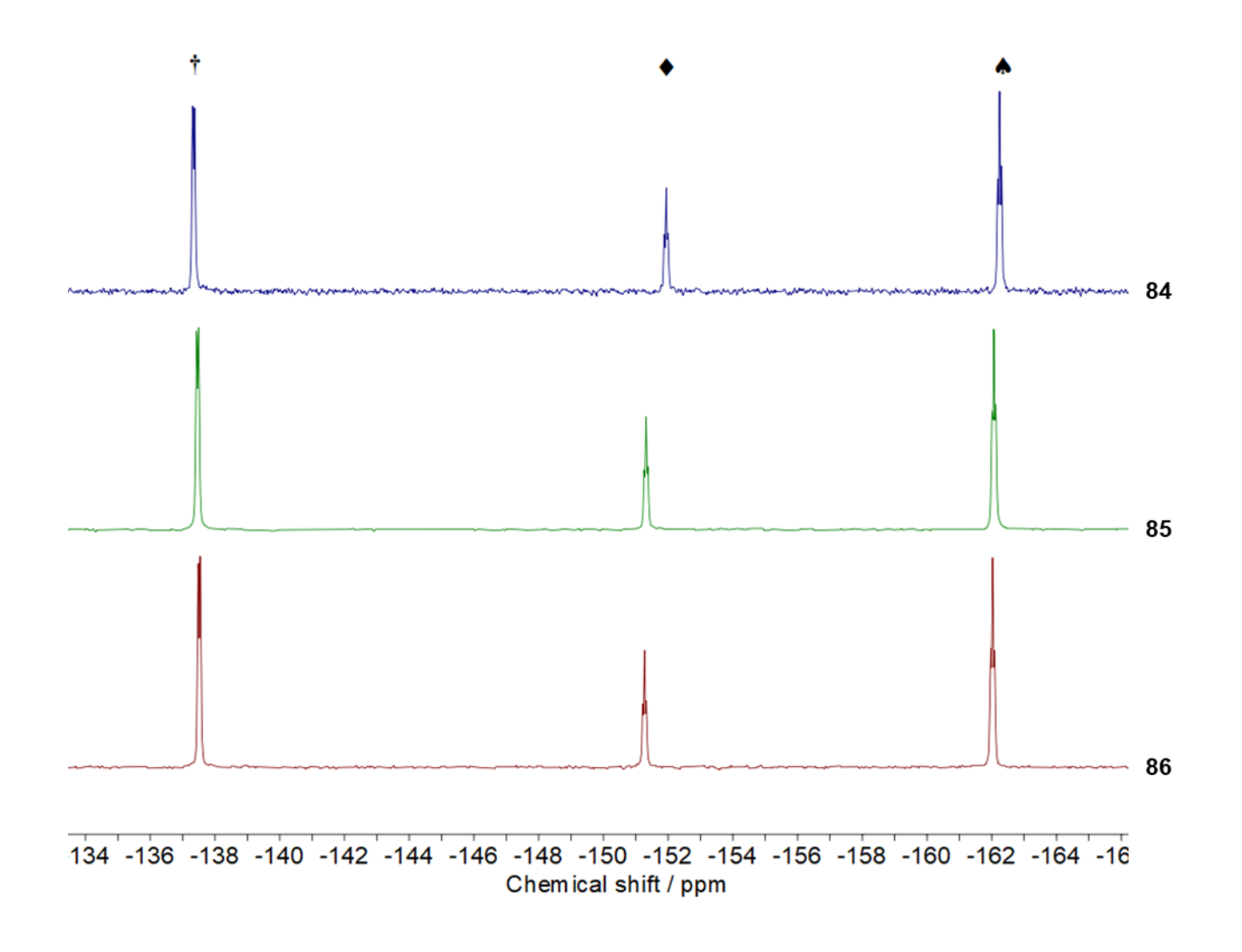


Figure 45 - Stacked ¹⁹F NMR spectra of reference sulfonamides synthesised, compounds **84**, **85** and **86** in acetonitrile.

The peaks most downfield, labelled †, between -137 ppm and -138 ppm represent the aromatic fluorine environment in the *ortho*-position to the sulfonamide moiety for all three compounds. This is due to the fluorine atoms in the *ortho*- position to the sulfonamide moiety exhibiting the greatest deshielding comparatively to the other fluorine environments in each reference compound 84-86. The peaks labelled ♠, between -162 ppm to -163 ppm, confirm the presence of the more shielded fluorine environment in the *meta*-position to the sulfonamide moiety. The fluorine environment in the *para*-position to the sulfonamide moiety for each compound is confirmed by the central triplet peaks between -151.32 ppm and –151.94 ppm, labelled ♦. From Figure 45 it can be seen that the ¹⁹F{¹H} NMR spectra for 84 and 85 have the peaks with closest chemical shift values in ppm for the references synthesised. This is due to the different positions of the nitro group on **84** and **85** only causing a small variance in the chemical shifts. Whereas by substituting the 4-nitro group of **84** with a chlorine atom in the same position in reference **86**, the chemical shifts exhibited by the fluorine peaks is greater. This is caused by the chlorine group having greater electron withdrawing ability than the nitro groups in 84 and 85.

3.1.1.5 Crystallographic data

Compound **85** crystallised in the space group P-1. Sodium ions are coordinated to four different ligands and two water molecules. The water molecules are arranged *cis* to one another. The H₂O-Na-OH₂ bond angle is 89.35°. Bond angles for the three *trans* O-Na-O arrangements are 154.53°, 171.75° and 176.58°. The two

bond angles that are closer to 180° both involve a water molecule. The sodium ion is again in a distorted octahedral geometry.

In the crystal structure, π - π stacking is visible when viewed along vector a. The centroid-to-centroid distance, linked by symmetry code x-1, y, z, between phenyl rings of the same molecule is 3.576 Å. The same distance is again observed between phenyl rings of adjacent molecules in the lattice.

Interestingly, the sulphonate group oxygens, with respect to their coordination to sodium ions, alternate between both being both involved or only one of the atoms being involved. This is shown in Figure 46.

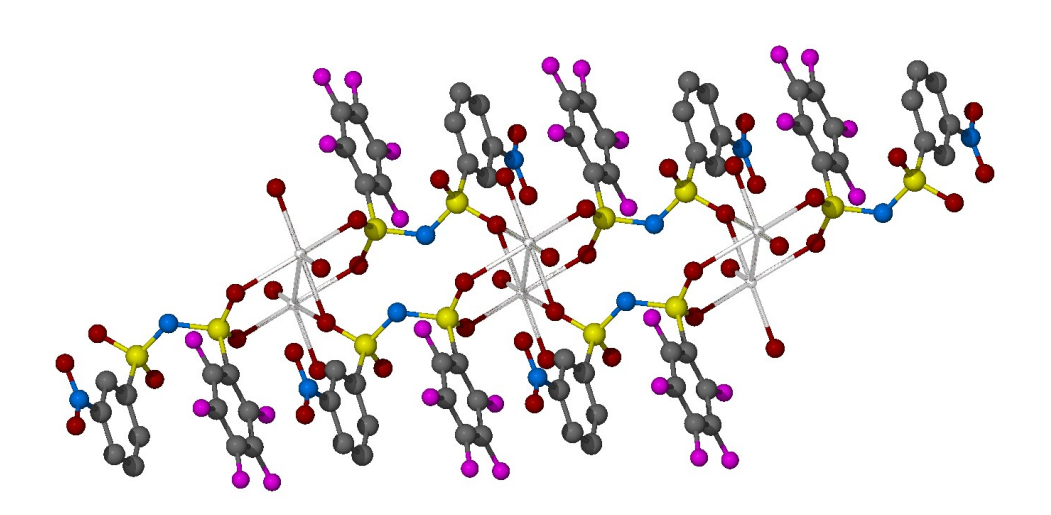


Figure 46 - Ball and stick representation of the X-ray crystallographic structure of **85** that showcases the coordination to sodium ions by ligand molecules in lattice. Atom labelling: carbon (black), oxygen (red), nitrogen (blue), fluorine (pink), sulfur (yellow), sodium (silver).

86 crystallised in the P-1 space group and was isolated as the coordinated sodium complex. In the crystal structure, two different types of sodium ion are present. All together three sodium ions are present in the asymmetric unit with a total occupancy of 2.5. The unit cell is shown in Figure 47; five sodium ions are present. Two sodium ions both have fully occupancy in the asymmetric unit with each ion being coordinated to four different ligands through an oxygen atom of each sulphonate ligand. Each sodium ion is in a distorted octahedral environment (*trans* O-Na-O bond angles are 174.06°, 160.78° and 171.10°). The remaining two coordination sites are occupied by two water molecules. Each water molecule bridges two sodium ions (bond angles for Na-O-Na are 116.20° and 116.63°). The hydrogen atoms for the bridging water molecules could not be found in the difference map.

The second type of sodium ion only has half occupancy. Again, it is coordinated to four different ligands through the oxygen atoms from a sulphonate group and to two water molecules. Unlike compound **85**, the water molecules are disordered over two positions with a 52%:48% probability of being in either position. Again, the H-atoms could not be located for these oxygen atoms from the difference map. One of the nitrogen atoms that is adjacent to two sulphonate groups is also disordered over two positions with exactly the same probability as the water molecule oxygen atoms. Furthermore, the oxygen atoms of one of the sulphonate groups is also disordered.

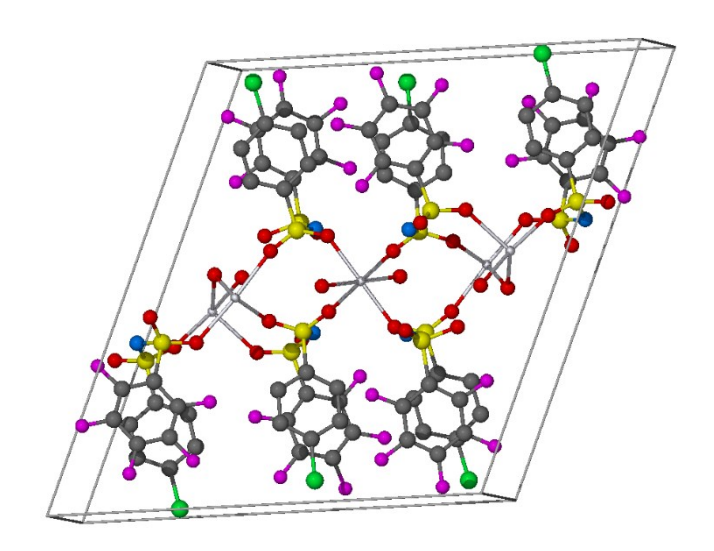


Figure 47 - Ball and stick representation of the X-ray crystallographic unit cell contents of **86** with H atoms omitted for clarity. Atom labelling: carbon (black), oxygen (red), nitrogen (blue), fluorine (pink), sulfur (yellow), sodium (silver), chlorine (green).

For atoms that are disordered over two positions, only one position is shown. The sodium ion in the centre of the unit cell has half the ligands possess π - π stacking which is evident along the b-c plane (Figure 48). The centroid-to-centroid distance between the two phenyl rings of the ligands reveal that the closest contact is 3.539 Å (symmetry code = x, y, z). The same contact distance links centroids of adjacent rings of symmetry-linked elements. This π - π distance is very similar to that observed for **85**.

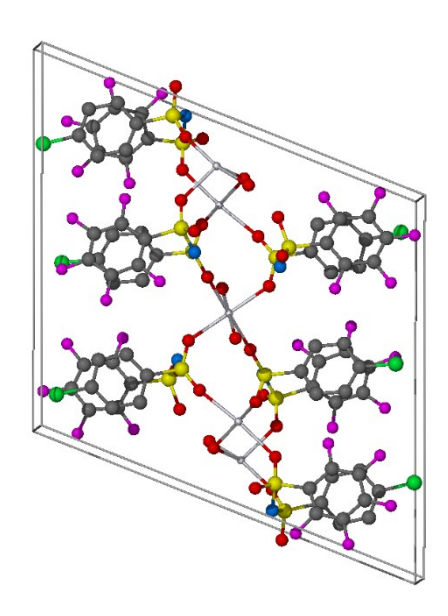


Figure 48 - Ball and stick representation of the X-ray crystallographic unit cell contents of **86** viewed along the b-c plane. H atoms have been omitted for clarity. For atoms that are disordered over two positions, only one position is shown. Atom labelling: carbon (black), oxygen (red), nitrogen (blue), fluorine (pink), sulfur (yellow), sodium (silver), chlorine (green).

3.1.2 Control ¹⁹F{¹H} NMR titration using two synthesised sulfonamides as reference compounds

Prior to determining the pK_a value of the Brønsted acid **59**, a control ¹⁹F{¹H} NMR titration was performed using two of the reference sulfonamides compounds, **84** and **85**, with known pK_a values. This enabled comparison between the calculated pK_a values from the ¹⁹F{¹H} NMR titration and literature values.⁷⁶ To ensure the sulfonamide compounds were appropriate for use throughout the pK_a determination experiment, the ¹⁹F{¹H} NMR spectra of **84** and **85** in neutral, fully protonated and fully deprotonated forms were compared. The sulfonamide

references **84** and **85** were fully protonated using an excess of a super acid, neat triflic acid, and deprotonated by addition of a very strong base, neat phosphazene base P₁-tBu. ¹⁹F{¹H} NMR chemical shift values for each fluorine environment of **84** and **85** obtained in their neutral, acidic and basic forms are reported in Table 7. As evidenced in Table 7, the neutral forms of the acids have similar ¹⁹F{¹H} chemical shifts to their fully deprotonated forms. This is indicative of a strong acid.

Table 7 – ¹⁹F{¹H} NMR spectrum chemical shifts (ppm) for sulfonamides **84** and **85** in neutral, fully protonated and deprotonated forms

	Sulfonamide 84 meta fluorine peak	Sulfonamide 84 para fluorine peak	Sulfonamide 84 ortho peak	Sulfonamide 85 ortho peak	Sulfonamide 85 para fluorine peak	Sulfonamide 85 meta peak
Neutral forms	164.31	154.07	139.33	164.26	154.02	139.27
Fully protonated form	161.09	145.98	138.1	161.04	145.92	138.04
Fully deprotonated form	164.38	154.17	139.34	164.32	154.13	139.29

The data in Table 7 provides evidence that the reference compounds **84** and **85** were suitable for the determination of the pK_a value of **59**. Since all the peaks in the ¹⁹F{¹H} NMR spectra experience adequate chemical shift upon protonation and deprotonation, this enables differentiation between the two forms to be made and thus provides observable start and end points for subsequent titrations.

A control titration was undertaken using the reference compounds **84** and **85** in order to check the accuracy of the pKa titrations. The reference compounds used had a difference in pKa values of 0.13 meaning that the accuracy of pKa values calculated was only affected by the method itself, since the difference was less than one pKa unit. The literature pKa values for compound 85 is 6.73 and 6.60 for compound **85.** The two pK_a values calculated from a titration involving compounds 85 and 84 were 6.72 and 6.61 respectively. Since the pKa difference stated in the literature was 0.13 and the difference in the calculated values was 0.11, the pKa values calculated for the reference compounds were only out by 0.02 pKa units. During this titration, equimolar amounts of both acids were used, however, the spectra could not be integrated to ensure the amounts were in a perfect 1:1 ratio and thus may not have been within 1% from each other. This was due to the peaks of the compounds being too close together to resolve at such low concentrations on a 400 MHz spectrometer. This suggests that for titrations using compounds with greater chemical shift differences in the ¹⁹F{¹H} NMR spectra that could be integrated to ensure a 1:1 ratio may have an even higher accuracy than calculated during this control titration. This titration ensured that the ¹⁹F{¹H} NMR titrations are an appropriately accurate method to determine the pKa for the phosphinic acid **59**, provided that the difference in calculated pKa values is less

than 1 pK_a unit and the spectral peaks for both acids could be integrated to within 1% of each other.

3.1.3 pKa Determination: preliminary chemical shift tests for Brønsted acid **59**

To calculate the pK_a value of **59** using the equations previously outlined, pages 112-113, the ¹⁹F{¹H} NMR spectra of **59** and one of the reference compounds, sulfonamides **84-86**, were required in different forms. The chemical shifts of the fully protonated, fully deprotonated and partially protonated and deprotonated forms of **59** with one reference sulfonamide was required. This was best achieved by fully protonating **59** and a reference compound within the same sample NMR tube, and then deprotonating with aliquouts of base to obtain a mixture of partially protonated and deprotonated forms. Aliquots of base would continue to be added until the fully deprotonated forms of **59** and the reference compound were obtained.

In the first titration, compound **59** and reference **84** (5.71 mM) were dissolved in 0.7 mL acetonitrile. Hexafluorobenzene in CD₃CN (7.18 × 10⁻³ mol dm⁻³), was used as an internal standard to allow the compound peaks in the spectra to be referenced to its single ¹⁹F signal at –164.90 ppm. This would enable accurate values for the chemical shifts to be obtained throughout the experiment as hexafluorobenzene is not susceptible to the acid or base used in the titration. Compounds **59** and **84** were then analysed by ¹⁹F{¹H}NMR spectrometry as fully protonated and fully deprotonated forms, as well as partially protonated and deprotonated forms. The spectra from this preliminary chemical shift test of **59** using **84** as a reference is shown in Figure 49 as an example.

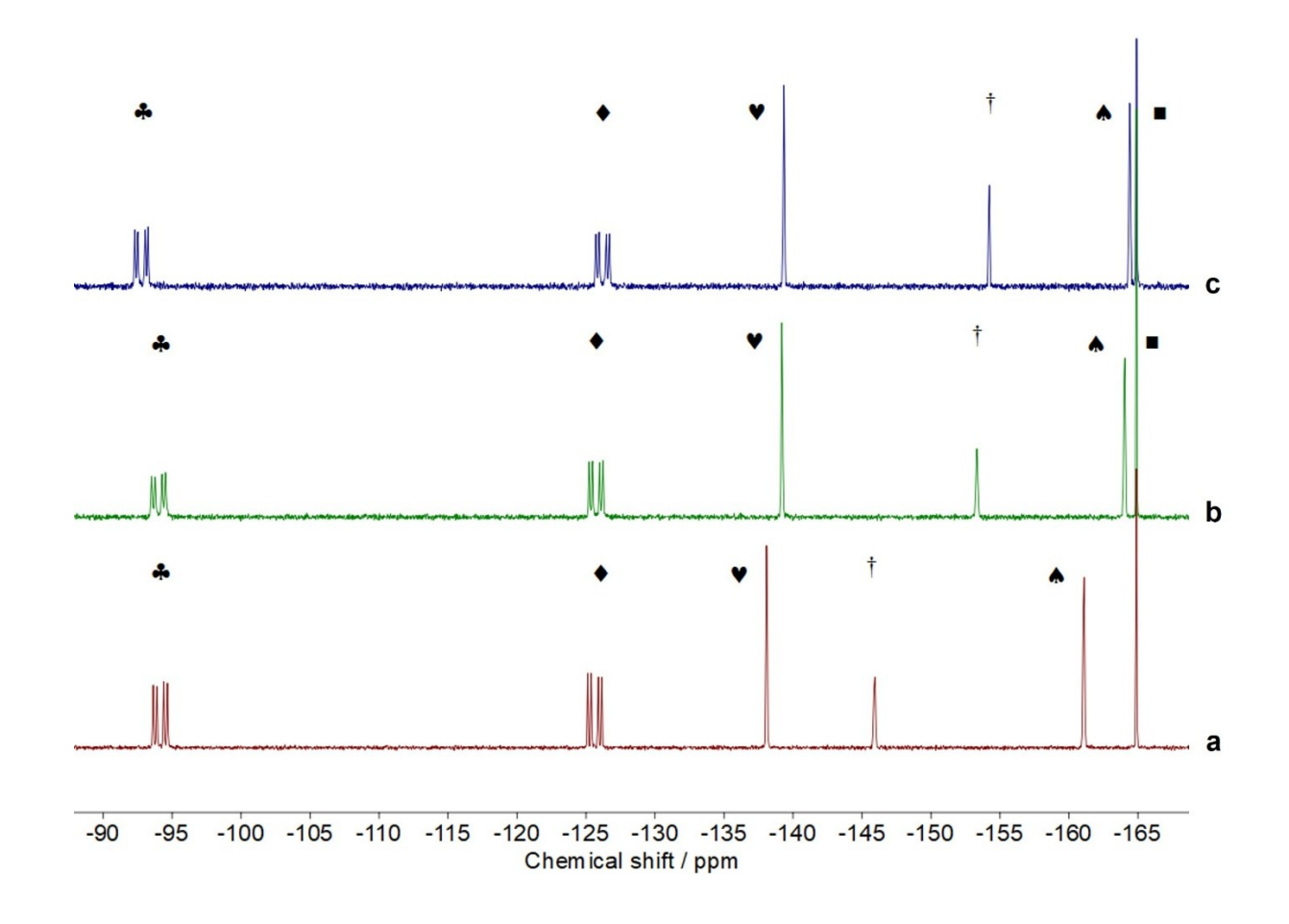


Figure 49 – Exemplar ¹⁹F{¹H} NMR spectra from a preliminary chemical shift test of Brønsted acid **59** using sulfonamide **84** as a reference. Spectrum 49a represents the fully protonated compounds **59** and **84**, spectrum 49b represents the partially protonated and deprotonated forms of **59** and **84** and spectrum 49c represents the fully deprotonated forms of compounds **59** and **84**.

Figure 49a is the ¹⁹F{¹H} NMR spectrum that correlates to the fully protonated forms of Brønsted acid **59** and reference sulfonamide **84**, which was obtained using neat triflic acid. Figure 49b correlates to the mixure of partially protonated Brønsted acid **59** and reference sulfonamide **84**. Lastly, Figure 49c correlates to the fully deprotonated forms of **59** with **84**. There was a significant chemical shift in the fluorine peaks (ca. 1-2 ppm) between the fully protonated and fully deprotonated spectra of 59 in the presense of the reference sulfonamides 84-86: this is exemplified in Figure 49 wherein 84 was used as a reference. This confirmed the methodology could be used to determine the pKa value of the Brønsted acid 59 using a reference sulfonamide; since the equations used to determine the pK_a value require a change in the chemical shifts for both compounds within the same NMR sample tube upon protonation and deprotonation. Despite the low concentrations within the NMR sample due to the low solubility of **59**, the peaks were sufficiently resolved from one another. Each peak could therefore be integrated separately; enabling integration of the peaks to ensure the compounds were titrated in a 1:1 ratio. This allowed the pKa values from each titration to be calculated irrespective of the concentrations.

The two doublet of doublet peaks, ♣ and ♦ at –94.15 ppm and –125.63 ppm in Figure 49a are the fluorine environments of **59**, whereas the three peaks ♥, † and ♠ at –138.11 ppm, –145.91 ppm and –162.35 are the *meta-*, *para-* and *ortho-*fluorine signal respectively of compound **84**. All of these peaks provide the ppm values for the fully protonated forms of **59** with **84** in acetonitrile after addition of the super acid triflic acid to the mixed system. The strong base phosphazene P₁-¹Bu, was then added to partially deprotonate the system, which resulted in the ¹¹9F{¹H} spectrum depicted in Figure 49b. The peaks ♣ and ♦ for **59** shifted to

-93.88 ppm and -126.23, whilst the peaks for reference compound, 84, ♥, † and ♠ shifted to -139.18, -153.33 and -164.04 ppm. To ensure the mixture was fully deprotonated, the system was treated with an excess of the same strong base, until the peaks for both compounds no longer exhibited further chemical shift; the resulting ¹9F{¹H} spectrum obtained is shown in Figure 49c. The signals observed in the ¹9F{¹H}NMR spectrum (Figure 49c) correlated to the complete deprotonated forms i.e. -92.78 ppm and -126.21 ppm for 59, and -139.35 ppm, -154.21 ppm and -164.42 ppm for 84. The pKa value of 59 could have been calculated using these values alone, however, to improve the accuracy of the value determined, ¹9F{¹H}NMR spectra were required from multiple points throughout the entire NMR titration.

This preliminary test was then repeated twice more using Brønsted acid **59** with the other reference sulfonamides synthesised, **85** and **86**. It was concluded from the chemical shifts observed in the preliminary tests of the mixed systems that the methodology could be used to determine the pK_a of the potential Brønsted acid as previously described. The spectra obtained in all tests were relatively weak due to the low solubility of **59**. Although the solubility of **59** is low in acetonitrile, the number of transients used to generate a spectrum was increased to 64 from 8. This could have been increased to further improve the resolution and reduce the spectral noise at the baseline, however, this would have impacted the experiment time considerably. Each spectrum took 7 minutes to acquire. For a 40-point titration this required over 4 and a half hours of spectrometer time. This does not include the time to make the acid and base solutions or the time required to ensure that each compound integrated 1:1 in the ¹⁹F{¹H} NMR spectrum to reduce error. Neither did that time include the time between spectra collection which

consisted of sample tube ejection, the refitting of the sample tube to the Konte equipment in another laboratory, and subsequent addition of base and sample reinsertion. The fastest this could be done was around 5 minutes, however, on average the time between spectra collection doubled the experiment time. To effectively run each titration at least 10 hours was required. Since only the chemical shift values were required from this experiment, increasing the number of scans for minimal improvement on the quality of the spectra was not feasible. Each spectrum obtained consisted of 64 scans and a recycle delay of 3 seconds was used. A T₁ of 0.04 was calculated using a saturation recovery experiment, according to the literature.⁸¹

3.1.4 Optimised ¹⁹F NMR titration data

The optimised full ¹⁹F{¹H}NMR titration of Brønsted acid **59** with reference compounds **84-86** were undertaken to obtain data for the accurate determination of the pK_a value of **59**. The extreme chemical shift values for the fully protonated and fully deprotonated mixed systems from the preliminary tests were used as starting and end points respectively for the titrations. The chemical shift values, recorded in Table 8, for both the fully protonated and fully deprotonated forms of compound **59** with the reference sulfonamides **84-86** were obtained from spectra of the final, optimised experiments.

Table 8 - Chemical shift values used for the fully protonated and fully deprotonated forms of **59** relative to the reference standards **84-86** in the ¹⁹F{¹H} NMR titration experiments performed.

	Compound 84 up-	Compound 84 para	Compound 84	Compound 59 up-	Compound 59
	field peak	fluorine peak	downfield peak	field peak	downfield peak
Fully protonated	-161.08	-145.92	-138.08	-125.63	-94.14
Fully	-164.39	−154.23	-139.33	-126.14	-92.78
	Compound 85 up- field peak	Compound 85 para fluorine peak	Compound 85 downfield peak	Compound 59 up-	Compound 59 downfield peak
Fully protonated	-161.31	-146.01	-138.11	-125.51	-94.07
Fully deprotonated	-164.66	−154.38	-139.22	-126.21	-92.80

	Compound 86 up-field peak	Compound 86 para fluorine peak	Compound 86 downfield peak	Compound 59 up-field peak	Compound 59 downfield peak
Fully protonated	-161.11	-146.15	-138.01	-125.47	-93.99
Fully deprotonated	-164.57	-154.76	-139.19	-126.08	-92.51

Despite the values from Table 8 enabling the pK_a value of **59** to be calculated, the chemical shift values from each titration point were utilised in the pK_a calculation to ensure the value determined was accurate. The individual ¹⁹F{¹H} NMR spectra from each titration point were stacked and analysed simultaneously in each titration undertaken. The results from the optimised ¹⁹F{¹H} NMR titration using reference compound **84** against phosphinic acid **59** are shown in Figure 50 as an example.

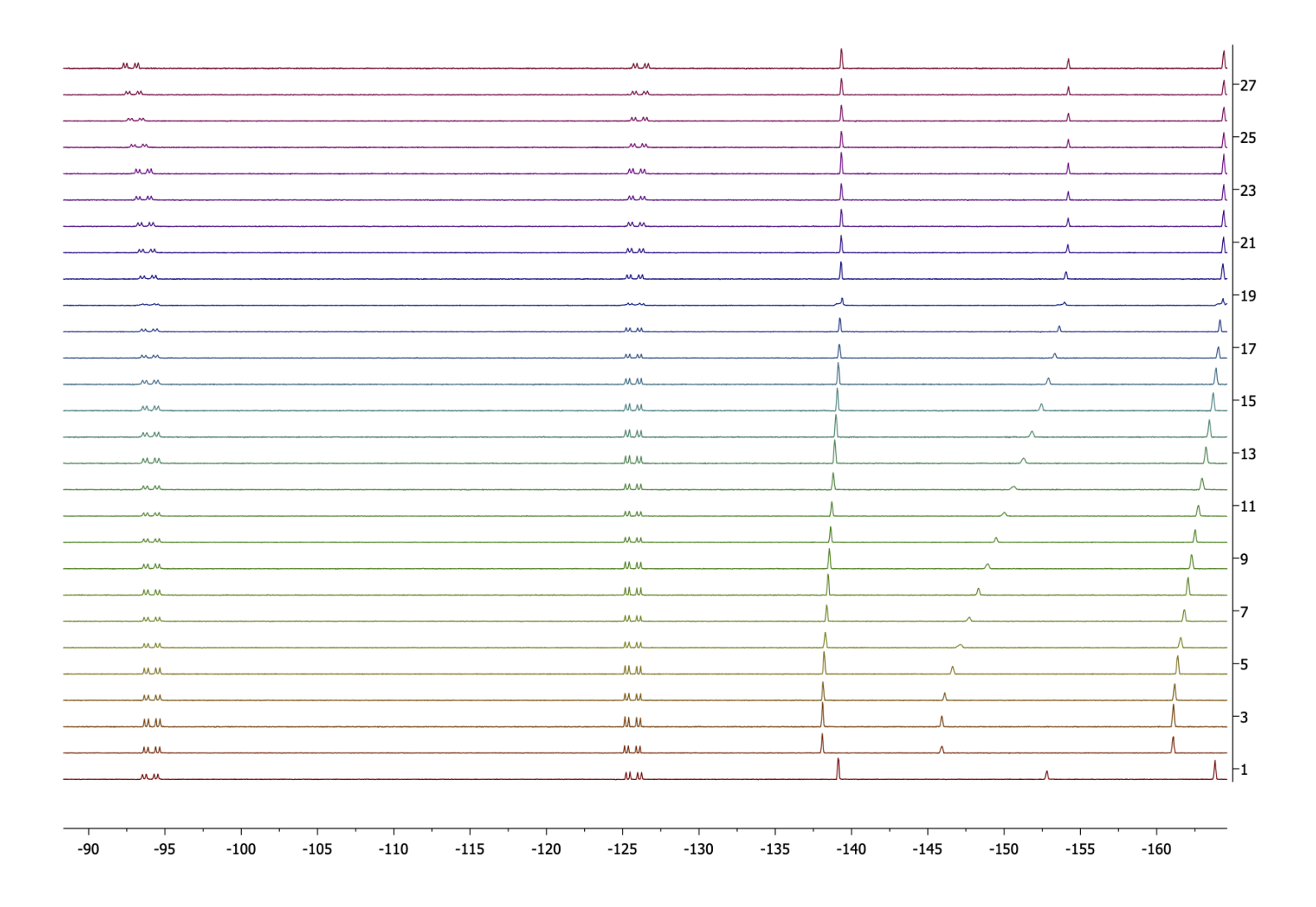


Figure 50 - Stacked ¹⁹F{¹H} NMR spectra results from the optimised titration of **59** using reference compound **84**.

The data from spectrum 1 was used to ensure the phosphinic acid **59** and the reference compound **84** were within 1% integral size of each other (integrals should be 1:1) prior to fully protonating the samples to ensure equal molarities were present in the sample. The integrations of **59** and **84** equating to 1:1 showed that the concentrations of both compounds were equal to within 1% of each other. The concentration of the sample is not required to calculate the change in pK_a as long as the molar amounts are equal.⁷³ The data from spectrum 1 also accounted for the observed values, δ_i^{obs} and δ_j^{obs} for the pK_a calculation, where *i* and *j* represent phosphinic acid **59** and reference compound **84** respectively. Spectrum 2 in the stacked spectral plot shown in Figure 50, represents the starting point of the titration. Each subsequent spectrum, spectra 3 to 27, correlate to the addition of 20 µL ¹Bu-P₄ phosphazene base in acetonitrile solution (4.56 mM) until the end point was reached and both compounds were fully deprotonated (spectrum 29, Figure 50). The peak intensities decrease after each addition of base. This is due to the samples being effectively diluted during the course of the experiment.

It is stated in the literature that the bigger the change of the chemical shifts, the smaller the uncertainty of the determined pK_a value.⁷⁵ Hence the chemical shift values for the downfield peak of phosphinic acid **59** and the central peak of reference compound **84** were used for the pK_a determination calculations, where **59** is *i* and **84** is *j*. Depending on the spectrum used for the chemical shift values of the partially deprotonated form, the change in pK_a calculated varied slightly. Therefore, the following calculation was performed using data from all spectra recorded throughout the titration and an average was taken. The chemical shift values from the titrations were used to calculate the pK_a of **59** using Equation 1 and **84** from the literature,⁷³ as shown below. The twelfth reading from the 27-point

titration was used here as the values for the partially protonated and partially deprotonated forms of **59** and **84**, represented by i and j, as an example.

$$=\frac{K_{a_i}}{K_{a_i}} = \frac{(94.06 - 92.755)(145.89 - 151.8)}{(151.8 - 154.21)(94.15 - 94.06)}$$

$$=\frac{K_{a_i}}{K_{a_i}}=35.6$$

$$\Delta p Ka = log \frac{K_{a_i}}{K_{a_i}} = \pm 1.55$$

The average of the values calculated for each spectrum were taken to give a final change in pK_a value of ± 1.73 . As the reference compound deprotonated first in all titrations attempted, this confirmed they were the stronger acid in each experimental system and therefore had the lowest pK_a, which in this case for **84** is known to be $6.60.^{75}$ This enabled the pK_a of **59** to be determined as 8.33 using reference **84**. This provided evidence that the difluoromethyl substituents of Brønsted acid **59** significantly lower the pK_a value in comparison to Brønsted acids with similar structures. The BINOL-phosphinic acids, which were grouped together on the scale by Rueping *et al.*, shown in Figure 40, are around half the pK_a value of **59** with pK_a values of 12-14. The results from all optimised titrations are shown in Table 9.

Table 9 - pKa values determined by $^{19}F\{^1H\}$ NMR titrations.

Compound	pK _a value calculated	Reference used
O OO O F S N S F F F 84	6.73	O OO O F S N S F F F NO ₂ 85
O OO O F N F F NO ₂ 85	6.60	O_2N O_2N O_3 O_5 $O_$
F F O P O H F F S S S S S S S S S S S S S S S S S	8.33	$O_{2}N \xrightarrow{O_{2}O_{0}O_{0}F} F$ $H F F$ $R F$ $R F$ $R F$ $R F$ $R G$ R
F F O OH F F	8.54	O OO O F NO ₂ F F NO ₂ 85

Unfortunately, since the pK_a values calculated for **59** using reference sulfonamides 84 and 85 were greater than one pKa unit from the reference compounds, the values determined were not as reliable as possible. 73 although they are comparable to one another. A more accurate pKa value for 59 using the third reference synthesised, sulfonamide **86** was calculated to be 8.12. The reference compound 86 is a slightly weaker acid than 84 and 85, with a higher pKa value of 7.57.75 The reference compound is the weakest acid of the reference compounds due to the decreasing electron withdrawing properties of the chloro- group in comparison to the nitro-group. The weaker electron withdrawing properties of the chlorine atom enables a stronger N-H bond for the acidic proton and so the compound does not deprotonate as readily. Thus, **59** is a weaker acid in comparison to the other references (84 and 85) which possess a nitro-substituent. The higher pK_a value for the third reference was closer to the true pK_a value of phosphinic acid 59 and therefore a more accurate pKa value was determined using 86 as a reference, as the change in pKa should, in theory, be less than one pKa unit different.

As reported in the literature, the greater the change of the chemical shifts, the smaller is the uncertainty of the determined pK_a value.⁷³ Therefore the compound peaks with the greatest chemical shifts throughout the titrations were used to calculate the most accurate pK_a value. In this case, it was the *para* signal for the reference compound **86** and the most downfield signal for the phosphinic acid **59**. The pK_a values reported in Table 9 were calculated using the equations previously described. As with the previous calculations, an average value from all spectra obtained at each titration point were used for δ_i^{obs} and δ_j^{obs} to improve accuracy and the final pK_a value calculated using sulfonamide **86** was 8.12. The spectra for

this titration were integrated to a 1:1 ratio, meaning that the amounts of acid **59** and reference **86** were equal to within 1% of each other. The control titration using two sulfonamides with known pK_a values provides evidence that this optimised titration using **86** as a reference has determined the most accurate result for the pK_a of the phosphinic Brønsted acid **59**, as 8.12 ± 0.02 .

3.2 Conclusions

Three sulfonylamide reference compounds (**84-86**) were synthesised in a two-step procedure in yields of 5-27% and characterised using ¹H, ¹³C and ¹⁹F{¹H} NMR and mass spectrometry. The characterisation data obtained agreed with data reported in the literature. A control titration involving reference compounds **84** and **85** confirmed that an ¹⁹F{¹H} NMR titrations could be used to obtain accurate pK_a values as a pK_a difference of 0.13 was obtained. This compares well with the literature pK_a values of 6.60 and 6.73 for **84** and **85** respectively, which is a difference of 0.11.

The pK_a of **59** was determined using a ¹⁹F{¹H} NMR titration method. Three titrations were conducted, and for each titration a different reference compound was employed. The method involved fully protonating 59 and the reference compound using the superacid triflic acid. Resultingly, the strong base phosphazene base P₁-tBu was added in aliquots and a ¹⁹F{¹H}NMR spectrum was acquired after each addition. The pK_a values were determined to be 8.33, 8.54 and 8.12 using reference compounds 84, 85 and 86 respectively. The pKa value of 8.12 was considered the most accurate value calculated, due to the difference in pKa to the reference compound being less than 1 pKa unit different to 59. This pKa value shows a significant increase in acidity in comparison to other BINOLphosphinic acids, which tend to have pK_a values between 12-14.²⁰ This increased acidity is due to the substitution of two difluoromethylene groups at the α -position to the phosphorus atom. The pK_a values obtained using reference compounds 84 and **85** (8.33 and 8.54 respectively) were not considered as accurate as the value 8.12 obtained using **86** as a reference, due to them having pK_a values greater than one unit from the Brønsted acid **59**. However, there is strong correlation in terms

of the pK_a values obtained being in the range 8.12-8.54. This pK_a range determined is significant as it provides evidence that the CF₂ substitutions have successfully increased the acidity of the BINOL-derived phosphinic acid.

3.3 Future Work

This work has the potential to be extended by increasing the size of the library of target fluorinated compounds for pK_a determination by the ¹⁹F{¹H} NMR titration. Mikami *et al.*²⁵ increased the number of fluorine atoms of the phosphinic acid **59** by substituting the methylene groups of the 7-membered ring with CF₂CF₃ groups, as well as the CF₂ groups that were investigated in this work. The pK_a of the compounds with CF₂CF₃ groups near the acid site could be determined using this ¹⁹F{¹H} NMR titration method. The library could also have been extended by fluorinating the phosphinic acid **59** even further by substituting the same methylene groups with larger CF₂CF₂CF₃ groups. The synthesis of novel phosphinic acids, based on acid **59**, fluorinated at the 3, 3'-positions could have been investigated and the pK_a of these novel compounds could have been determined by this method.

Utilising Brønsted phosphinic acids in asymmetric catalysis

4.1 Introduction: Applications of phosphinic acids in asymmetric catalysis

A substantial area of organic synthesis today is the creation of novel, chiral phosphonic acids for use in asymmetric catalysis. Since the first synthesis of the new class of phosphonic ligands, derived from BINOL, many chiral, phosphorus-based ligands today are designed to have a similar atropisomer backbone. 10, 12, 15-17, 20, 41, 71 The atropisomerism associated with such structures enables high enantioselectivity for many reactions when employed as phosphorous-based Brønsted acid catalysts. An early example of the asymmetric application of these catalysts, obtaining high enantiomeric excess (*ee*) values, is in the direct Mannich reaction, reported by Terada, Akiyama and co-workers (Figure 51). 42, 45

87

88

Ar = Ph, ee(%) = 95
Ar =
$$\rho$$
-MeC₆H₄, ee(%) = 98
Ar = ρ -FC₆H₄, ee(%) = 98
Ar = ρ -MeC₆H₄, ee(%) = 92

 $R = 4-\beta$ -naph- C_6H_4

Figure 51 - Early application of BINOL-derived phosphoric acid atropisomers in the direct Mannich reaction by Terada and Uraguchi.⁴⁵

The application of phosphoric acid **90** by Terada and Uraguchi in the direct Mannich reaction of 2,4-pentadione **88** with the aldimine **87**, shown in Figure 51, obtained the corresponding adduct **89** with *ee* values that sparked early interest in the area. With *ee* values up to 98% and product yields of 99% in multiple asymmetric conversions, the transition states of these new BINOL derived atropisomer catalysts were investigated. The nine-membered zwitterion transition state of a BINOL-derived phosphorous atropisomer with an aldimine, was proposed by Yamanaka *et al.*, Figure 52.⁸²

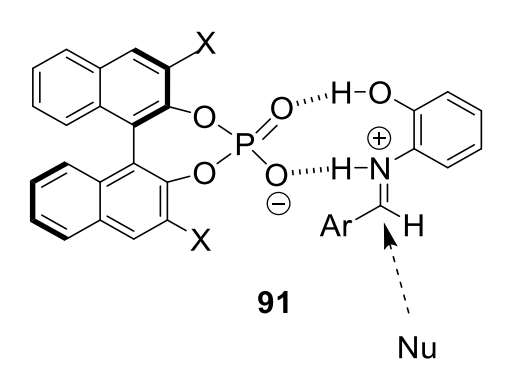


Figure 52 - Nine-membered zwitterion transition state proposed by Yamanaka *et al.*, showing the dual interaction of new chiral phosphoric Brønsted acids.

The transition state highlighted in Figure 52 is just one example published in 2007, though more examples were reported at the time. 82, 83 Though mono-coordinated, smaller transition states were proposed, mechanistic studies showed the nine-membered, dual-activation transition states lead to the high ees obtained from using the BINOL-derived phosphoric acids. 82 The examples reported form similar nine-membered cyclic transition states, similarly to **91** with aldimines (Figure 52). 42, 82 The di-coordination of the BINOL-derived phosphorous acid catalysts made them successful in many other chiral conversions, another very well-known example is in the Nazarov cyclisation reaction, initially reported by Rueping and co-workers (Figure 53). 84

Figure 53 - Nazarov cyclisation reaction catalysed by Brønsted phosphorous acids, published by Rueping *et al.* 2007.⁸⁴

The Nazarov cyclisation reaction depicted in Figure 53 was particularly poignant as it was the first publication of an organocatalytic electrocyclisation reaction.

Using the phosphoric acid catalysts **94a-e**, where X = OH, the product enantiomer **93a** was obtained with *ees* of 82% and **93b** with *ees* of 96% when the catalysts **94f-g** were employed. The application of phosphoric acids to successfully obtain enantiopure products are important not only in synthetic conversions as the cyclisation highlighted (Figure 53), but are paramount in the production of pharmaceutical and biologically relevant compounds. An early example of the application of the BINOL-derived phosphorous atropisomers as catalysts towards biologically active compounds was reported by Terada and Sorimachi in the synthesis of 1-indolyl-1-alkylamine derivatives, **97** (Figure 54).

Figure 54 - Friedel-Crafts reaction of indole **95** with imine **96**, catalysed by the BINOL-derived phosphoric acid **94a** to obtain the biologically active adduct **97** in high enantiomeric excess.⁸⁵

Terada and Sorimachi investigated the use of the phosphoric acid catalyst **94a** in the Friedel-Crafts reaction shown in Figure 54 since it is a very powerful reaction in the formation of new carbon-carbon bonds. The example shown was the first enantioselective Friedel-Crafts reaction of electron-rich alkenes activated by any chiral Bronsted acid catalyst.⁸⁵ The pair succeeded in providing an easy and practical method of accessing enantioenriched 1-indoyl-1-alkylamine derivatives, from indole **95**, with biological importance.⁸⁵ More recently, Mikami and coworkers have tested their novel fluorinated phosphinic acid catalysts in a Friedel-Crafts reaction with similar reagents, Figure 55.²⁵

4.1.1 Aims

Mikami *et al.* utilised their new class of perfluoroalkyl phosphinic acids in the Freidel-Crafts reaction shown, Figure $55.^{25}$ The group employed the catalysts shown for the Friedel-Crafts reaction towards tosylamide **100** and found that, as predicted, the more fluorinated the phosphinic acid catalyst at the α -site to phosphorous, the better catalytic ability of the atropisomer.

Figure 55 - Procedure for catalytic Friedel-Crafts reaction of (*E*)-*N*-benzylidene-4-methylbenzensulfonamide with indole.

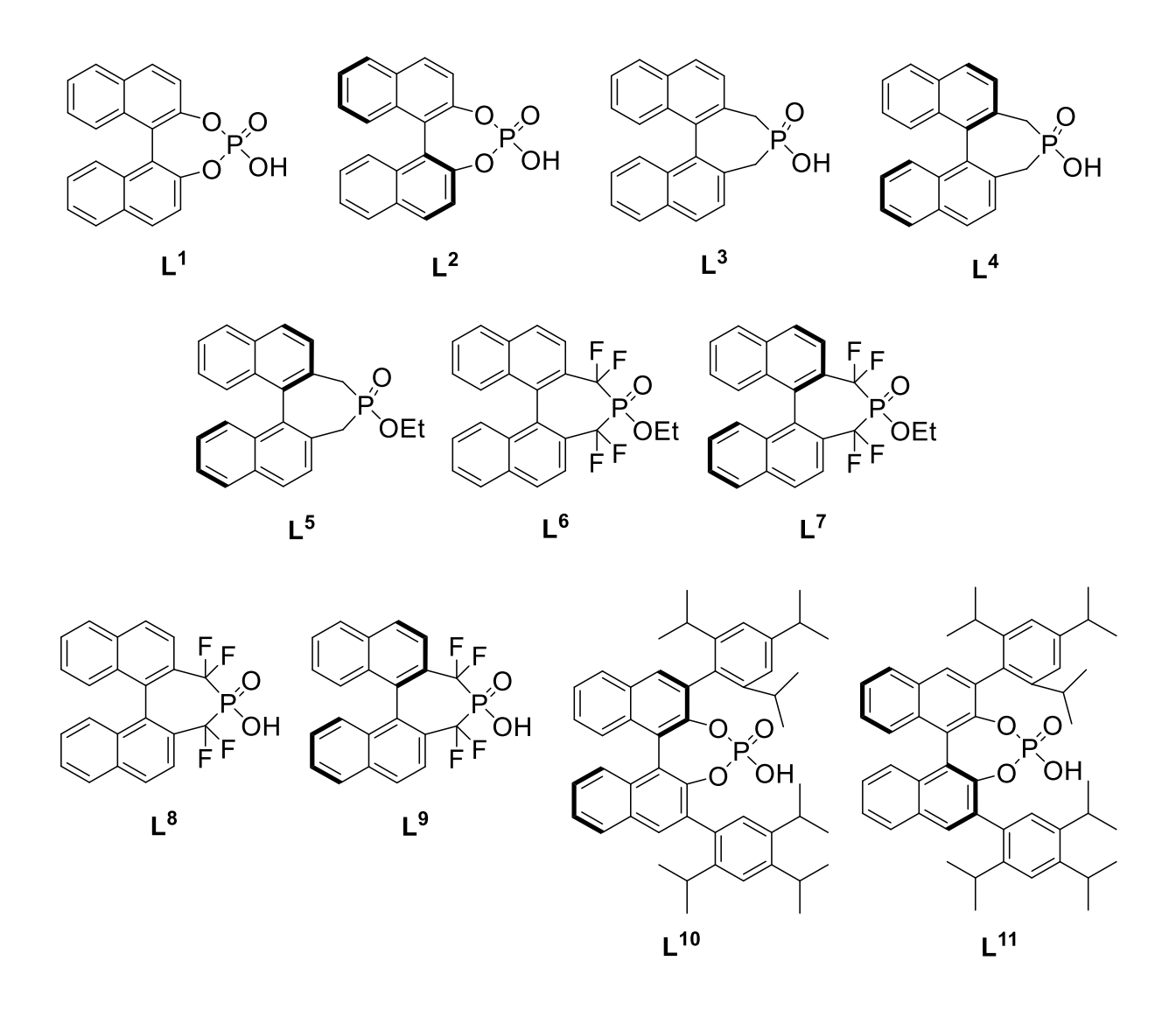
The highest yield reported was 89% and obtained utilising catalyst **101a**, with an enantiomeric excess (*ee*) value of 52%. Though the highest *ee* value reported (64%) was also obtained using this catalyst, the yield for this particular trial was a moderate 60%. Both the *ee* values and yields decreased from these results with a decreasing number of fluorine atoms in the catalysts. Catalyst **c** produced tosylamide **100** with 56% yield and an *ee* value of just 9%. The fluorinated catalysts did, however, produce greater yields and *ee* values than phosphoric acid, the non-fluorinated catalyst without groups at the 3,3'-positions trialled, catalyst **101d**. The yield using this catalyst was 42% and *ee* values obtained were 11%, though interestingly this catalyst produced a higher proportion of the (*S*) isomer instead of the (*R*). The use of 3,3'-substituted phosphoric acid, catalyst **101e**, produced **100** with a yield of 80% and *ee* of 49%, comparible to the non-substituted fluorinated acid catalyst **101a**, though the fluorinated catalyst **a** did provide the best results in this investgation.

Despite Mikami and co-workers showing the significance of fluorinating at the α -position to the phosphorous atom for this class of catalysts, the ee values and yields obtained for the Friedel-Crafts reaction have the potential to be improved on.

This chapter aims to utilise the catalysts, previously synthesised in this work, in this Friedel-Crafts reaction to improve the enantiomeric excess values and yields obtained in literature.²⁵ More catalysts will also be trialled, particularly for a direct comparison of the fluorinated acid **101c** with the non-fluorinated counterpart, compound L⁴, which has not been previously investigated, Figure 56. The catalyst L⁷ has not yet been reported in the literature and is another new entry for this particular reaction.

4.1.2 Results and discussion

To further investigate the phosphinic acid class of asymmetric catalysts, a larger library of catalysts than in the Mikami group publication were used in the Friedel-Crafts reaction towards tosylamide **100**, Figure 55.²⁵ The catalysts (and racemic control catalysts) that were employed in the Friedel-Crafts reaction have been highlighted in Figure 56. Catalyst L¹ and L² were employed for the direct comparison of the racemic yield to the chiral, as well as for a comparison of the ee values to the previous literature.²⁵ L³ and L⁴ were utilised as catalysts not yet reported for this reaction and for use as a direct comparison to the fluorinated catalysts, L³ and L⁴ were used to compare the catalytic ability of the novel chiral ester L⁻ synthesised during this work. The catalysts L¹⁰ and L¹¹¹, (R) and (S)-TRIP, respectively, are frequently used in numerous asymmetric reactions and have been included in this study to compare the results obtained from using phosphoric acid catalysts with substituents at the 3,3'-positions of the atropisomeric back bone. The results are summarised in Table 10.



 $L^1 = (rac)-1,1'-binaphthyl-2,2'-diylhydrogenphosphate$

L²= (S)-1,1'-binaphthyl-2,2'-diylhydrogenphosphate

 $L^3 = (rac)-4,5$ -dihydro-5-hydroxy-3H-dinaphtho-[1,2-c:2',1'-e]-phosphepine-5-oxide

 $L^4 = (R)-4,5$ -dihydro-5-hydroxy-3H-dinaphtho-[1,2-c:2',1'-e]-phosphepine-5-oxide

 $L^5 = (R)$ -ethyl-2,2'-bis(methylene)-1,1'-binaphthyl phosphinate

L⁶ = (rac)-ethyl 2,2'-bis(difluoromethylene)-1,1'-binaphthyl phosphinate

 $L^7 = (R)$ -ethyl 2,2'-bis(difluoromethylene)-1,1'-binaphthyl phosphinate

 $L^8 = (rac)$ -bis(difluoromethylene)-1,1'-binaphthyl phosphinic acid

 $L^9 = (R)$ -bis(difluoromethylene)-1,1'-binaphthyl phosphinic acid

 $L^{10} = (R)$ -TRIP

 $L^{11} = (S)$ -TRIP

Figure 56 - Catalysts employed in the Friedel-Crafts reaction of (E)-N-benzylidene-4-methylbenzensulfonamide with indole.

Table 10 - Catalyst screening results for the reaction of (*E*)-*N*-benzylidene-4-methylbenzensulfonamide with indole to produce tosylamide **100**.

Catalyst	Cat. molar eq.	Yield	ee
L ¹	0.1 eq	49%	N/A (rac)
L^2	0.1 eq	38%	7%
L^3	0.1 eq	90%	N/A (rac)
L ⁴	0.1 eq	9%	15%
L ⁵	0.1 eq	28%	34%
L ⁶	0.1 eq	78%	N/A (rac)
L ⁷	0.1 eq	34%	40%
L ⁸	0.1 eq	87%	N/A (<i>rac</i>)
L ⁹	0.1 eq	57%	39%
L ¹⁰	0.1 eq	48%	48%
L ¹¹	0.1 eq	19%	17%
	L ¹ L ² L ³ L ⁴ L ⁵ L ⁶ L ⁷ L ⁸ L ⁹ L ¹⁰	L¹ 0.1 eq L² 0.1 eq L³ 0.1 eq L⁴ 0.1 eq L⁵ 0.1 eq L° 0.1 eq L³ 0.1 eq L³ 0.1 eq L³ 0.1 eq L¹0 0.1 eq	L¹ 0.1 eq 49% L² 0.1 eq 38% L³ 0.1 eq 90% L⁴ 0.1 eq 9% L⁵ 0.1 eq 28% L° 0.1 eq 78% L° 0.1 eq 34% L° 0.1 eq 87% L° 0.1 eq 57% L¹0 0.1 eq 48%

Entries 1 and 2, Table 10, show the screening of racemic and (S)-phosphoric acid, L¹ and L², respectively. The product obtained using the chiral acid L² gave a low ee value of 7%. Despite this being quite a poor enantioselectivity, it is comparable to the literature value of 11%.²⁵ Interestingly, the racemic control gave a higher yield of the racemic mixture of toslyamide 100. This was the case in the comparisons for all racemic controls against their chiral counterparts, highlighting the need for better asymmetric catalysts for increased enantiocontrol. Comparing entries 5 and 7 for catalyst L⁵ against the novel fluorinated ester catalyst L⁷, the fluorinated new ester catalyst obtained the product in a higher yield of 34% with an ee of 40%. When comparing this to the ee of 9%, obtained using phosphinic acid **101c**, reported by Mikami et al. the novel ester is a significant improvement for the application in this Friedel-Crafts reaction. It may be considered as effective as the perfluoro phosphinic acid catalysts 101a and 101b. Surprisingly, it was as successful as the fluorinated phosphinic acid catalyst L⁹, which obtained **100** with an ee value of 39% in a 57% yield. This result (entry 9, Table 10) is also an improvement on both the yield and ee obtained in the literature using acid 101c, previously discussed.²⁵ A key comparison to be made is between entry 4 and entry 9, for L⁴ and L⁹ respectively. These results show the direct comparison between the fluorinated and non-fluorinated phosphinic acid catalysts, which has not yet been investigated in the literature. There is a clear correlation between fluorination and catalytic ability for this asymmetric reaction. The use of the non-fluorinated catalyst L⁴ provided **100** in a relatively low yield of 9%, whereas the fluorinated catalyst L⁹ obtained yields of 57%. The enantiomeric control using the fluorinated Bronsted acid L⁹ was also significantly higher than the non-fluorinated acid L⁴ with an ee value of 15% obtained by L⁴ and 39% for L⁹.

The racemic and chiral fluorinated catalysts L^8 and L^9 were both better at catalysing the Friedel-Crafts reaction than both (R) and (S)-TRIP, obtaining greater yields. Surprisingly, L^9 also provided **100** in better ee than (S)-TRIP, L^{11} . These results suggest that the phosphinic catalysts, fluorinated at the α -positions to phosphorous, are akin to larger catalysts, such as L^{10} and L^{11} . By extension, substituting these new fluorinated phosphinic catalysts at the 3,3'-positions to add steric hindrance, may produce greater asymmetric catalysts still.

4.1.3 Conclusion

Numerous catalysts were screened in the asymmetric Friedel-Crafts reaction towards tosylamide **100**, including the novel fluorinated ester catalyst L⁷. The new ester provided positive results, obtaining **100** in a better yield and *ee* than the non-fluorinated ester L⁵, showing the fluorination of the ester proved to be beneficial for this asymmetric conversion. The new ester L⁷ was also a comparable catalyst to the fluorinated phosphinic acid L⁹, with similar yields and *ee* values obtained for both catalysts. The screening of the catalyst L⁹ also showed a significant improvement to the *ee* values previously reported for this acid, with similar yields of 57% and *ee* of 39% from 9% in the literature. The direct comparison between catalyst L⁴ and L⁹ provides significant evidence that fluorinating the BINOL-derived phosphinic acid catalysts at the α-positions to the phosphorous atom enhanced both catalytic ability and enantiomeric control when utilised in this Friedel-Crafts reaction.

4.1.4 Future Work

The work in this chapter could be improved in the future by determining the ee values more accurately, utilising a mass spectrometry method with a chiral column; as opposed to the method in this work which used a polarimeter. This work may have also been extended by using this library of catalysts in further asymmetric reactions. For example, the Nazarov cyclisation and Diels-Alder reactions, previously discussed in other chapters, may have been investigated by employing these asymmetric catalysts.^{17, 18}

5. Experimental

5.1 Chemicals

All reagents used for synthetic procedures were of analytical grade, purchased from Fisher Scientific, Sigma Aldrich, Strem Chemicals, Fluorochem or Acros Organics and were used as received, unless otherwise stated. All reactions were carried out in inert conditions under either argon or nitrogen using standard Schlenk techniques. The anhydrous solvents THF, CH₂Cl₂, Et₂O and toluene were dried and obtained using an Innovative Technology Pure Solv solvent drying system and stored over molecular sieves of appropriate sizing for the solvent. The solvents used were of general purpose or HPLC grade and were purchased from Fisher Scientific. Thin layer chromatography analysis was performed using Sigma Aldrich silica gel 60 F254 aluminium plates and visualised by UV light. If required, basic potassium permanganate was used as a stain for visualisation. Purification by column chromatography was performed using silica gel pore size 60, 230-400 mesh and for flash chromatography purification. The eluents used for each compound are stated. When required, acetonitrile, tetramethylethylenediamine, ethyl dichlorophosphate and triethylamine were dried as follows: acetonitrile was stored over phosphorous pentoxide for a minimum of two days prior to distillation and storage in Schlenk flasks under argon; tetramethlethylenediamine was refluxed for a minimum of 2 h over lithium aluminium anhydride prior to distillation and stored under argon over molecular sieves 4 Å; ethyl dichlorophosphate was distilled under argon before immediate use; triethylamine was dried and stored over 3 Å molecular sieves for prolonged storage. The concentrations of *n*butyllithium (in hexanes) solutions was confirmed by titrations in section 5.3.

5.2 Instrumentation

NMR spectra were obtained from either a JEOL ECS 400 MHz FT or a JEOL ECS 500 MHz FT NMR spectrometer. Melting points were obtained using a Cole-Parmer melting point apparatus. All gas chromatography—mass spectrometry (GC-MS) analysis was performed on an Agilent 7890B BC coupled to an Agilent 5977B Mass Spectrometer (Agilent Technologies, Cheadle, UK). Infrared spectra were collected using a Thermo Nicolet 380 FT-IR. Mass spectra and accurate mass data were obtained on an Aglient Technologies 6540 UHD Accurate-Mass Q-TOF LC/MS.

5.3 Titration of *n*-butyl lithium solutions

General procedure for the titration of stock *n*-butyllithium solutions: A flame dried 25 mL two neck flask was charged with *n*-benzylbenzamide (300.5 mg) and dry THF (10 mL). The reaction mixture was cooled to -40° C using a cryostat (Labtex Huber) and cooling bath of ethylene glycol:water, 1:1, prior to the dropwise addition of *n*-butyllithium via syringe. The end point was reached when the solution remained a pale blue, a single drop past this point permanently changed the solution colour to a deep blue.

Optimised ¹⁹F{¹H} NMR titration experiments for the determination of the pK_a of the Brønsted acid 2,2'-bis(difluoromethylene)-1,1'-binaphthyl phosphinic acid

A single pulse experiment was altered for the optimised ¹⁹F{¹H} NMR spectra titration experiments. The sweep width was set to 200 ppm and offset to −150 ppm. Each spectrum was acquired using 16384 points, 64 scans and 2 prescans. The flip angle was set to 30° and a recycle delay of 3 seconds was used. The optimised titration was carried out under an argon atmosphere using Kontes taps to establish the inert atmosphere. The Kontes tap was fitted with a rubber septum to enable the addition of base throughout the titration while maintaining the inert atmosphere throughout the duration of the titration. The solvent used for all pKa titrations was deuterated acetonitrile (CD₃CN). The concentration of the reference compounds **81** and **82** were 9.90×10^{-3} mol dm⁻³ and 10.6×10^{-3} mol dm⁻³ for the reference compound 83. The concentration of the fluorinated phosphinic Brønsted acid (59) was 10.3×10^{-3} mol dm⁻³. The superacid used to fully protonate all species prior to the titration was a solution of triflic acid in CD₃CN (100 µL, 0.063 mol dm⁻³). The strong base used throughout the titrations was a solution of phosphazene base P₁-tBu in CD₃CN (0.021 mol dm⁻³) in 20 μL additions per spectrum recording. An internal standard solution of hexafluorobenzene in CD₃CN $(7.18 \times 10^{-3} \text{ mol dm}^{-3})$ was used as a reference point for each titration spectrum and was sealed into a melting point tube to ensure the pKa titration results were unaffected.

5.5 X-ray data collection and structural refinement

Single crystal X-ray diffraction data were collected on a Rigaku Saturn724+ CCD diffractometer, using either MoK α X-rays of λ =0.71073 Å or CuK α X-rays of λ =1.541840 Å. When MoK was employed as the radiation source, crystals were cooled to 150 K during data collection.

Refinement of F^2 was performed against all reflections. The weighted R-factor, wR, and goodness of fit, S, are based on F^2 , conventional R-factors (R) are based on F, with F set to zero for negative F^2 . The threshold expression of $F^2 > 2\sigma F^2$) is used only for calculating R-factors(gt) etc. and is not relevant to the choice of reflections for refinement. R-factors based on F^2 are statistically about twice as large as those based on F, and R-factors based on ALL data will be even larger.

Structures presented were solved by direct methods. All non H-atoms are refined anisotropically. Hydrogen atoms were fixed in idealised positions and refined using a riding model, with C-H distances of 0.97 Å, N-H distances of 0.91 Å, and U_{iso} 1.5 times U_{eq} of the carrier atom. All Ortep representations show ellipsoids at the 50% probability level.

The data collection, cell refinement and data reduction was conducted using CrysAlisPro. The solution and refinement of the data was achieved using SHELXL-97.

5.6 Synthesis of reference sulfonamides

5.6.1 General procedure for the amination of sulfonyl chlorides

Adapted from Supuran *et al.*: The corresponding sulfonyl chloride derivative (1.00 g, 4.5 mmol) was dissolved in an excess of ammonium hydroxide (8 mL) and heated under reflux until completion indicated by TLC analysis. The reaction mixture was left to cool down and the resulting precipitate was filtered and washed with ice-cold water to obtain the pure sulfonamide derivative.⁷⁸

5.6.2 Amination of 4-nitrobenzenesulfonyl chloride⁷⁸

Following the general procedure, 4-nitrobenzenesulfonyl chloride (1.0 g, 4.5 mmol) was reacted with ammonium hydroxide (8 mL, 10 wt%) for 12 h. The solid obtained was washed with ice cold water (1 mL) to obtain pure 4-nitrobenzenesulfonamide (760 mg, 84%); 1 H NMR (400 MHz, DMSO- d_6) δ 8.42 (d, J = 8.0, 2H), 8.06 (d, J = 8.0, 2H), 7.75 (s, 2H); 13 C{ 1 H} NMR (100 MHz, DMSO- d_6): 149.4 (C), 149.2 (C), 127.2 (CH), 124.4 (CH); IR (cm $^{-1}$): 3332 (N-H primary amine), 3247 (C-H), 3128 (C-H), 1515 (N=O asymmetric nitro stretch), 1346 (N-O symmetric nitro stretch), 1158 (S=O sulfoxide). Data in accordance with literature.²¹

5.6.3 Amination of 3-nitrobenzenesulfonyl chloride⁷⁸

$$O_2N$$
 O_2N
 O_2N

Following the general procedure, 3-nitrobenzenesulfonyl chloride (1.0 g, 4.5 mmol) was dissolved in ammonium hydroxide (8 mL, 10 wt%) and the solution was heated to reflux for 5 h. The reaction mixture was left to cool overnight to room temperature. White crystals of 3-nitrobenzenesulfonamide were obtained by filtering the slurry (861 mg, 95 %); ¹H NMR (400 MHz, DMSO- d_6) δ 8.59 (s, 1H), 8.45 (d, J = 8.0 Hz, 1H), 8.24 (d, J = 8.0, 1H), 7.89 (t, J = 8.0 Hz, 1H), 7.68 (s, br, 2H); ¹³C{¹H} NMR (100 MHz, DMSO- d_6) δ 147.7, 145.6, 131.7, 131.1, 126.5, 120.6.

5.6.4 Amination of 4-toluenesulfonyl chloride⁷⁸

4-Toluenesulfonyl chloride (1.1 g, 5.8 mmol) was dissolved in ammonium hydroxide (8 mL, 10 wt%) and heated to reflux for 2.5 h. The reaction mixture was left overnight to cool to room temperature. A white precipitate formed immediately after the heat source was removed. The solid 4-toluenesulfonamide was collected after filtration (662 mg, 67%); 1 H NMR (400 MHz, CDCl₃) δ 7.81 (d, J = 8.2 Hz, 2H), 7.32 (d, J = 8.2 Hz, 2H), 4.74 (s, 2H), 2.44 (s, 3H); 13 C{ 1 H} NMR (100 MHz, CDCl₃) δ 143.8, 139.5, 129.9, 126.6, 21.7.

5.6.5 Amination of 4-chlorobenzene sulfonyl chloride⁷⁸

4-Chlorobenzene sulfonyl chloride (2.0 g, 9.5 mmol) was dissolved in ammonium hydroxide (30 mL, 10 wt%) and stirred at 30°C for 3 h. The reaction mixture was left to cool slowly to room temperature before isolating the product by filtration. 4-Chlorobenzene sulfonamide was obtained as a white solid and washed using ice-cold hexane before being dried over P_2O_5 for a week to yield the final product (1.4 g, 77%); ¹H NMR (400 MHz, DMSO- d_6) δ 7.82 (d, J = 8.0 Hz, 2H), 7.65 (d, J = 8.0 Hz, 2H), 7.46 (br s, 2H); ¹³C{¹H} NMR (100 MHz, DMSO- d_6) δ 143.0, 136.6, 129.1, 127.6.

5.6.6 Synthesis of 2,3,4,5,6-pentafluoro-N-(4-nitrobenzene-1-sulfonyl)benzene-1-sulfonamide (84)⁸⁶

$$O_2N$$
 O_2
 O_3
 O_4
 O_5
 O_5

Procedure adapted from the literature.⁷⁵ 4-nitrobenzenesulfonamide (557 mg, 2.8 mmol) was dissolved in NaOH (5%, 2 mL). The solution was heated to 60°C and pentafluorobenzenesulfonyl chloride (785 mg, 2.9 mmol) was added over 1 h. The temperature and pH were monitored throughout. A pale-yellow slurry was obtained and the reaction was left to stir at the same temperature for a further 20 minutes, prior to the addition of 1 M NaOH (1.5 mL). Reaction completion was ascertained using both ¹⁹F NMR and ¹H NMR spectroscopy. The slurry was filtered to obtain the crude product as a sodium salt. The crude salt was dissolved in a minimum

amount of water and heated to 50 °C for better dissolution. Insoluble solids were removed by filtering the solution. The salt was acidified using concentrated HCI. The solution was transferred to a petri dish to recrystalise by evaporation and white crystals were obtained (29 mg, 2%); ¹H NMR (400 MHz, DMSO- d_6) δ 8.22 (d, J = 8 Hz, 2H), 7.97 (d, J = 8 Hz, 2H); ¹ºF{¹H} NMR (376 MHz, DMSO- d_6) δ −138.80 (d, J = 26.3 Hz, 2F), −153.56 (s, 1F), −163.8 (d, J =18.8 Hz, 2F); LC-MS (Q-TOF, ESI, neg.): RT = 4.268, target mass ([M]+) = 431.95092, mass found ([M]+), 431.95261.

5.6.7 Synthesis of 2,3,4,5,6-pentafluoro-N-(3-nitrobenzene-1-sulfonyl)benzene-1-sulfonamide (**85**)⁸⁶

3-Nitrobenzenesulfonamide (511 mg, 2.5 mmol) was dissolved in NaOH (5%, 2.3 mL) and heated to 60 °C. Pentafluorobenzenesulfonylchloride (677 mg, 2.5 mmol) was added in small portions over 1.5 h. The reaction mixture was filtered to afford the crude product. The crude product was dissolved in a minimum amount of hot water and left to cool to room temperature to afford crystals (300 mg, 28 %); ¹H NMR (400 MHz, CD₃CN) δ 8.22 (d, J = 8.7 Hz, 2H), 7.97 (d, J = 8.7 Hz, 2H); ¹³C{¹H} NMR (101 MHz, CD₃CN) δ 147.74, 145.59, 131.72, 131.13, 126.53, 120.54; ¹³C{¹⁹F} NMR (101 MHz, CD₃CN) δ 129.6 (d, J = 6.14), 128.3 (d, J = 6.38), 125.2-125.1 (m), 123.8-123.7 (m), 122.1; ¹⁹F{¹H} NMR (376 MHz, DMSO- d_6) δ –138.77 (d, J = 22.6 Hz), –153.44 (m), –163.71 (m); LC-MS (QTOF, ESI, neg.) RT = 4.272, target mass = 431.95092 ([M]+), mass found = 430.94543 ([M-H]⁺).

Table 11: Crystal data for the structural refinement of **85**.

Compound number	85	
Formula	C ₂₄ H ₁₈ N ₄ O ₁₆ F ₁₀ Na ₂ S ₄	
M, g mol ⁻¹	982.64	
Crystal system	Triclinic	
Space group	P-1	
a/Å	7.2301(2)	
b/Å	8.0035(2)	
c/Å	33.1658(8)	
α/deg	86.251(2)	
β/deg	86.228(2)	
γ/deg	63.409(2)	
V/ų	1711.07(8)	
T/K	293(2)	
Z	2	
ρ, calc [g cm ⁻³]	1.9070	
λ°/ Á	1.54184	
Data Measured	27410	
Ind. Refins	6761	
Rint	0.0734	
Reflns with I	5830	
l > 2σ(l)		
Parameters	565	
Restraints	8	
R ₁ d (obs), wR ₂ (all)	0.0686, 0.0774	
Goodness of fit	1.129	
Largest residuals/ e Á ⁻³	1.344, -0.718	

5.6.8 Synthesis of 2,3,4,5,6-pentafluoro-N-(4-chloro-1-sulfonyl)benzene-1-sulfonamide⁸⁶ (**86**)

Procedure adapted from the literature⁷⁵. 4-Chlorobenzenesulfonamide (1.40 g, 7.3 mmol) was dissolved in NaOH (5%, 6 mL) and heated to 60°C.

Pentafluorobenzenesulfonylchloride (2.00 g, 7.5 mmol) was added in small portions over 1 h. The pH was maintained between 9-11 by addition of 5% NaOH as necessary. The reaction mixture was stirred for a further 25 minutes at the same temperature and left to stir overnight at 60°C. The reaction mixture was cooled slowly to room temperature and a white solid precipitated formed. The white solid was collected by filtration to afford the crude product. The crude product was recrystallised from the minimum amount of MeOH and conc. HCl (1:4) to afford white crystals (150 mg, 5%); 1 H NMR (400 MHz, DMSO- d_6) δ 7.62 (d, J = 8.5 Hz, 2H), 7.48 (d, J = 8.6 Hz, 2H); 13 C{ 1 H} NMR (101 MHz, DMSO- d_6) δ 143.4, 135.6, 128.4, 128.2; 19 F{ 1 H} NMR (376 MHz, CD $_{3}$ CN) δ –163.56, –163.50, –163.45, –152.98, –138.51, –138.46; LC-MS (QTOF, ESI, pos.) RT = 12.922, m/z = 443.91595 ([M+Na] $^{+}$), target mass = 420.92687, found mass = 420.92609.

Table 12: Crystal data for the structural refinement of **86**.

	86
Compound number	
Formula	C ₇₂ H ₂₄ Cl ₆ F ₃₀ N ₆ Na ₅ O ₃₀ S ₁₂
M, g mol ⁻¹	2735.34
Crystal system	Triclinic
Space group	P-1
a/Å	7.4286(2)
b/Å	17.9262(7)
c/Å	19.3116(8)
α/deg	111.638(4)
β/deg	92.039(3)
γ/deg	92.300(3)
V/ų	2385.00(16)
T/K	293(2)
Z	1
ρ, calc [g cm ⁻³]	1.904
λ°/ Á	1.54184
Data Measured	39761
Ind. Refins	9274
R _{int}	0.0667
Reflns with I	7384
l > 2σ(l)	
Parameters	774
Restraints	31
R ₁ d (obs), wR ₂ d (all)	0.1042, 0.1262
Goodness of fit	1.064
Largest residuals/ e Á ⁻³	2.571, -2.041

5.7 Synthesis of Brønsted phosphinic acids for asymmetric catalysis.

5.7.1.1 General synthesis of 2,2'-bistriflate-1,1'-binaphthyl (52)^{27, 49, 51}

Triflic anhydride (19.1 mL, 113 mmol) was added dropwise at 0 °C to a solution of 1,1'-binaphthol (15.0 g, 52 mmol), pyridine (15.9 mL, 197 mmol) and dry CH₂Cl₂ (250 mL) over a 15 minute period. The reaction mixture was then stirred at room temperature overnight. The solvent was removed *in vacuo* and the resulting yellow solid was dissolved in ethyl acetate (250 mL) before washing with HCl (5%, 200 mL); aq. NaHCO₃ (sat., 200 mL) and brine (200 mL). The organics were combined, dried over anhydrous MgSO₄ and the solvent was removed under vacuum to obtain a yellow crude product. The solid crude material was passed through a short pad of silica gel, eluting with CH₂Cl₂ to give the product as a white solid.

(*rac*)-2,2'-bistriflate-1,1'-binaphthyl Obtained as a white, powdered solid (9.5 g, 98%). ¹H NMR (500 MHz, CDCl₃) δ 8.14 (d, J = 8 Hz, 2H), 8.01 (d, J = 8 Hz, 2H), 7.63 (s, 1H), 7.61 (s, 1H), 7.60 – 7.58 (m, 2H) 7.43 – 7.40 (m, 2H), 7.27 (s, 1H), 7.25 (s, 1H). ¹³C{¹H} NMR (125.77 MHz, CDCl₃) δ 145.5, 133.3, 132.5, 132.1, 128.5, 128.1, 127.5, 126.9, 123.6, 119.5, 117.0. ¹⁹F{¹H} (470.62 MHz, CDCl₃) δ - 74.46; R_f = 0.72 (Hexane/EtOAc: 3/1).

(*R*)-2,2'-bistriflate-1,1'-binaphthyl Obtained as a white crystals (28.7 g, 100%). 1 H NMR (500 MHz, CDCl₃) δ 8.15 (d, J = 5.0 Hz, 2H), 8.01 (d, J = 10.0 Hz,

2H), 7.62 (d, *J* = 10.0 Hz, 2H), 7.59 (m, *J* = 15.0 Hz, 2H), 7.41 (m, *J* = 15.0 Hz, 2H), 7.26 (d, *J* = 10.0 Hz); ¹³C{¹H} NMR (125.77 MHz, CDCl₃) δ 145.5, 133.3, 132.5, 132.1, 128.5, 128.1, 127.5, 126.9, 123.6, 119.5, 117.0; ¹⁹F{¹H} NMR (470.62 MHz, CDCl₃) δ -74.46; R_f = 0.70 (Hexane/EtOAc: 3/1).

5.7.1.2 Synthesis of 2,2'-dimethyl-1,1'-binaphthyl (53)

To a stirred solution of 2,2'-bistriflate-1,1'-binaphthyl (5.0 g, 9.1 mmol) and Ni(dppp)Cl₂ (345 mg, 0.6 mmol) in Et₂O (80 mL) was added MeMgBr (12 mL, 3.0 M in Et₂O) dropwise at 0°C. The reaction mixture was heated under reflux for 12 h and quenched afterwards on ice with 5% HCl. The reaction mixture was extracted with EtOAc (3 × 50 mL) and the combined organic extracts were washed with aqueous NaHCO₃ (sat., 50 mL). The combined organic extracts were dried over anhydrous magnesium sulfate, filtered and the solvent removed under reduced pressure to afford the product as a white solid.

(*rac*)-2,2'-dimethyl-1,1'-binaphthyl Obtained as colourless crystals (1.10 g, 86%); 1 H NMR (500 MHz, CDCl₃) δ 7.90 (s, 4H), 7.50 (s, 2H), 7.40 (s, 2H), 7.20 (s, 2H), 7.04 (s, 2H), 2.03 (s, 6H); 13 C{ 1 H} NMR (125.77 MHz, CDCl₃) δ 135.0, 134.4, 132.9, 132.4, 128.9, 128.1, 127.6, 126.2, 125.8, 125.0, 20.1; R_f = 0.40 (Hexane).

(*R*)-2,2'-dimethyl-1,1'-binaphthyl Obtained as white solid (2.50 g, 99%); ¹H NMR (500 MHz, CDCl₃) δ 7.93 (m, 4H), 7.56 (d, *J* = 10.0 Hz, 2H), 7.42 (t, *J* = 15.0 Hz, 2H), 7.23 (t, *J* = 15.0 Hz, 2H), 7.04 (d, *J* = 10.0 Hz, 2H), 2.05 (s, 6H); ¹³C{¹H}

NMR (125.77 MHz, CDCl₃) δ 135.6, 135.0, 133.3, 132.9, 129.4, 128.6, 128.0, 126.6, 126.0, 125.5, 20.3; R_f = 0.41 (Hexane).

Table 13: Crystal data for the structural refinement of (*R*)-2,2'-dimethyl-1,1'-binaphthyl (**53**)

Compound number	53
Formula	C ₂₂ H ₁₈
M, g mol ⁻¹	282.39
Crystal system	Monoclinic
Space group	C ₂ /c
a/Å	17.0224(3)
b/Å	7.4345(10)
c/Å	24.9292(4)
α/deg	90
β/deg	101.364(2)
γ/deg	90
V/ų	3093.02(9)
T/K	293(2)
Z	8
ρ, calc [g cm ⁻³]	1.2127
λ°/ Á	1.541840
Data Measured	26663
Ind. Refins	3106
R _{int}	0.0291
Reflns with I	2825
l > 2σ(l)	
Parameters	89
Restraints	0
R₁ ^d (obs), wR₂ ^d (all)	0.0709, 0.0753
Goodness of fit	1.058
Largest residuals/ e Á ⁻³	0.607, -0.415

5.7.1.3 Attempted synthesis of ethyl-2,2'-bis(methylene)-1,1'-binaphthyl phosphinate (**56**) from **53**.

To a solution of 2,2'-dimethyl-1,1'-binaphthyl (500 mg, 1.8 mmol) in dry THF (5 mL) was added TMEDA (0.64 mL, 2.4 eq., 4.3 mmol,) dropwise at −72°C. The reaction mixture was stirred for 1 h before the dropwise addition of *n*-butyllithium (2.14 mL, 2.23 M in hexanes, 1.1 eq. to TMEDA) at the same temperature. The reaction mixture was stirred for 6 h before leaving to warm to room temperature overnight, until the mixture had completed a colour change to crimson red. At −72°C, ethyldichlorophosphate (0.23 mL, 1.9 mmol) was added and stirred for a further 8 h prior to being stirred overnight at room temperature. The reaction mixture was quenched with saturated NH₄Cl at 0°C, CH₂Cl₂ was then added and the mixture was separated. The aqueous layer was extracted with CH₂Cl₂ (3 × 100 mL). The organics were washed with water and brine (3 × 100 mL). The organics were combined and dried using MgSO₄, prior to filtration by gravity. The solvent was removed under reduced pressure to afford the crude white solid.

(*rac*)-ethyl-2,2'-bis(methylene)-1,1'-binaphthyl phosphinate . ¹H NMR (500 MHz, CDCl₃) δ 7.89 (t, J = 15.76 Hz, 4H), 7.51 (d, J = 10.00 Hz, 2H), 7.39 (m, J = 15.0 Hz, 2H), 7.21 (m, J = 15.0 Hz, 2H), 7.05 (d, J = 8.50 Hz, 2H), 4.10 (m, 1H), 3.64 (t, 1H) 1.32 (m, 3H); ³¹P{¹H} NMR (202.47 Hz, CDCl₃) δ 64.6.

(*R*)-ethyl-2,2'-bis(methylene)-1,1'-binaphthyl phosphinate ¹H NMR (500 MHz, CDCl₃) δ 7.89 (t, J = 15.76 Hz, 4H), 7.51 (d, J = 10.00 Hz, 2H), 7.39 (m, J = 15.0

Hz, 2H), 7.21 (m, J = 15.0 Hz, 2H), 7.05 (d, J = 8.50 Hz, 2H), 4.10 (m, 1H), 3.64 (t, 1H) 1.32 (m, 3H); $^{31}P\{^{1}H\}$ NMR (202.47 Hz, CDCl₃) δ 64.6.

5.7.1.4 Synthesis of (R)-2,2'-di(bromomethyl)-1,1'-binaphthyl (**54**).

A mixture of solid 2,2'-dimethyl-1,1'-binaphthylene (2 g, 7.08 mmol), *N*-bromosuccinimide (NBS) (2.51 g, 14.10 mmol) and AIBN (azobisisobutyronitrile) (116 mg, 0.71 mmol) was dissolved in dry CH₂Cl₂ (60 mL) and refluxed for 6 h. Further AIBN (3 portions, 116 mg, 0.71 mmol each time) were added over the period of five days at regular intervals. The mixture was then left to cool to room temperature before filtration by gravity and the solvent was then removed *in vacuo*. The remaining residue was dissolved in EtOAc (20 mL) and washed with water (20 mL × 3) and sat. brine (20 mL × 3). The combined organic layers were dried over anhydrous magnesium sulfate, filtered and the solvent removed *in vacuo*. The product was recrystalised from CH₂Cl₂ and hexane to afford yellow crystals (1.8 g, 69%); ¹H NMR (500 MHz, CDCl₃) δ 8.02 (d, J = 8.7 Hz, 2H), 7.92 (d, J = 8.3 Hz, 2H), 7.75 (d, J = 8.6 Hz, 2H), 7.49 (s, 2H), 7.31 – 7.23 (m, 2H), 7.08 (d, J = 8.4 Hz, 2H), 4.26 (s, 4H); ¹³C{¹H} NMR (125.77 MHz, CDCl₃) Rf = 0.31 (Hexane). Data in accordance with the literature.^{25, 49}

5.7.1.5 Synthesis of (R)-2,2'-bis(methylene)-1,1'-binaphthyl phosphinic acid (55)

To a stirred solution of anilinium hypophosphite (1.3 g, 8.17 mmol) in CH₂Cl₂ (50 mL), was added N,N-Diisopropylethylamine (DIPEA) (7.3 mL, 41.80 mmol) dropwise at 0°C and stirred at room temperature for 30 minutes. Me₃SiCl (5.3 mL, 41.77 mmol) was then added at 0°C and the reaction mixture was stirred at room temperature for 2 h. A solution of (R)-2,2'-di(bromomethyl)-1,1'-binaphthyl (1.8 g, 4.19 mmol) in CH₂Cl₂ (20 mL) was added dropwise at 0°C and the reaction mixture was left to stir at room temperature for 3 d. The reaction mixture was cooled to 0°C and quenched slowly with water. The organics were washed with 5% HCl (2 × 50 mL) and water (2 × 50 mL) and brine (2 × 50 mL) before drying with anhydrous magnesium sulfate. The mixture was filtered by gravity and the solvent was removed in vacuo to obtain the crude product as a cream solid. The crude solid was triturated using CH₂Cl₂ and pentane to obtain a white solid (707) mg, 64%); ¹H NMR (500 MHz, CDCl₃) δ 7.97 (d, 8.4 Hz, 4H), 7.54 (dd, J = 8.4, 1.4 Hz, 2H), 7.47 (m, 2H), 7.24 (m, 2H), 7.18 (d, J = 8.3 Hz, 2H), 3.10 (m, 4H); ${}^{13}C\{{}^{1}H\}$ NMR (125.77 MHz, CDCl₃) δ 133.9, 133.0, 132.3, 130.1, 129.4, 128.4, 128.2, 127.1, 126.5, 125.8, 35.6; $^{31}P\{^{1}H\}$ NMR (202.47 Hz, CDCl₃) δ 67.98. Data in accordance with the literature. 25, 49

5.7.1.6 Synthesis of (R)-ethyl-2,2'-bis(methylene)-1,1'-binaphthyl phosphinate (**56**)

A solution of (*R*)-2,2'-bis(methylene)-1,1'-binaphthyl phosphinic acid (91.3 mg, 0.27 mmol) and SOCl₂ (2 mL, excess) was heated to reflux for 6 h and stirred at room temperature for a further 14 h. The volatiles were removed *in vacuo* and the remaining residue was cooled to 0°C prior to the dropwise addition of pyridine (2 mL, 24.7 mmol) and absolute ethanol (2 mL, 34.2 mmol). The reaction mixture was quenched at 0°C with HCl (2M, 20 mL). Aqueous layer was extracted with CH₂Cl₂ (20 mL × 3). The organics were dried over MgSO₄, filtered and solvent removed *in vacuo* to obtain ester 56 as a white solid, which was purified by silica gel chromatography eluting with hexane/EtOAc (2/1). (83 mg, 84%). ¹H NMR (500 MHz, CDCl₃) δ 7.98 (s, 1H), 7.97 (d, J = 5 Hz, 1H), 7.94 (d, J = 10 Hz, 2H), 7.63 (d, J = 10 Hz, 1H),7.48-7.42 (m, 3H), 7.24-7.17 (m, 4H), 4.23-4.09 (m, 2H), 3.19-3.00 (m, 4H), 1.33 (t, 3H); ³¹P{¹H} NMR (202.47 Hz, CDCl₃) δ 67.98. Rf = 0.56 (EtOAc). Data is in accordance to the literature.⁴⁹

5.7.1.7 Synthesis of (R)-ethyl 2,2'-bis(difluoromethylene)-1,1'-binaphthyl phosphinate (57)

A solution of (R)-ethyl-2,2'-bis(methylene)-1,1'- binaphthylphosphinate (57) (2.68 g, 7.2 mmol) in THF (100 mL) was added, over a period of 3 mins, to a solution of NaHMDS (0.132 g, 7.2 × 10^{-4} mol) in THF (100 mL) at -78 °C. The resulting red solution was stirred for 1 h at -78°C and a solution of N-fluorobenzenesulfonimide $(0.3 \text{ g}, 9.5 \times 10^{-4} \text{ mmol})$ in THF (5 mL) was added over a period of 3 mins. The reaction was stirred at -78 °C for a further 2 h. The reaction was allowed to warm up to room temperature over a period of 5 mins and quenched with 1 M aq. HCl (5 mL). The reaction mixture was then reduced in vacuo. The mixture was extracted with EtOAc (3 × 10 mL) and combined, prior to being dried over MgSO₄. The solution was then concentrated under reduced pressure before being purified by silica gel chromatography eluting with CH₂Cl₂ to give pure (R)-ethyl 2,2'bis(difluoromethylene)-1,1'-binaphthyl phosphinate as a cream coloured solid (30 mg, 53%); R_f: 0.4 (CH₂Cl₂). ¹H NMR (CD₂Cl₂): δ 8.18 (t, J = 9 Hz, 2H, Ar), 8.03 (d, J = 8 Hz, 2H, Ar), 7.85 (dd, J = 21 Hz, J = 9 Hz, 2H, Ar), 7.60 (t, J = 7 Hz, 2H, Ar),7.32 (t, J = 8 Hz, 2H, Ar), 7.14 (d, J = 9 Hz, 2H, Ar), 4.43 (m, 2H, P-O-CH2-), 1.38 (t, J = 7 Hz, 3H, -CH₃); ¹³C{¹H} NMR (CD₂Cl₂): δ 134.9, 132.9, 130.5, 130.4, 128.8, 128.3, 127.7, 127.4, 126.9 (br s), 121.8 (dd, J = 27 Hz, J = 14 Hz), 118.3 (dt, 1 J_{C-P} = 138 Hz, 1 J_{C-F} = 271 Hz, -CF₂-P). ¹⁹F{¹H} NMR (CD₂Cl₂): δ -91.5 (dd, ² J_{F-F} = 277 Hz, ${}^{2}J_{F-P}$ = 87 Hz, 1F), -93.5 (dd, ${}^{2}J_{F-F}$ = 295 Hz, ${}^{2}J_{F-P}$ = 110 Hz, 1F), -121.7 (ddd, $^{2}J_{\text{F-F}} = 283 \text{ Hz}, ^{2}J_{\text{F-P}} = 98 \text{ Hz}, ^{4}J_{\text{F-F}} = 12 \text{ Hz}, 1\text{F}), -123.8 (ddd, ^{2}J_{\text{F-F}} = 294.8 \text{ Hz}, ^{2}J_{\text{F-F}}$

 $_{P}$ = 93 Hz, $^{4}J_{F-F}$ = 12 Hz, 1F); $^{31}P\{^{1}H\}$ NMR (CD₂Cl₂): δ 25.6 (pseudo-pent, $^{2}J_{P-F}$ = 95 Hz); LCMS (ESI+), 70 eV [M+H]⁺ with m/z = 445.1 R_f = 0.4 (CH₂Cl₂).

5.7.1.8 (*R*)-bis(difluoromethylene)-1,1'-binaphthyl phosphinic acid (59)

Solid **57** was dissolved in CH₂Cl₂ (2 mL) and MeOH (2 mL) was added and stirred for 10 minutes. NaOH (2 M, 2 mL) was added dropwise at 0°C and the mixture stirred for 1 h. Reaction mixture was quenched at 0°C with HCl (10 mL, 1 M) and aqueous layer extracted with EtOAc (3 × 10 mL). Organics were washed with brine (sat. 10 mL), dried with MgSO₄ before filtration by gravity. The solvent was removed in vacuo to obtain **59** as a white solid (17 mg, 79%). ¹H NMR (CDCl₃): δ 7.90 (m, 4H), 7.52 (m, 8H); ¹⁹F{¹H} NMR (CDCl₃): –93.37 (dd, 2F), –124.21 (dd, 2F) ³¹P NMR (CDCl₃): δ 38.24. Data correlated to the literature.²⁵

5.7.1.9 General procedure for the esterification of 1,1'-binaphthyl-2,2'-diyl hydrogenphosphate (15)

Solid 1,1'-binaphthyl-2,2'-diyl hydrogenphosphate (0.25 g, 0.72 mmol) was dissolved in thionyl chloride (1 mL) and heated to reflux for 2.5 h. The reaction mixture was allowed to cool to room temperature and volatiles removed over vacuum. The resulting residue was dissolved in CH₂Cl₂ (3 mL) and cooled to 0°C prior to the addition of pyridine (0.12 mL, 1.44 mmol), followed by ethanol (12 mL).

The reaction mixture was left to slowly warm to room temperature and stirred for a further 12 h. Reaction was quenched using HCl (2M) at 0°C. Aqueous layer was extracted with DCM (3 × 20 mL), organics combined and washed with brine prior to drying with MgSO₄. Mixture was filtered and solvent removed in vacuo to obtain **70** as a solid used without further purification.

(rac)-4-ethoxydinaphtho[2,1-d:1',2'-f][1,3,2]dioxaphosphepine 4-oxide:

Obtained as yellow/orange solid; ¹H NMR (500 MHz, CD₃OD) δ 8.06 (d, 2H), 7.95 (d, 2H), 7.51 (d, 2H), 7.42 (m, 2H), 7.22 (m, 4H), 4.92 (d, 4H), 3.27 (m, ¹H); ³¹P{¹H} NMR (202.47 Hz, CD₃OD) δ 4.01 (s).

(R)-4-ethoxydinaphtho[2,1-d:1',2'-f][1,3,2]dioxaphosphepine 4-oxide:

Obtained as orange solid; ¹H NMR (500 MHz, CD₃OD) δ 8.04 (d, 2H), 7.93 (d, 2H), 7.51 (d, 2H), 7.40 (m, 2H), 7.20 (m, 4H), 4.93 (d, 3H), 3.5 (m), 1.31 (t) 1.13 (t); ³¹P{¹H} NMR (202.47 Hz, CD₃OD) δ 4.18 (s).; R_f = 0.42 (EtOAc).

(S)-4-ethoxydinaphtho[2,1-d:1',2'-f][1,3,2]dioxaphosphepine 4-oxide:

Obtained as yellow solid (impure ~11%); ^{1}H NMR (500 MHz, CD₃OD) δ 8.05 (d, 2H), 7.95 (d, 2H), 7.51 (d, 2H), 7.42 (m, 2H), 7.22 (d, 4H), 4.90 (s, 6H), 4.00 (m, 0.5 H), 3.57 (q, 1H), 3.27 (m, 1H), 1.33 (m, 1H), 1.14 (t, 1H); $^{31}P\{^{1}H\}$ NMR (202.47 Hz, CD₃OD) δ 4.18 (and 3.22); $R_f = 0.42$ (EtOAc).

5.8 Friedel-Crafts reactions

5.8.1 General procedure for the catalytic asymmetric Friedel-Crafts reaction of (*E*)-*N*-Benzylidene-4-methylbenzenesulfonamide with indole.

Catalysts L¹, L², L¹⁰ and L¹¹ were purchased from Sigma Aldrich and used as received. Catalysts L³⁻⁹ were synthesised as previously described. All catalysts were used for the above Friedel-Crafts reaction, as described below.

Catalyst (L¹-L¹¹) (4.1 mg, 9 ×10⁻³ mmol) was added to a solution of (*E*)-*N*-benzylidene-4-methylbenzensulfonamide (25.5 mg, 0.098 mmol) in toluene (0.5 mL) at -60 °C. The reaction mixture was stirred for 10 minutes and indole (58 mg, 0.49 mmol) was added in one portion before stirring for a further 3 h at -60 °C. The mixture was allowed to warm to room temperature and stirred for a further 21 h, monitoring by TLC analysis. The reaction mixture was quenched at room temperature with saturated aqueous ammonium chloride and washed with ethyl acetate. The organic layer was washed with brine and dried using anhydrous magnesium sulfate. Solvent was removed *in vacuo* and resulting solid was purified by silica gel chromatpgraphy eluting with hexane/EtOAc (2/1) to give to corresponding tosylamide (9-90%, highest yield utilised L³).

¹H NMR (500 MHz, CDCl₃): δ 8.00 (s, 1H), 7.57 (d, J = 8.3 Hz, 2H), 7.30 (d, J = 8.3 Hz, 1H), 7.26 (s, 1H), 7.20 (m, 6H), 7.12 (d, J = 7.9 Hz, 2H), 7.00 (ddd J = 8.1,

7.1, 1.1 Hz, 1H), 6.69 (d, J = 1.5 Hz, 1H), 5.86 (d, J = 7.6 Hz, 1H), 5.05 (d, J = 6.7 Hz, 1H), 2.37 (s, 3H). The data correlates with the literature.²⁵

6. Conclusion and Future work

6.1 Conclusions

The chiral Brønsted acid **59** was successfully synthesised from BINOL using a seven step synthetic route. To improve the synthetic route towards new fluorinated phosphinic acids, a novel reaction was extensively trialled to circumvent three synthetic steps that had low atom economies and negative environmental impacts. This new reaction step found success in the direct cyclisation of compound **53** into ester **56** however isolation was unsuccessful. The previously published, longer synthetic route was amended to utilise unrestricted reagents successfully, improving the accessibility of the new class of fluorinated phosphinic acid asymmetric catalysts. A novel chiral fluorinated ester was synthesised

A ¹⁹F{¹H} NMR spectroscopy titration was optimised and successfully validated using a small library of fluorinated sulfonamides that were synthesised for this purpose. Novel crystallographic data were obtained for the sulfonamide sodium salts **84** and **86**. The pK_a value of the racemic fluorinated phosphinic acid **48** was determined to be in the range of 8.12-8.54, using the validated ¹⁹F{¹H} NMR experiment. This pK_a determination proved that fluorinating the phosphinic acids at the α-position enhances their acidity significantly from the expected region of 14-12 for phosphoric acid catalysts with similar structures to 8.12-8.54.

A library of BINOL-derived phosphorous atropisomers, including the new chiral fluorinated phosphinic ester L^7 , were screened in the asymmetric Friedel-Crafts reaction of indole with (*E*)-*N*-benzylidene-4-methylbenzensulfonamide towards the corresponding tosylamide. The new chiral ester L^7 showed a similar catalytic ability to the corresponding fluorinated acid L^9 , obtaining the tosylamide with

similar yields and ees. The catalysts screened provided a new, direct comparison of the catalytic abilities of BINOL-derived phosphorous atropisomers to their fluorinated counterparts. The direct comparison between L^4 and L^9 provided evidence to support that enhancing the acidity of phosphinic acid catalysts by fluorinating at α -positions to the phosphorous atom produced a catalyst with better catalytic ability and enantiomeric control.

6.2 Future work

Larger catalysts based on the structure of the fluorinated acid catalyst 59 have the potential to be targeted with further reaction trials of the novel "LICKOR" reaction using bulkier substituent groups at the 3,3'-positions to enhance catalytic stereocontrol. The novel esterification reaction from compound 53 to 56 has the potential for isolation of the ester, to improve the overall synthetic route towards the fluorinated phosphinic acid catalysts. The fluorination reactions in this work have the potential to be extended to a large scope of similar P(V) containing atropisomeric catalysts, previously discussed. Fluorinated P(III) containing phosphine compounds may be alternative targets for applications in asymmetric catalysis for comparison to the P(V) examples and for other chiral reactions. For example, the fluorination of the P(III) acid 3, Figure 2, initially synthesised by Beller et al. could be tested. 11 Another method to target P(III) acids would be to build on Chusov et al.'s work by oxidising the P(V) catalysts to P(III) phosphines for applications in asymmetric catalysis.⁵ Since acidity is enhanced by adding electron withdrawing groups to the α positions of the phosphorous atom of the phosphinic acids, other perfluoroalkyl groups could be targeted. Fluorine substituents on the

aromatic backbone may also be targeted for further applications in asymmetric catalysis.

The pK_a value of the novel chiral fluorinated ester **57** synthesised has the potential to be determined utilising the 19 F{ 1 H} NMR spectrometry titration, established through this work. By extension, the pK_a values of any future catalysts in this new class of phosphinic acids, fluorinated at the α -position to the phosphorous atom, could be determined by amending the same method. The pK_a values obtained may be used to influence the asymmetric reactions these catalysts could be screened in going forward. The asymmetric reactions that have the potential to be explored, depending on the pK_a values, could employ the library of compounds for detailed comparisons of small but significant catalyst structural amendments. Reactions with the possibility to be explored are the Nazarov cyclisation, Diels-Alder reactions and more. Furthermore, fluorinated phosphinic catalysts with larger groups at the 3,3-positions may be synthesised to enhance catalyst enantiocontrol, for applications in these asymmetric reactions and their pK_a values assigned.

7. References

- 1. J. L. Montchamp, Acc. Chem. Res., 2013, 47, 77-87.
- 2. F. H. Westheimer, *Science*, 1987, **235**, 1173-1178.
- 3. J. L. Montchamp, *Phosphorus, Sulfur, Silicon, Relat. Elem.* 2013, **188**, 66-75.
- 4. M. Kloda, S. Ondrusova, K. Lang and J. Demel, *Coord. Chem. Rev.*, 2021, **433**, 213748.
- 5. D. Chusov, E. Kuchuk and E. Podyacheva, *Tetrahedron. Lett.*, 2019, **60**, 575-582.
- 6. M. Collinsova and J. Jiracek, *Curr. Med. Chem.*, 2000, **7**, 629-647.
- 7. W. R. Roush and J. M. Methot, *Adv. Synth. Catal.*, 2004, **346**, 1035-1050.
- 8. S. Deprèle and J.-L. Montchamp, *J. Organomet. Chem.*, 2002, **643-644**, 154-163.
- 9. J. Montchamp and Y. Dumond, J. Am. Chem. Soc., 2001, **123**, 510-511.
- 10. J. L. Montchamp, J. Organomet. Chem., 2005, **690**, 2388-2406.
- 11. K. Junge, G. Oehme, A. Monsees, T. Riermeirer, U. Dingerdissen and M. Beller, *Tetrahedron Lett.*, 2002, **43**, 4977.
- 12. H. Sugihara, K. Daikai, X. Lan, H. Furuno and J. Inanaga, *Tetrahedron*, 2002, **43**, 2735-2739.
- 13. G. J. Mei, W. L. Koay, C. Y. Guan and Y. Lu, *Chem*, 2022, **8**, 1855-1893.
- 14. J. K. Cheng, S. H. Xiang, S. Li, L. Ye and B. Tan, *Chem. Rev.*, 2021, **121**, 4309-5094.
- 15. M. Terada, K. Soga and N. Momiyama, *Angew. Chem. Int. Ed.*, 2008, **47**, 4122-4125.
- 16. T. Akiyama, J. Itoh, K. Yokota and K. Fuchibe., *Angew. Chem. Int. Ed.*, 2004, **43**, 1566-1568.
- 17. D. Parmar, E. Sugiono, S. Raja and M. Rueping, *Chem. Rev.*, 2014, **114**, 9047-9153.
- 18. N. Momiyama, H. Tabuse and M. Terada, *J. Am. Chem. Soc.*, 2009, **131**, 12882-12883.
- 19. H. Kagan and O. Riant, *Chem. Rev.*, 1992, **92**, 739-1140.
- 20. K. Kaupmees, N. Tolstoluzhsky, S. Raja, M. Rueping and I. Leito, *Angew. Chem. Int. Ed.*, 2013, **52**, 11569-11572.

- 21. A. Kütt, I. Leito, I. Kaljurand, L. Sooväli, V. M. Vlasov, L. M. Yagupolskii and I. A. Koppel, *J. Org. Chem.*, 2006, **71**, 2829-2838.
- 22. C. H. Martínez and C. Dardonville, ACS Med. Chem. Lett., 2013, 4, 142-145.
- 23. M. Schlosser, G. Katsoulos and S. Takagishi, *Synlett.*, 1990, 747.
- 24. F. W. Bennett, H. J. Emeleus and R. N. Haszeldine, *J. Chem. Soc.*, 1954, **881**, 3598-3603.
- 25. K. Fujii, H. Todani, S. Ito and K. Mikami, *Org. Lett.*, 2019, **21**, 3387-3391.
- 26. M. M. Abdou, P. M. O'Neill, E. Amigues and M. Matziari, *Drug Discov. Today*, 2019, **24**, 916-929.
- 27. Y. Uozumi, A. Tanahashi, S. Y. Lee and T. Hayashi, *J. Org. Chem.*, 1993, **58**, 1945-1948.
- 28. C. S. Ewig and J. R. V. Wazer, *J. Am. Chem. Soc.*, 1985, **107**, 1805-2202.
- 29. L. D. Quin, Heteroat. Chem., 2013, 24, 243-344.
- 30. A. W. Hofmann, Ber. Chem., 1872, 5, 104.
- 31. A. W. Frank, Chem. Rev., 1960, **61**, 313-424.
- 32. J.-L. Montchamp and K. Bravo-Altamirano, *Tetrahedron Lett.*, 2007, **48**, 5755-5759.
- 33. E. A. Boyd, M. E. K. Boyd and F. Kerrigan, *Tetrahedron Lett.*, 1996, **37**, 5425-5426.
- 34. E. E. Nifant'ev, Russ. Chem. Rev., 1978, 47, 835-858.
- 35. K. Bravo-Altamirano, Z. Huang and J. L. Montchamp, *Tetrahedron*, 2005, **61**, 6315-6329.
- 36. K. Bravo-Altamirano and J. L. Montchamp, Org. Synth., 2008, 85, 96-105.
- 37. K. Bravo-Altamirano and J. L. Montchamp, *Org. Lett.*, 2006, **8**, 4169-4171.
- 38. E. A. Boyd, A. C. Regan and K. James, *Tetrahedron Lett.*, 1994, **35**, 4223-4226.
- 39. J. Stawinski and M. Kalek, *Tetrahedron*, 2009, **65**, 10406-10412.
- 40. T. Hirao, T. Masunaga, Y. Ohshiro and T. Agawa, *Synthesis*, 1981, DOI: 10.1055/s-1981-29335, 56-57.
- 41. J. Cornforth, *Proc. R. Soc. Lond.*, 1978, **203**, 101.
- 42. T. Akiyama, *Chem. Rev.*, 2007, **107**, 5744-5758.
- 43. I. Coric and B. List, *Nature*, 2012, **483**, 315-319.

- 44. M. Monaco, R. Properzi and B. List, *Synlett*, 2016, **27**, 591-594.
- 45. D. Uraguchi and M. Terada, *J. Am. Chem. Soc.*, 2004, **126**, 5336-5654.
- 46. E. M. Silva, H. D. A. Vidal, M. A. P. Januario and A. G. Correa, *Molecules*, 2023, **28**, 12-33.
- 47. J. L. Vasse, R. Stranne, R. Zalubovskis, C. Gayet and C. Moberg, *J. Org. Chem.*, 2003, **68**, 2997-3366.
- 48. M. Bose and D. B. Berkowitz, *J. Fluorine Chem.*, 2001, **112**, 13-33.
- 49. J. A. Dixon, Ph.D. Thesis, MMU, 2017.
- 50. J. F. Yang, R. H. Wang, Y. X. Wang, W. W. Yao, Q. S. Liu and M. Ye, *Angew. Chem. Int. Ed.*, 2016, **55**, 14116-14120.
- 51. M. Vondenhoff and J. Mattay, *Tetrahedron. Lett.*, 1990, **31**, 985-988.
- 52. R. A. Arthurs, D. L. Hughes and C. J. Richards, *Eur. J. Inorg. Chem.*, 2022, **2022**, e202101077.
- 53. S. T. Chadwick, R. A. Rennels, J. L. Rutherford and D. B. Collum, *J. Am. Chem. Soc.*, 2000, **122**, 8640-8647.
- 54. L. M. Engelhardt, W. P. Leung, C. L. Raston, G. Salem, P. Twiss and A. H. White, *J. Chem. Soc., Dalton Trans.*, 1988, 2403-2409.
- 55. A. F. Burchat, J. M. Chong and N. Nielsen, *J. Organomet. Chem.*, 1997, **542**, 281-283.
- 56. M. L. Nielsen, J. V. Pustinger Jr. and J. Strobel, *J. Chem. Eng. Data*, 1964, **9**, 161-320.
- 57. L. P. Miller, J. A. Vogel, S. Harel, J. M. Krussman and P. R. Melvin., *Org. Lett.*, 2023, **25**, 1799-1998.
- 58. A. Barba-Bon, A. M. Costero, S. Gil, R. Martínez-Máñez and F. Sancenóna., *Org. Biomol. Chem.*, 2014, **12**, 8745-8751.
- 59. W. P. Chappell, N. Schur, J. A. Vogel, G. M. Sammis, P. R. Melvin and N. D. Ball, *Chem.*, 2024, **10**, 1644-1654.
- 60. F. N. Diauudin, J. I. A. Rashid, V. F. Knight, W. M. Z. W. Yunus, K. K. Ong, N. A. M. Kasim, N. A. Halim and S. A. M. Noor., *Sens. Bio-Sens. Res.*, 2019, **26**, 100305.
- 61. S. Mukherjee and R. D. Gupta., *J. Toxicol.*, 2020, **2020**, 1-16.
- 62. P. Savignac, D. Carmichael and B. lorga, C. R. Acad. Sci, 2000, 821-829.
- 63. S. S. Zhu, D. R. Cefalo, D. S. La, J. Y. Jamieson, W. M. Davis, A. H. Hoveyda and R. R. Schrock, *J. Am. Chem. Soc.*, 1999, **121**, 8251-8259.

- 64. P. M. Pihko, Angew. Chem. Int. Ed., 2004, 43, 2062-2064.
- 65. N. T. McDougal and S. E. Schaus, *J. Am. Chem. Soc.*, 2003, **125**, 12094-12095.
- 66. L. Bernardi, M. Fochi, M. Comes Franchini and A. Ricci, *Org. Biomol. Chem.*, 2012, **10**, 2911-2922.
- 67. P. R. Schreiner, *Chem. Soc. Rev.*, 2003, **32**, 289-296.
- 68. J. F. Blake, D. Lim and W. L. Jorgensen, J. Org. Chem., 1994, **59**, 803-805.
- 69. M. R. Gholami and B. A. Talebi, *J. Phys. Org. Chem.*, 2003, **16**, 79-83.
- 70. F. G. Bordwell, Acc. Chem. Res., 1988, **21**, 456-463.
- 71. P. Christ, A. G. Lindsay, S. S. Vormittag, J.-M. Neudörfl, A. Berkessel and A. C. O'Donoghue, *Chem. Eur. J.*, 2011, **17**, 8524-8528.
- 72. J. Reijenga, A. van Hoof, A. van Loon and B. Teunissen, *Anal. Chem. Insights*, 2013, **8**, 53-71.
- 73. R. Shivapurkar and D. Jeannerat, *Anal. Methods*, 2011, **3**, 1316-1322.
- 74. J. J. H. Ackerman, G. E. Soto, W. M. Spees, Z. Zhu and J. L. Evelhoch, *Magn. Reson. Med.*, 1996, **36**, 674-683.
- 75. E. Parman, L. Toom, S. Selberg and I. Leito, *J. Phys. Org. Chem.*, 2019, **32**, e3940.
- 76. I. Leito, E. Raamat, A. Kütt, J. Saame, K. Kipper, I. A. Koppel, I. Koppel, M. Zhang, M. Mishima, L. M. Yagupolskii, R. Y. Garlyauskayte and A. A. Filatov, *J. Phys. Chem. A.*, 2009, **113**, 8421-8424.
- 77. D. B. Berkowitz, K. R. Karukurichi, R. de la Salud-Bea, D. L. Nelson and C. D. McCune, *J. Fluorine Chem.*, 2008, **129**, 731-742.
- 78. N. Pala, L. Micheletto, M. Sechi, M. Aggarwal, F. Carta, R. McKenna and C. T. Supuran, *ACS Med. Chem. Lett.*, 2014, **5**, 927-930.
- 79. R. Chen, S. Xu, F. Shen, C. Xu, K. Wang, Z. Wang and L. Liu, *Molecules*, 2021, **26**, 5551.
- 80. E. Hayashi, Y. Yamaguchi, Y. Kita, K. Kamata and M. Hara, *Chem. Commun.*, 2020, **56**, 2095-2098.
- 81. R. Wei, C. L. Dickson, D. Uhrin and G. C. Lloyd-Jones, *J. Org. Chem.*, 2021, **86**, 9023-9029.
- 82. M. Yamanaka, J. Itoh, K. Fuchibe and T. Akiyama, *J. Am. Chem. Soc.*, 2007, **129**, 6664-6964.
- 83. I. D. Gridnev, M. Kouchi, K. Sorimachi and M. Terada, *Tetrahedron Lett.*, 2007, **48**, 497-500.

- 84. M. Rueping, W. Ieawsuwan, A. P. Antonchick and B. J. Nachtsheim, *Angew. Chem.*, 2007, **119**, 1971-2169.
- 85. M. Terada and K. Sorimachi, *J. Am. Chem. Soc.*, 2006, **129**, 244-451.
- 86. S. Şanli, Y. Altun, N. Şanli, G. Alsancak and J. L. Beltran, *J. Chem. Eng. Data*, 2009, **54**, 3014-3021.